Thermochemistry, bonding, and reactivity of Ni+ and Ni2+ in the gas phase

Otilia Mó, Manuel Yáñez, Jean-Yves Salpin, Jeanine Tortajada

Thermochemistry, Bonding and Reactivity of Ni^+ and Ni^{2+} in the gas phase

Otilia Mó and Manuel Yáñez

Departamento de Química, C-9. Universidad Autónoma de Madrid. Cantoblanco, 28049-Madrid. Spain

Jean-Yves Salpin and Jeanine Tortajada

Université d'Evry Val d'Essonne

Laboratoire Analyse et Modélisation pour la Biologie et l'Environnement (LAMBE), UMR CNRS 8587

Bâtiment Maupertuis, Boulevard François Mitterrand, 91025 EVRY CEDEX (France)

In this review we present a general overview on the studies carried out on Ni^+ and Ni^{2+} containing systems in the gas phase since 1996. We have focused our attention in the determination of binding energies in parallel with an analysis of the structure and bonding of the complexes formed by the interaction of Ni^+ with one ligand, or in clusters where this metal ion binds several identical or different ligands. Solvation of Ni^{2+} by different ligands is also discussed, together with the theoretical information available of doubly charged Ni-containing species. The final section of this review is devoted to an analysis of the gas-phase uni- and bimolecular reactivity of Ni^+ and Ni^{2+} complexes.

I. INTRODUCTION

The study of the reactivity and thermochemistry of transition metal ions in the gas phase is a very active area of research because transition metals, either as neutrals or

as singly or multiply charged ions, play a crucial role in a variety of chemical processes. In spite of that many questions, such as the mechanism behind the activation of methane by transition metal ions or that associated with the hydrogenation of ethane using heterogeneous catalysts, such as Raney nickel, are still a technological challenge. On the other hand our knowledge on the nature of the bonding between transition metal cations and the different ligands is far from being complete and the amount of accurate experimental binding energies is not very large either. The first important and exhaustive compilation of thermochemical data involving metal cations in general and transition metal cations in particular was published in 1996 (Freiser, 1996). For this reason, in this review we examined exclusively articles and reviews published since 1996, to assure a reasonable continuity with the compilation mentioned above. We have been invited to focus our attention on the reactivity and thermochemistry of Ni^+ and Ni^{2+} ions, which is a distinguished member of the family of transition metals.

Ni^+ presents indeed some peculiarities from the reactivity point of view that will be analyzed along this review. Just to mention one, while the reaction of Fe^+ and Co^+ with ethylene oxide to produce the corresponding methylidene complexes, MCH_2^+, is exothermic and very efficient, it is endothermic and highly inefficient for Ni^+. But also its thermochemistry presents peculiarities which are not well understood yet. For instance, it is often found that the Ni^+ binding energies to certain ligands correspond to a maximum within the first row, even though the electrostatic interactions should be greater for Cu^+, since the ionic radius of the metal decreases from left to right across the periodic table, and therefore under this assumption a greater Cu^+ binding energy should be expected. At this point it can be argued that, as it is indeed the case, other factors, besides the electrostatic ones enter into play. However, the weight of these factors change depending on the nature of the ligand, and for some of them Cu^+ binding

energies (BE) are greater than Ni^+ BE. On the other hand, Ni is between the ten essential transition metals found in biological systems, and one of the few that are commonly coordinated to sulphur (Stiefel & Matsumoto, 1996). The biochemical activity of $Ni^+$is reflected in a significant number of studies of the reactions of Ni^+ with relatively small systems of biochemical relevance. It has been often argued in this respect, that the behavior of a biochemical system is not well represented by its reactivity in the gas phase, which provides, in turn, information on the intrinsic reactivity of the system. However, many biological processes take place in essentially non-polar environments and whereas they cannot always be rationalized in terms of reactivity in solution, the gas-phase reactivity provides useful hints on what is going on in the process. A paradigmatic example is provided by uracil. It has been well established that the pK_a values for the N1 and N3 sites of uracil are virtually the same (Kurinovich & Lee, 2002; Miller et al., 2004), whereas the corresponding gas-phase acidities differ by more than 40 kJ mol^{-1}. Interestingly, the stability of anionic uracil in the active site of uracil-DNA glycosylase, established by means of contemporary NMR techniques, is consistent with the enhanced intrinsic acidity of the N1 site, and contrary to the expectation based on solution acidities (Drohat & Stivers, 2000; Lee, 2005).

A significant attention was also devoted to Ni^+-complexes from the theoretical point of view. Most of this work was done within the framework of the density functional theory (DFT) through the use of the B3LYP approach. This method, that combines Becke's three-parameter nonlocal hybrid exchange potential (Becke, 1993) with the nonlocal correlation potential of Lee, Yang and Parr (Lee et al., 1988), has been shown to yield reliable geometries in particular for complexes containing transition metal cations (Sim et al., 1992; Kim & Jordan, 1994; Bauschlicher, 1995; Bauschlicher & Partridge, 1995; Mebel et al., 1995; Llamas-Saiz et al., 1995; Luna et al., 1997; Luna et al., 1998a;

Montgomery Jr. et al., 1999; Curtiss et al., 2001), as well as relatively good binding energies. In much less opportunities the BPW91 method, that combines the gradient corrected exchange functional of Becke (Becke, 1988) with the correlation functional of Perdew-Wang (Perdew & Wang, 1992) has been used.

Many calculations have been also carried out using high-level ab initio methods, rather than DFT approaches. Among them, besides those based on the use of the Moller-Plesset perturbation theory, the most reliable one is the coupled cluster theory including single and double excitations (Bartlett, 1981) as well as the effect of the connected triples in a perturbative manner (CCSD(T))(Raghavachari et al., 1989). It should be emphasized that also from the theoretical point of view Ni^+ presents important challenges, derived from the fact that for this metal cation there are two or more states very close in energy at the HF level. The immediate consequence is that single-reference procedures, even those including a significant amount of dynamical correlation such as CCSD(T), might fail completely. $NiOH^+$ or the sandwich-type dimers between Ni^+ and pyrrole are paradigmatic examples. In the former, there are two ^3A" states whose energies differ by only 0.8 kJ/mol (Ricca & Bauschlicher, 1997). The latter may exist either as C_{2h}- or as C_2-symmetry complexes, and both configurations differ by less than 1.2 kJ/mol (Gapeev et al., 2000).

In what follows we shall present an overview of the thermochemistry of Ni^+ complexes, ranging from complexes in which the metal cation interacts with one or two ligands, to clusters in which the metal is solvated by several ligands, typically from 3 to 6, because the individual bond dissociation energies can change significantly as the degree of ligation changes, due to concomitant changes in geometric and electronic structures. As we shall have the opportunity to illustrate in forthcoming sections, in this area there are still some open questions. For instance, why in Ni^+L_2 complexes,

depending on the nature of the ligand L, the LNi^+-L bond dissociation energy (BDE) is some times larger, some times smaller than L-Ni^+ BDE. Even in some cases the most stable structure of the Ni^+ complexes is not known. Although, this information is very often available from ab initio or density functional theory (DFT) calculations, not always the theoretical structures have been reported. For this reason, in some instances, we will offer some complementary information based on calculations carried out by us, and not reported before in the literature.

Among complexes involving only one ligand, a particular attention deserve those in which the ligand is an aromatic system, because, in general, large biological molecules exhibit a low vapour pressure and therefore are difficult to produce in the gas phase, but their π-interactions with a metal cation can be reasonably well mimicked using some of the small aromatic compounds that are their basic components. In all cases particular attention will be paid to the existence of periodic trends in the binding when information for other transition metal cations of the same row is available.

In the second section we will analyze the nature of the bonding between Ni^+ and different ligands. The third part of this review will concentrate on the uni- and bimolecular reactivity of bare and ligated Ni(I) and Ni(II) ions.

II. THERMOCHEMISTRY OF Ni^+ INTERACTIONS

An interesting review on the different experimental techniques usually employed to measure metal cation binding energies has been published three years ago (Operti & Rabezzana, 2003). In this section we shall discuss in the first place those papers in which singly ligated complexes are investigated, the ligand being a non-aromatic system.

A. Ni^+-L (L = C, CH, CH_2,CH_3, CH_4) complexes

As mentioned in the introduction, an understanding of the activation of methane is to date an important challenge. This motivated the study of the reaction of $Ni^+(^2D)$ with methane by means of guided ion beam mass spectrometry techniques (Liu et al., 2005). The reaction of Ni^+ with methane yields, besides the $NiCH_4^+$ adduct, the following product ions: NiH^+, NiC^+, $NiCH^+$, $NiCH_2^+$, $NiCH_3^+$. Consequently, new thermochemical information on these products, with the exception of NiC^+, which is observed in the mass spectrum only at high energies, was reported. From the thresholds measured for the corresponding cross sections the bond dissociation energies reported in Table 1 were obtained. For NiH^+ the reported value is in good agreement with the one determined previously from the reactions of Ni^+ with H_2 (Armentrout & Kickel, 1996). For $NiCH^+$ the value in Table 1 was obtained as the weighted average between the BDEs measure for the CH_4 and CD_4 systems, after including the zero point energy (ZPE) correction obtained from theoretical vibrational frequencies evaluated at the B3LYP/6-311+G* level of theory. No previous estimates were reported in the literature to compare with. The BDE for $NiCH_2^+$ is 13.4 kJ/mol smaller than the first theoretical estimates (Bauschlicher et al., 1992b), but in good agreement with more recent values based on B3LYP all-electron calculations (Holthausen et al., 1995). This BDE is also in good agreement with previous values published by the same group and with values obtained from photodissociation studies (Husband et al., 2000). In these photodissociation studies (Husband et al., 2000) $NiCH_2^+$ is produced in reactions between Ni^+, obtained by laser ablation of a metal rod, with ethylene oxide (c-C_2H_4O). As mentioned in the Introduction, this reaction is endothermic and highly inefficient, but although the photodissociation cross sections are one order of magnitude lower than for other transition metal ions, such as Fe^+ or Co^+, a threshold at 406 nm is clearly

observed yielding a $D_0(Ni^+-CH_2) \leq 295 \pm 5$ kJ/mol. For $NiCH_3^+$ the value in Table 1 is somewhat lower than previous estimates obtained from analyses of reactions in which $NiCH_3^+$ is the predominant product ion. The Ni-CH_4^+ BDE was obtained in reactions between this ion with Xe, which yielded $NiXe^+$ demonstrating that $D_0(Ni^+-CH_4) < D_0(Ni^+-Xe)$. From the threshold for the simple collision-induced dissociation process the BDE value reported in Table 1 was obtained. Interestingly, this value is in good agreement with other measurements using equilibrium methods.

TABLE 1. Bond Dissociation Energies (BDE, kJ/mol) of complexes between Ni^+ and different ligands

Ligand	BDE	Ligand	BDE
H	154 ± 7[a]	S	238 ± 4[h] 237 ± 4[i]
CH	301 ± 11[a]	CS	234 ± 9[i]
CH_2	309 ± 8[a] ≤ 295 ±5[b]	CO	175 ± 11[j]
CH_3	170 ± 7[a]	OH	271 ± 9[k]
CH_4	96 ± 5[a]	imidazole	283 ± 9[l]
C_2H_2	188 ± 8[c]	pyrimidine	244 ± 9[m]
C_2H_4	184 ± 8[c]	pyridine	256 ± 15[n]
C_3H_8	148.9[d]- 143.2[e]	adenine	297 ± 10[p]
C_4H_{10}	134[f]	formamide	229.7[q]
Coronene	242.7[g]	urea	277.4[r]
Tribenzocyclyne	463.6[g]	glycine	348.1[s]

[a] (Liu et al., 2005). [b](Husband et al., 2000). [c](Surya et al., 1997). [d](Yi et al., 1998) (theory). [e](Corral et al., 2003c)(theory) .[f](Blomberg et al., 1999). [g](Klippenstein & Yang, 2000)(theory) [h](Husband et al., 2001). [i](Rue et al., 2002). [j](Armentrout & Kickel, 1996).[k](Thompson et al., 2000). [l](Rannulu et al., 2004). [m](Amunugama & Rodgers, 2001). [n](Rodgers & Armentrout, 2000).[p](Rodgers & Armentrout, 2002).[q](Rodríguez-Santiago & Tortajada, 2002)(theory). [r](Rodríguez-Santiago et al., 2003)(theory). [s](Rodríguez-Santiago et al., 2001) (theory)

B. $NiOH^+$ and $NiOH^+(H_2O)$

Transition metal hydroxides have received some attention because the MOH^+ solvated species are frequently found in electrospray mass spectra where they are formed by charge reduction reactions of the solvated dications:

$$Ni^{2+}(H_2O)_n \rightarrow NiOH^+(H_2O)_{n-2} + H_3O^+ \qquad (1)$$

Besides, these metal hydroxides are important components of atmospheric aerosols and can play also a role in surface chemistry (Duncan, 1997; Eller & Schwarz, 1991).

Some papers dealing with the evaluation of the BDE of $NiOH^+$ using either collision-induced dissociation (CID) techniques (Magnera et al., 1989) or ion-molecule reactions in a guided ion beam apparatus (Armentrout & Kickel, 1996) were reported before 1996. The most recent evaluation of the BDE of $NiOH^+$ was carried out by means of photofragment spectroscopy (Thompson et al., 2000). In this study $NiOH^+$ is produced using an electrospray source, which also yields the monohydrated species $NiOH^+(H_2O)$. The photofragmentation of the ion in the 275 to 500 nm range occurs exclusively via loss of OH:

$$NiOH^+ + h\nu \rightarrow Ni^+ + OH \qquad (2)$$

Photofragmentation of $NiOH^+(H_2O)$ occurs by two different pathways:

$$NiOH^+(H_2O) + h\nu \begin{cases} \rightarrow NiOH^+ + H_2O \\ \rightarrow Ni^+H_2O + OH \end{cases} \qquad (3)$$

However, in the 400 nm region, it has been observed that photodissociation occurs overwhelmingly by loss of H_2O. Loss of OH occurs below 370 nm and becomes the primary dissociation pathway only below 330 nm. From the observed spectroscopic thresholds the upper bounds for the corresponding BDEs are those shown in Table1. Several points deserve to be commented. The $NiOH^+$ BDE estimated from the photofragment spectra is significantly higher than the first reported value (Magnera et al., 1989) based in CID experiments (176.6 ± 12 kJ/mol) and also higher than the values obtained in ion-beam experiments (235.5 ± 19 kJ/mol) (Armentrout & Kickel, 1996). Theoretical calculations on $NiOH^+$ carried out using the CCSD(T) method and employing B3LYP optimized geometries, have been reported (Ricca & Bauschlicher, 1997) also in the period of time under review. For Ni-containing systems, even high-level methods such as CCSD(T) may be in error because of the multireference character of the system. This is the case of $NiOH^+$ for which the T1 index that measures the adequacy of a single-reference approach is relatively high. From this fact the authors considered that their CCSD(T) estimates are 12.5 kJ/mol too low, so they proposed as the best theoretical estimate (224.7 kJ/mol) The value so obtained is 37.7 kJ/mol larger than the CID experimental value (Magnera et al., 1989); but still ca. 11 kJ/mol lower than the experimental one obtained in ion-beam experiments (Armentrout & Kickel, 1996), which were the only ones known when this theoretical paper was published, and 46 kJ/mol lower than the photofragmentation derived value. New B3LYP/6-311+G(2df,2p) calculations (Luna et al., 2002) yielded a BDE (248.9 kJ/mol) slightly higher than the CID experimental value, but within the error bars of the experiment, but still too low with respect to the photofragmentation derived value. This seems to indicate that, very likely the CID value (Magnera et al., 1989) is far too low, and likely the upper limit from photofragment spectra(Thompson et al., 2000) far too high.

Interestingly, the BDE of $NiOH^+(H_2O)$ is significantly larger than D_0 (Ni^+-H_2O) (180 ± 3 kJ/mol). This implies that the interaction of water with $NiOH^+$ is significantly stronger than its interaction with bare Ni^+. A similar effect was reported before on hydrated $MgOH^+$ species (Sanekata et al., 1995; Watanabe et al., 1995), that was explained as a result of the OH halfway oxidizing the cation to Mg^{2+}, due to its high electronegative character. A similar mechanism, although quantitatively less strong, is responsible for the enhanced strength of the $NiOH^+$-H_2O interaction with respect to the Ni^+-H_2O one. The attachment of OH to Ni^+ results in a significant charge transfer from the metal cation to the hydroxyl group, leaving a Ni with a charge larger than 1 (+1.3 as estimated from B3LYP calculations) (Thompson et al., 2000) rendering the electrostatic interaction with the water dipole much stronger.

C. NiS^+, $NiCS^+$

As we have mentioned in the Introduction, Ni appear commonly coordinated to sulfur when it interacts with biological systems. This fact motivate some interest in the study of the bare Ni^+ sulfide in the gas phase (Husband et al., 2001; Rue et al., 2002) in order to gain some insight into the intrinsic properties of the Ni-sulfur bond. Besides, these sulfides react (Jackson et al., 1986) with a variety of small alkanes yielding products which result from elimination of either an alkene or H_2S, in an almost even distribution. In the NiS^+ photodissociation study (Husband et al., 2001) the metal sulfide is produced in a reaction of the metal cation with methanethiol (methyl mercaptan):

$$Ni^+ + CH_3SH \rightarrow NiS^+ + CH_4 \qquad (4)$$

including N_2 in the mix to produced vibrationally cold ions.

The photofragment spectrum of NiS^+ shows a threshold at 19900 cm^{-1} which leads to an upper limit to the Ni^+-S bond dissociation energy of 238 ± 4 kJ/mol (see Table 1). This value is significantly lower than the value reported before (Hettich et al., 1986) using similar techniques, but in nice agreement with the value obtained one year later (Rue et al., 2002) using guided-ion beam mass spectrometry (See Table 1). In this latter study, NiS^+ is produced by the reaction of Ni^+ either with CS_2 or with COS:

$$Ni^+ + CS_2 \rightarrow NiS^+ + CS \quad (5)$$

$$Ni^+ + COS \rightarrow NiS^+ + CO \quad (6)$$

Reaction (5) competes with other two processes in which $[Ni,C,S]^+$ + S and CS_2^+ + Ni are formed. In reaction (6) the formation of NiS^+ competes with the formation of $NiCO^+$. Surprisingly, the thresholds from the CS_2 and COS reactions yield rather different BDEs (222 ± 9 and 238 ± 4 kJ/mol, respectively). However, the authors argue that the determination of the NiS^+ threshold in the CS_2 reactions is probably less accurate than in the COS reaction because competition with the $NiCS^+$ channel shifts the NiS^+ threshold to slightly higher energies, leading to a lower BDE. Hence, the $D_0(Ni^+\text{-}S)$ reported value (238 ± 4 kJ/mol) is the one derived in the reaction with COS. It is worth noting that the trends in the MS^+ (M = Ni, Cu, Zn) bond energies Ni > Cu > Zn is comparable to those observed for the corresponding oxides. However, while the nickel-oxide cation bond energy is stronger than that of the nickel-sulfide cation, for Cu^+ and Zn^+ is the other way around. If one assumes that electrostatic interactions are dominant, the relative stabilities of the sulfides and oxides would depend essentially on the polarizabilities of sulfur and oxygen that are 2.90 and 0.81 $Å^3$, respectively. This would explain the behavior of Cu^+ and Zn^+ but not that of Ni^+. This seems to imply that

covalent interactions play a significant role in this case, as it is common for transition metals. Clearly, further theoretical investigations on the characteristics of the Ni^+-S bonding are needed.

From the threshold to form $NiCS^+$ in the reactions of Ni^+ with CS_2 a bond dissociation energy of 234 ± 9 kJ/mol was obtained (Rue et al., 2002) for this ion. This value is significantly larger than the previously reported value of $D_0(Ni^+\text{-CO})$ = 175 ± 11 kJ/mol (Armentrout & Kickel, 1996; Khan et al., 1995; Kretzschmar et al., 2001) for the oxygen analogue. This is not surprising because the polarizability of CS should be larger than that of CO. Besides, an analysis of the molecular orbitals of CS and CO reveals that both the π-acceptor and the σ-donor orbitals of the former are lower in energy than those of the latter, contributing to an enhancement of the metal-to carbon interactions.

D. Ni^+- C_3H_8, -C_4H_{10}, -C_2H_8Si, -C_2H_8Ge

The reaction of ground-state $Ni^+(^2D_{5/2})$ with propane (Noll et al., 1998) and *n*-butane (Blomberg et al., 1999) at a collision energy of formally 0.01 eV was studied under single-collision crossed-beam conditions using pulsed time-of-flight mass spectrometry (Noll et al., 1998). Although these studies were focused on reactivity, that will be discussed in forthcoming sections, it could be established unambiguously the formation of long-lived $NiC_3H_8^+$ and $NiC_4H_{10}^+$ complexes. The former is formed almost exclusively (≥ 96%) at the aforementioned collision energies, while the latter constitutes roughly 11% of the products, although this proportion increases up to 21% at 0.21 eV collision energy. An estimation of the binding energy (134 kJ/mol) for the $NiC_4H_{10}^+$ complex based on B3LYP calculations, was reported in the same paper (Blomberg et al., 1999), although similar calculations reported one year before (Yi et al., 1998) yield

a much larger value (148.9 kJ/mol). More recently, a new theoretical value (143.2 kJ/mol) obtained at the B3LYP/6-311+G(2df,2p) level of theory has been published (Corral et al., 2003c). Very interestingly, in the same publication it has been shown that the corresponding silanes and germanes, namely ethylsilane and ethylgermane, exhibit enhanced Ni^+ BDEs (200.2 kJ/mol and 206.9 kJ/mol) with respect to the propane, due to the existence of stabilizing agostic-type interactions involving the Si-H and Ge-H bonds that will be discussed in forthcoming sections. The existence of these agostic-type interactions are also responsible for the fact that the α,β-unsaturated analogues, that is, vinylsilane and vinylgermane, yield as global minima of the PES non-conventional π-complexes, in which Ni^+, interacts simultaneously with the C=C unsaturated moiety and with one of the X-H bonds (X = Si, Ge) (see figure 1). As we shall discuss later, these interactions are very weak for C-H bonds and accordingly propene yields a conventional π-complex as the most stable structure (see Figure 1)

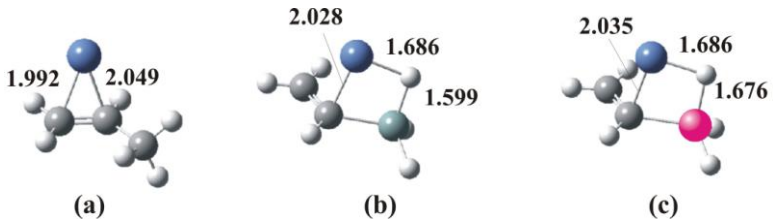

FIGURE 1. B3LYP/6-311G(d,p) optimized geometries of Ni^+ complexes with: (**a**) propene, (**b**) vinylsilane, (**c**) vinylgermane reported by (Corral et al., 2003c), showing that while propene yields conventional π-complexes, vinylsilane and vinylgermane yield non-conventional π-complexes as the most stable structures. Bond lengths are in Å.

E. Ni^+ complexes with formamide, urea and glycine

Due to the ubiquitous presence of Ni^+ in the biological media, several studies have been devoted to investigate the reactivity of this metal ion with small model compounds, such as formamide, which can be consider the simplest model of a peptide function (Rodríguez-Santiago & Tortajada, 2002). Also studies on the reactivity toward urea (Rodríguez-Santiago et al., 2003) and glycine (Rodríguez-Santiago et al., 2001) have

been reported. Although these investigations were focused on reactivity, useful information on the structure and bonding of the corresponding Ni^+ complexes, obtained through the use of B3LYP calculations, was provided. It is worth noting, that only for glycine the most stable structure corresponds to a η^2-N,O bisligated structure in which Ni^+ bridges between the carbonyl group of the acidic function and the amino group (see Figure 2) . For urea, a similar structure was found to be 10 kJ/mol less stable than a single coordinate complex, in which Ni^+ is attached to the carbonyl oxygen (see Figure 2). The most stable structure for formamide-Ni^+ is the oxygen adduct in which Ni is *trans* with respect to the amino group (see Figure 2), the *cis* isomer being 10 kJ/mol less stable.

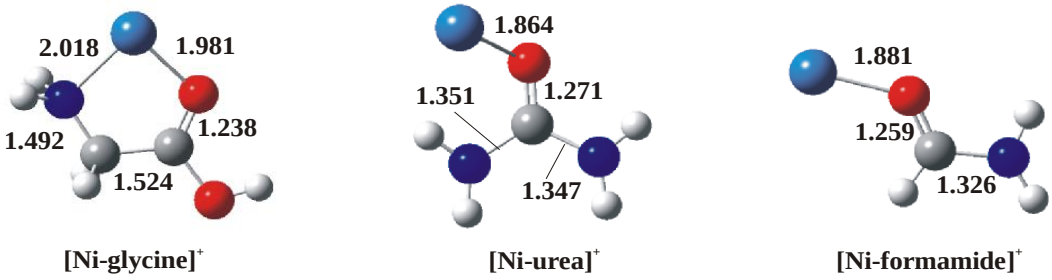

FIGURE 2. B3LYP optimized geometries for $[Ni\text{-glycine}]^+$ (Rodríguez-Santiago et al., 2001), $[Ni\text{-urea}]^+$ (Rodríguez-Santiago et al., 2003) and $[Ni\text{-formamide}]^+$ (Rodríguez-Santiago & Tortajada, 2002). Distances are in Å.

Ni^+ association triggers a sizable activation of the C=O bond, which is maximum in urea. Also in glycine, where the metal cation interacts with the amino group, a significant lengthening of the corresponding C-N bond is observed. It is also worth noting that although the zwiterionic form of glycine is not a minimum of the PES, it is stabilized by interaction with Ni^+, yielding a complex which lies 59 kJ/mol above the global minimum, and in which the metal cation is bisligated to the two oxygens. In all these complexes, the bonding is as expected dominantly electrostatic, although the

charge transfer from the base to the metal cation, evaluated using the NBO formalism, is not negligible (around 0.15 e).

The calculated binding energies (See Table 1) clearly reflect the chelation effects present in glycine, which exhibits a BDE (348 kJ/mol) significantly larger than that of urea (277 kJ/mol) and formamide (230 kJ/mol). The larger BDE of urea with respect to formamide reflects its larger polarizability and the inductive effect of the second amino group. In all cases, it is also found that Ni^+ BDEs are larger than those estimated for Cu^+ at the same or similar levels of accuracy.(Hoyau & Ohanessian, 1997a; Luna et al., 2000c; Hoyau & Ohanessian, 1997b) The energy gaps (33 kJ/mol for glycine, 17 kJ/mol for urea and 11 kJ/mol for formamide) followed the same trend as the corresponding BDEs.

F. Ni^+ complexes with aromatic systems

In the period of time under scrutiny not many experimental studies on the direct interaction of Ni^+ with aromatic systems have been reported in the literature. Besides the works on $Ni^+(benzene)_n$ and $Ni^+(pyrrole)_n$ (n = 1, 2) clusters (Meyer et al., 1995; Gapeev et al., 2000; Jaeger & Duncan, 2005b; Jaeger et al., 2004) that will be discussed in the following sub-section, to the best of our knowledge only the bonding to pyridine (Rodgers et al., 2000), pyridine and its mono-, di- and tri-substituted methyl derivatives (Wong et al., 1997a), pyrimidine (Amunugama & Rodgers, 2001), imidazole (Rodgers & Armentrout, 2002) and adenine (Rannulu et al., 2004) has been analyzed (See Table 1). In these studies the corresponding BDEs were determined in guided ion beam CID experiments. For pyridine, the BDE so measured is in very good agreement with that obtained previously using the Cooks kinetic method (Wong et al., 1997a), while for pyrimidine, imidazole and adenine no previous determinations were available to compare with. The structure and bonding of both Ni^+-pyridine (Rodgers et al., 2000),

Ni^+-pyrimidine (Amunugama & Rodgers, 2001) and Ni^+-imidazole (Rannulu et al., 2004) complexes was also investigated by means of B3LYP calculations. These three derivatives may behave, like benzene, as π-donors, but also as electron σ donors, essentially from the lone pair on their nitrogen atoms. As expected, for the three compounds, the metal ion prefers to be bound to the nitrogen atom rather than to the π cloud of the aromatic ring. For imidazole binding of Ni^+ at the N3 site is preferred over N1 site. Due to this dominant contribution from the σ-donations, pyridine, pyrimidine and imidazole resemble closer the behavior of ammonia and water when binding to transition metal ions than the behavior of benzene. A clear increase of 6, 10 and 45 kJ/mol is observed in the Ni^+ BDE in going from ammonia to pyrimidine, pyridine and imidazole respectively. This trend reflects (Amunugama & Rodgers, 2001) a parallel increase of the polarizability in going from ammonia to pyridine and pyrimidine (2.16, 8.61 and 9.51 $Å^3$, respectively), but not the large binding energy of imidazole, which has a polarizability smaller that the other two aromatic systems (7.17 $Å^3$). Nevertheless, imidazole has a larger dipole moment (3.67 D) than pyridine (2.21 D) and pyrimidine (2.33 D) that can explain its larger Ni^+ binding energy, although differences in the covalent interactions cannot be discarded. Adenine exhibits the largest Ni^+ BDE of this set of compounds (Rodgers & Armentrout, 2002), due to its large polarizability (13.1 $Å^3$) and its rather large dipole moment (2.54 D), and to the fact that although Ni^+ binds preferentially at the N7 position of the imidazolic ring (analogous to the N3 position in imidazole) it also interacts with the lone pair of the amino group.

There are interesting dissimilarities between the four compounds when the BDEs with respect to Ni^+ are compared with those of other late-transition metal ions. For pyridine, when CID methods were used (Rodgers et al., 2000), the following trend was observed: $Co^+ < Ni^+ > Cu^+$, while for pyrimidine the trend is: $Co^+ \approx Ni^+ < Cu^+$, and for imidazole

Co^+ <Ni^+ < Cu^+. Also surprisingly, the observed trend for adenine resembles that found for pyrimidine and not that found for imidazole, which would be the one expected taking into account that the interaction involves the N atom of the imidazolic ring. Although the Co^+ < Ni^+ < Cu^+ trend is the one that could be expected in terms of the decreasing size of the cation, the increase in the occupation of the 3*d* orbitals leads to the opposite trend Co^+ > Ni^+ > Cu^+. Hence, it is usually argued that due to an increased occupation of the 3dσ orbital Cu^+ BDE are smaller than Ni^+ BDE (Rodgers et al., 2000), but such an explanation obviously fails for pyrimidine and imidazole. Interestingly, the theoretical estimates for these two compounds (Rodgers et al., 2000; Rannulu et al., 2004) are at variance with the experimental values and predict for pyrimidine and imidazole the same trend observed for pyridine, i.e. Co^+ < Ni^+ > Cu^+. However, this is not very conclusive either because, in general, the agreement between these theoretical values and the experimental ones for the BDEs of the first-row transition metal cations is not very good, the mean absolute deviation being 9 ± 5 kJ/mol (Amunugama & Rodgers, 2001). On the other hand, at variance with CID experiments, the kinetic method (Wong et al., 1997a) predicts that Co^+ and Ni^+ are equally bound to pyridine.

Methyl substitution leads to a moderate increase in Ni^+ binding energies to pyridine. This increase is equal or slightly smaller than 6 kJ/mol for the monosubstituted compounds, 12 kJ/mol for disubstituted compounds and 13 kJ/mol for the 2,4,6-trisubstituted pyridine. This basicity enhancement is much smaller than that observed for the corresponding proton affinities, for which methyl substitution accounts typically for increases of ca. 25 kJ/mol. Nevertheless, an excellent linear correlation between the relative Ni^+ affinities of *meta*- and *para*-substituted pyridines and their proton affinities exists (Wong et al., 1997a). This was taken as an indication of the similarities in the underlying electronic effects and of the non-negligible covalent character of the Ni^+

interactions. A similarly good linear correlation was reported between calculated Ni^+ binding energies for a variety of N and O containing bases and their experimental proton affinities (Luna et al., 2002).

It is worth noting that the enhancement of Ni^+ affinities is clearly observed for all the *ortho* substituted derivatives, while it has been shown previously that the presence of alkyl substituents at the *ortho*-position of pyridine lowers the cation affinities of many other species such us for instance Cl^+ (Eberlin et al., 1994)), CN^+ (Yang et al., 1995), SF_3^+ (Wong et al., 1997b) or even Fe^+ (Ma et al., 1996), that was attributed to steric hindrance due to the presence of the alkyl group. Accordingly, it was concluded (Wong et al., 1997a) that in the interaction with Ni^+ the *ortho*-methyl-substituted pyridines show very small steric effects.

Cation-aromatic-π interactions have been suggested to play an important role in the molecular recognition of many biological and macromolecular systems (Ma & Doughterty, 1997; Dougherty, 1996). Hence, the interaction of transition metal ions in the gas phase with aromatic molecules was studied by many research groups.

A particularly interesting effect has been observed when complexation with coronene (COR) was compared with that of tribenzocycline (TBC) (See scheme 1) (Pozniak & Dunbar, 1997).

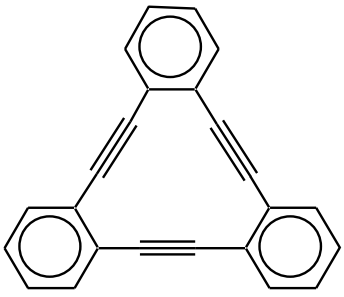

tribenzocycline (TBC)

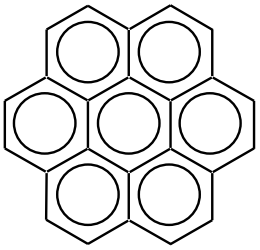

coronene (COR)

Scheme 1

Transition metal ions readily formed dimer sandwich complexes with COR, but for the smaller ions Ni^+ and Cu^+, no dimer formation was observed with TBC. This molecule has a central cavity potentially capable of accommodating small atomic cations, and the results observed with TBC suggested that Ni^+ and Cu^+ were inserted, at least partially into the cavity, thus obstructing the attachment of a second ligand for formation of a sandwich complex ("cavity effect"). B3LYP calculations on $M(COR)^+$ and $M(TBC)^+$ complexes (Klippenstein & Yang, 2000), showed COR binding energy (269.4 kJ/mol) to be, on average, 21 kJ/mol larger than those for the metal benzenes, due simply to the increased polarizability of the ligand. Interestingly, the metal ions bind more strongly to TBC than to COR (+194 kJ/mol for Ni^+) (see Table 1). This enhanced binding was related to the large central cavity, which allows for a closer approach of the metal ion into the ligand plane. (Pozniak & Dunbar, 1997).

This cavity effect appears also in the gas phase association of several transition metal ions and Ag^+ and cyclophanes by means of secondary ionization mass spectrometry (SIMS) (Grutzmacher et al., 2001). Cyclophanes (see Scheme 2) are

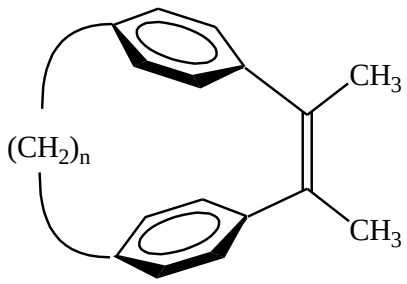

n	
3	**1**
4	**2**
5	**3**
6	**4**

Scheme 2

bridged aromatics having a molecular cavity, the size of which depends on the nature of the bridge between the two benzene rings. Presently, the cyclophanes considered

contained an etheno bridge and an oligomethylene chain (n=3-6). From CID experiments, it was concluded that the metal is strongly bound in the corresponding complexes, with the metal buried inside the cavity of the cyclophane. This was corroborated by AM1 semiempirical calculation carried out for complexes of Fe^+, Ni^+ and Co^+, which showed that the most stable structures correspond to asymmetric "inside-cavity" complexes, the metal being shifted toward the border of the cavity close to the oligomethylene chain.

G. NiL_n^+ (L = H_2, CH_4, C_2H_2, C_2H_4, C_6H_6, CO, CO_2, N_2 NH_3, CN, NO, O_2, H_2O) clusters

A number of studies on transition metal ions solvated by small ligands have been carried out with the main goal of determining sequential metal-ligand BDEs, which provide useful information about the interactions of the individual solvent molecules with the metal.

Equilibrium experimental methods, as well as high-level ab initio calculations applied to the sequential clustering of H_2 ligands to ground state Ni^+ ions (Kemper et al., 1998a) provided association enthalpies and entropies from 1 to 6 ligands, as well as useful ideas on the evolution of the bonding along the series.

The measured BDE of the Ni^+-H_2 was 72.4 kJ/mol (See Table 2), a value which is almost identical to those previously reported for $Fe^+(H_2)$ and $Co^+(H_2)$, but somewhat greater than that of $Cu^+(H_2)$, which, as mentioned above, is usually explained by arguing that metal-ligand repulsion must be stronger in Cu^+ (a $3d^{10}$ ion) because the ligands approach filled $3d_z^2$ orbital, whereas in Ni^+ (a $3d^9$ ion) they approach a half-filled $3d_z^2$ orbital. It is also worth noting that the strength of the Ni^+-H_2 bond is weaker than that of Ni^+-CH_4 (104.2 kJ/mol, see Table 2) (Zhang et al., 2001b) due to the larger

polarizability of methane and much weaker than that of Ni^+-CO (175 kJ/mol, see Table 2) (Khan et al., 1995), reflecting the existence of ion-dipole interactions in Ni^+-CO interactions and the presence of two π-interactions instead of one (Kemper et al., 1998a).

TABLE 2. Sequential Bond Dissociation Energies (BDE, kJ/mol) of Ni^+-L_n clusters

System	BDE	System	BDE
Ni^+-H_2	72 ± 1.2[a]	Ni^+-CH_4	104.2[h]
$Ni^+(H_2)$-H_2	75 ± 1.2[a]	$Ni^+(CH_4)$- CH_4	110.9[h]
$Ni^+(H_2)_2$-H_2	47 ± 1.2[a]	$Ni^+(CH_4)_2$- CH_4	38.9[h]
$Ni^+(H_2)_4$- H_2	18 ± 0.8[a]	$Ni^+(CH_4)_4$- CH_4	~ 8.4[h]
$Ni^+(H_2)_5$- H_2	3 ± 0.8[a]	$Ni^+(CH_4)_5$- CH_4	~ 8.4[h]
Ni^+NH_3	238[b]	Ni^+-N_2	111 ± 11[d]
$Ni^+(NH_3)$-NH_3	251[b]	$Ni^+(N_2)$- N_2	111 ± 11[d]
$Ni^+(NH_3)_2$-NH_3	93[b]	$Ni^+(N_2)_2$- N_2	56 ± 4[d]
Ni^+NO	228 ± 8[c]	$Ni^+(N_2)_3$- N_2	42 ± 9[d]
$Ni^+(NO)$-NO	123 ± 7[d]	Ni^+-CO	175 ± 11[d]
$Ni^+(NO)_2$-NO	115 ± 5[d]	$Ni^+(CO)$- CO	168 ± 11[d]
Ni^+pyrrole	255[e]	$Ni^+(CO)_2$- CO	95 ± 6[d]
Ni^+(pyrrole)-pyrrole	183[e]	$Ni^+(CO)_4$	72 ± 3[d]
$Ni^+C_6H_6$	243 ± 11[f]	Ni^+-C_4H_6	386[i]
$Ni^+(C_6H_6)$-C_6H_6	146 ± 11[f]	$Ni^+(C_4H_6)$- C_4H_6	279[i]
$Ni^+C_2H_4$	182 ± 11[g]		
$Ni^+(C_2H_4)$-C_2H_4	173 ± 14[g]		

[a](Kemper et al., 1998a). [b](Walter & Armentrout, 1998). [c](Thomas et al., 1997). [d](Khan et al., 1995). [e](Gapeev et al., 2000). [f](Meyer et al., 1995). [g](Sievers et al., 1998). [h](Zhang et al., 2001b). [i](Kandalam et al., 2004)

The second H_2 molecule binds with only a slightly larger binding energy than the first one (See Table 2), what is consistent with the fact that the MP2 calculated bond lengths are also nearly identical (1.654 Å in Ni^+-H_2 and 1.643 Å in Ni^+-$(H_2)_2$) (Kemper et al., 1998a). This feature is common to the interaction of several metal cations with different ligands and it has been explained in terms of sd_σ hybridization which tries to alleviate

Pauli repulsion by moving electron charge density away from the ligand. This hybridization has, no doubt an energetic cost which is already paid by the first ligand. Nevertheless, some word of caution is needed here, because, as we shall have the opportunity of illustrating along this review, there are clear exceptions in which the bonding of the second ligand is weaker or even much weaker than the bonding of the first ligand This is the case, for instance, of the $Ni^+(CO)_n$ clusters, in which the BDE of the second CO molecule is 6.7 kJ/mol smaller than the BDE of the first one (Khan et al., 1995) (*vide infra*).

The measured BDE for the third H_2 ligand is much smaller than the first two (See Table 2). A similar behavior was also found for the clusters with methane (Zhang et al., 2001b) and CO (Khan et al., 1995). This finding seems to be related to the repulsive interaction of the H_2 σ orbitals with the 3d shell of the metal cation. As a matter of fact, for the $Ni^+(H_2)_3$ cluster a D_{3h} structure is predicted in which the three H_2 molecules have a repulsive interaction with the $3d_z^2$ (a_1) and the two e' ($3d_{x^2-y^2}$ and $3d_{xy}$) orbitals of Ni^+.

A further decrease in the bonding strength is observed when the fourth H_2 or CO molecule is added to the cluster (See Table 2). The equilibrium structure of the $Ni^+(H_2)_4$ cluster, obtained in MP2 calculations, corresponds to a distorted trigonal pyramid, in such a way that the D_{3h} structure of the $Ni^+(H_2)_3$ is largely preserved. This means that the three equatorial ligands are strongly bound while the fourth ligand is more weakly attached, because it must approach the metal along the axis of the $3d_z^2$ orbital.

MP2 calculations show the Ni^+-$(H_2)_5$ clusters to be a trigonal bipyramid with two weakly bound H_2 ligands capping the planar $Ni^+(H_2)_3$ group. The BDE of the fifth H_2 molecule is about 12 kJ/mol smaller than that of the fourth one (see Table 2). It has been suggested (Kemper et al., 1998a) that in $Ni^+(H_2)_4$ cluster the $4p_z$ orbital is used to

polarize the *z* axis electron density away from the ligand, which would result in a strong repulsion when the fifth ligand is added opposite to the fourth. Nevertheless, this mechanism needs to be ratified by suitable theoretical calculations since the participation of the $4p_z$ orbital involves a highly energetic cost. The fifth addition closes the first solvation sphere, what is in contrast with early transition metal ions that add six H_2 ligands, as well as with Cu^+ which adds only four (Kemper et al., 1998b). Accordingly, the BDE obtained for the sixth H_2 molecule is very small (3.3 kJ/mol) indicating that it has been added to the second solvation shell.

Similarly to what has been discussed in previous paragraphs for $Ni^+(H_2)_n$ clusters, the sequential BDEs of $Ni^+(CH_4)_n$ (n = 1-6) have been measured (Zhang et al., 2001b) through the equilibrium:

$$Ni^+(CH_4)_{n-1} + CH_4 \leftrightarrows Ni^+(CH_4)_n \qquad (7)$$

As it was found before for H_2, the first two CH_4 ligands are relatively strongly bound (See Table 2), in good agreement with B3LYP calculations (Zhang et al., 2001b). The BDEs for the third and the forth CH_4 molecules are about 72 kJ/mol weaker than the first two (See Table 2), and again in good agreement with the theoretical estimates. For n = 5, 6 the BDEs are very small (see Table 2), suggesting that both molecules are already in the second solvation shell, likely due to the larger molar volume of methane.

It is interesting to compare the clustering of Ni^+ with other transition metals of the same row, such as Fe^+ and Co^+. Ni^+ and Co^+ exhibit a rather similar behavior. In both cases the second methane molecule is bound about 8.4 kJ/mol stronger than the first one, an effect similar to the one discussed above for clusters involving H_2. Conversely, for Fe^+ the BDE of the second methane molecule is 21 kJ/mol weaker than that of the first one,

that in turn is more than 29 kJ/mol lower than those for Ni^+ and Co^+. As a consequence, while for Fe^+ the BDE when n = 1 is significantly smaller than for Ni^+ and Co^+, the BDE energy of the second methane molecule is almost identical. It is well known that transition metal cations usually adopt a $3d^n$ configuration rather than a $3d^{n-1}4s^1$ to bind inert ligands, in order to reduce the metal/ligand repulsion. Co^+ and Ni^+ are already $3d^n$ species in their ground state, and therefore this problem does not arise. However, Fe^+ has a $^6D(3d^6\ 4s^1)$ ground state, so to adopt a $3d^7$ configuration in its interaction with CH_4 the reaction should involve the ^4F first excited state that lies 24 kJ/mol higher in energy. Apparently, the stabilization gaining, when only one ligand is involved in the interaction, is not enough to counterbalance this energetic cost and in the $Fe^+(CH_4)$ complex, the metal ion remains as a sextet (Schultz & Armentrout, 1993), and due to the large metal/ligand repulsion the BDE is much lower than in Ni^+ and Co^+ analogues. When the second ligand is added, the excitation to the first excited state, to gain a $3d^7$ configuration becomes energetically favorable and in the $Fe^+(CH_4)_2$ cluster the metal changed to a quartet (Schultz & Armentrout, 1993), with BDEs similar to those of the Ni^+ and Co^+ analogues. It is important however not to forget that also the nature of the ligand matters when considering the periodic trends in bonding. Although for CH_4 the BDEs follow the trend $Fe^+ < Co^+ < Ni^+$, for CH_2, as we have mentioned above, the observed trend is just the opposite (Husband et al., 2000).

$Ni^+(C_2H_2)_n$ (n = 1-8) were produced by laser vaporization in a pulsed supersonic expansion of 1% acetylene seeded in argon (Walters et al., 2002). These ions were then mass selected and analyzed with a reflectron time-of-flight spectrometer. The sequential loss of C_2H_2 molecules was then produced by the photodissociation of the clusters using a tunable infrared laser in the 2900-3400 cm^{-1} wavelength region. Very recently a new

investigation on *n* = 1-4 clusters, including a theoretical analysis of their structures was published (Walters et al., 2005b)

The dissociation energies of the complexes formed were not measured, but some interesting hints on the bond strengths were obtained (Walters et al., 2002). The mass spectra showed that apparently acetylene was present primarily as intact molecules, i.e., there is little evidence for fragmentation in the laser plasma. When irradiated with 2900-3400 cm^{-1} wavelengths no photodissociation signal is detected for complexes $Ni^{+}(C_2H_2)_n$ for n = 1, 2. A small amount of photodissociation could be seen for n = 3, while dissociation is highly efficient for clusters with n = 4-8. It was argued that since the calculated value for Ni^{+}-(C_2H_2) complex (Sodupe & Bauschlicher, 1991) is equivalent to 12300 cm^{-1}, the photodissociation of this complex in the 3000 cm^{-1} region requires a multiphoton process, and taking into account that the efficiency of these processes depends on the density of vibrational states which is usually rather low in the small complexes, it is reasonable to expect no dissociation for n < 3. These results must be taken however with caution since in this technique not all molecules undergo infrared multiphoton dissociation (IRMPD) due to the multiphotonic nature of this process. The mass spectrum has a drop of intensity for n = 3 suggesting a change in cluster stability after n = 3. This finding is consistent with the fact that for platinum complexes the most stable coordination sphere contains also three ethylene molecules (Heck, 1974; Csaszar et al., 1988). Taking into account that acetylene is a two-electron donor, the $Ni^{+}(C_2H_2)_3$ complex would have 15 valence electrons, which is less than the 18-electron configuration usually found in organometallic chemistry. The characteristics of the IR spectrum of the $Ni^{+}(C_2H_2)_3$ complex can aid to assure that indeed its most stable structure would correspond to three ethylene molecules in the same plane as the Ni atom in a D_{3h} structure. In that case only two IR-active vibrations should be

expected, while three active bands should be seen if the acetylenes are perpendicular to the plane defined by the metal and the C≡C bond centers (Walters et al., 2002). Unfortunately the quality of the IR spectra recorded in these first experiments was not good enough as to assign unambiguously the structure of this complex. However, in the more recent publication (Walters et al., 2005b), it was found that at the B3LYP/6-311+G** level of theory the most stable structure corresponds to an arrangement (structure *c* in Figure 3) in which only two acetylenes are equivalent and almost perpendicular (the dihedral angle being 113º) to the plane define by the C≡C bond of the third molecule and the Ni ion. To complement this information we have then considered it of interest to use the same theoretical model to characterize the cluster in which the three acetylene molecules lie in the same plane with the Ni atom. We found this structure (*a* in Figure 3) to be a saddle point with three imaginary frequencies that try to take the three acetylene molecules out of the plane. Furthermore, as it has been found before for the bis-acetylene $Ni^{+}(C_2H_2)_2$ complex (Sicilia & Russo, 2004) the acetylene moieties are not linear any more, the C≡C-H angle being 164.2 degrees. Also interestingly, similar calculations show that the D_{3h} configuration in which the three acetylene molecules are perpendicular to the plane that contains the metal and the centers of the three C≡C bonds (structure *b* in Figure 3) is not a stationary point of the PES. The forces and the displacements never converge because the system is forced to have a D_{3h} configuration, while lower in energy there exists the low-symmetry minimum described above (structure *c* in Figure 3).

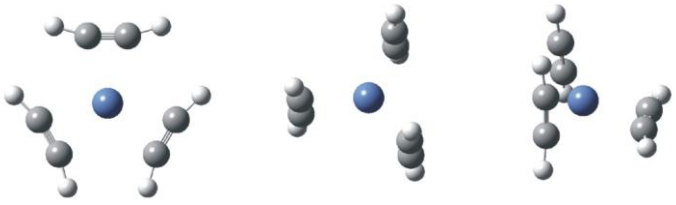

a ***b*** ***c***

FIGURE 3. B3LYP/6-311+G(d,p) optimized geometries of $Ni(C_2H_2)_3^+$ clusters. The D_{3h} structure ***a*** is a saddle point with three imaginary frequencies. The D_{3h} structure ***b*** is not a stationary point of the PES. The C_1 structure ***c*** is a minimum.

Quite interestingly, the n = 4 complex presents a rather simple spectrum that led to the conclusion that it is not a 3 +1 species, since the four ligands seem to be equivalent, even though the greater dissociation yield for n = 4 indicates that the binding energy for the fourth acetylene molecule is smaller than for n = 3. Two possible conformations will be consistent with four equivalent ligands. A square planar species with the acetylenes oriented perpendicular to the plane containing the metal and the ligand centre or a tetrahedral structure. The observed IR spectrum was consistent with either structure, but it did not allow distinguishing between them. This uncertainty was solved in a new publication (Walters et al., 2005b) in which it was found, by means of B3LYP/6-311+G** calculations, that in the $Ni^+(C_2H_2)_4$ cluster the four acetylenes are attached directly to the metal, and as 3 + 1 structure in which the fourth acetylene molecule is weakly bound to the inner-shell acetylenes, so that three of the acetylene molecules keep a similar arrangement as in the trimer, (structure *b* in Figure 4). We have also verified that the D_{4h} structure in which the four acetylene molecules are perpendicular to the plane containing the metal ion and the centers of the C≡C bonds (structure *a* in Figure 4) is a saddle point with two imaginary frequencies. It is worth noting that structure *b* is consistent with the fact that this cluster has photodissociation yields about 10 times greater than the *n* = 3 cluster (Walters et al., 2002), and with the calculated sequential BDEs from *n* = 1 to *n* = 4 (197, 161, 67 and 20 kJ/mol, respectively).

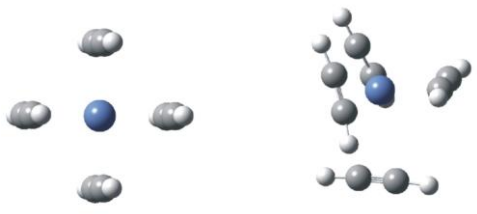

a ***b***

FIGURE 4. B3LYP/6-311+G(d,p) optimized geometries of $Ni(C_2H_2)_4^+$ clusters. The D_{4h} structure *a* is a saddle point with two imaginary frequencies. The C_1 structure *b* is a minimum.

Larger complexes with n = 5-8 show a very efficient photodissociation, what suggests that the additional ligands are not bound to the metal cation, similarly to what was found for CO_2 complexes, in which is possible to clearly distinguish between "core" ligands (those attached to the metal) and "surface" ligands (those bound externally). The characteristics of their IR spectra seem to be consistent with this assumption. The n = 5 complex exhibits new bands at 3248 and 3266 cm^{-1}, that are also present for n = 6, that have their origin in "surface" molecules. Consistently, as new molecules are added to the outer layer forming the n = 7, 8 clusters, these "surface" vibrational modes grow in intensity.

However, the most intriguing feature in the IR spectra of n = 5,6 clusters is the appearance of a strong new band at 3178 and 3176 cm^{-1}, respectively. The fact that these bands appear only in the larger clusters and are shifted further to the red than any others in the spectrum seems to indicate that they are originated in intracluster reactions (Walters et al., 2002), among which the most likely ones are the combination of two acetylenes to form a cyclobutadiene molecule. Although cyclobutadiene itself is not stable, the metal ion can be incorporated into the ring to form a metallacyclopentadienyl complex (**a** in Scheme 3). Alternatively, a π-bonded η_4 Ni-cyclobutadiene complex (**b** in Scheme 3) can be formed. The most significant features of the IR spectra of these clusters agree better with a metal-cyclobutadiene complex than with a metallacyclopentadienyl complex.

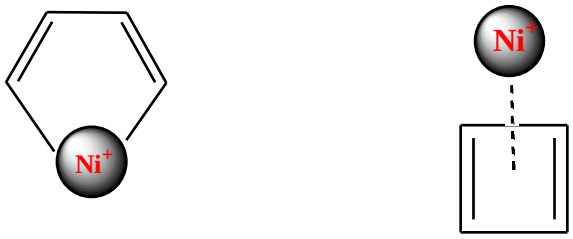

a **b**

Scheme 3

This particular problem was also addressed from the theoretical point of view (Sicilia & Russo, 2004), by exploring the $Ni^+(C_2H_2)_2$ potential energy surface using the B3LYP/DFT approach. The three different local minima that were located in this study are schematized in Figure 5. The bis-ligated metal-cation complex (I) presents a C_{2v} planar structure with Ni ion lying on the perpendicular bisector of the C≡C bonds. The metallacyclopentadienyl complex (II) presents also a C_{2v} planar structure. In complex III, Ni^+ is located over the centre of the ring of a distorted cyclobutadiene molecule in which two acetylene moieties are linked by two additional C-C (1.532 Å) bonds. The most significant finding however is that by far the most stable structure is that of the bis-acetylene complex, while that proposed in the IR study of $Ni^+(C_2H_2)_n$ complexes, is the least stable.

I **II** **III**

FIGURE 5. Local minima of the $Ni^+(C_2H_2)_2$ PES taken from (Sicilia & Russo, 2004). The global minimum corresponds to structure **I**.

Nevertheless, an analysis of the C-H stretching frequencies of the three local minima, shows that only for complex III, the agreement with the experimental values of

(Walters et al., 2002) is good, what seems to indicate, that even though the cyclobutadiene-Ni^+ complex is the least stable in the gas phase, apparently is the one formed under the experimental conditions in which the $Ni^+(C_2H_2)_n$ clusters were formed (Walters et al., 2002). However, it must be recalled here that IR methods do not need to sample all isomers necessarily. Taking into account that the intense absorptions at 3176-3178 cm^{-1} were only observed in the larger clusters, a question that remains to be answered would be why the "surface" molecules triggered the cyclization of ethylene to form cyclobutadiene.

To date, experimental studies on $Ni^+(C_2H_4)_n$ complexes have been reported for n=1, 2 (Sievers et al., 1998). The $D_0(Ni^+\text{-}C_2H_4)$ BDE determined in this guided ion beam mass spectrometry investigation (see Table 2), corrects the previous estimates reported in the literature (> 167.8 kJ/mol) (Jacobson & Freiser, 1983c; Armentrout & Beauchamp, 1981b), based on the exothermicity of the reaction:

$$Ni^+ + c\text{-}C_5H_{10} \rightarrow Ni^+(C_2H_4) + C_3H_6 \qquad (8)$$

but agrees nicely with previous studies of kinetic energy release distributions (184 ± 21 kJ/mol) (Hanratty et al., 1988). It should also be mentioned that this new value is significantly larger (30 kJ/mol) than the available theoretical estimates (Sodupe et al., 1992).

From the analysis of the cross sections for $Ni^+(C_2H_4)_2$ it could be established for the first time the value of the BDE of the second ethylene molecule to be equal to 173 ± 14 kJ/mol (see Table 2), that is, 9 kJ/mol lower than that of the first BDE. It is worth noting that while the BDE for the $M^+\text{-}C_2H_4$ complex is slightly smaller (4 kJ/mol) for Ni^+ than for Co^+, for the second BDE is the other way around (Sievers et al., 1998). Conversely,

the first Ni^+ BDE is 7 kJ/mol larger than the first Cu^+ BDE, while the second BDE is 1 kJ/mol larger for the Cu^+-containing system. There are also some dissimilarities when C_2H_4 is compared with CO. For instance, CO binds Ni^+ slightly (1 kJ/mol) stronger than Co^+ and much stronger (26 kJ/mol) than Cu^+. However, the second BDE for CO resembles closely that measured for C_2H_4.

The clustering of Ni^+ with benzene is of particular relevance since benzene constitutes the paradigmatic model of aromatic systems. The sequential bond energies $Ni(C_6H_6)_n^+$ (n = 1, 2) (see Table 2), have been determined by collision-induced dissociation with Xe in a guided ion beam tandem mass spectrometer (Meyer et al., 1995). The BDE for n = 1 (243 ± 11 kJ/mol) was found to be smaller than that of Co^+ (256 ± 11 kJ/mol) and larger than that of Cu^+ (218 ± 9 kJ/mol). This behavior resembles that observed for complexes with C_2H_4 (Sievers et al., 1998) and was explained (Meyer et al., 1995) as a result of the repulsion between the benzene π-system and the ligand. It seems well established (Bauschlicher et al., 1992a) that a significant enhancement of the interaction between transition metal ions and benzene arises from electron donation from metal 3*d* orbitals into the π* orbitals of benzene. In the C_{6v} symmetry complex the orbitals involved in these donations are $3de_2(\delta)$, while the $3de_1(\pi)$ ones (empty in early transition metal cations) overlap with the benzene π-system and are antibonding. For Co^+, Ni^+ and Cu^+, with 8, 9 and 10 3*d* electrons, these orbitals become increasingly occupied leading to a parallel increase of the repulsion with benzene. Very likely a similar mechanism explains the trends in the interactions with C_2H_4. However, in clear contrast with C_2H_4, a significant decrease in the BDE is observed in going from n = 1 to 2 for benzene. A similar decrease was also observed for other later transition metals such as Fe^+, Co^+ and Cu^+ (Meyer et al., 1995). In contrast for Ti^+ and V^+ early transition metal ions, both BDEs are rather similar. This has been explained (Meyer et al., 1995)

by assuming a fluxional η^4-like bonding of the benzene ligand rather than a η^6-bonding mode. Recent B3LYP/6-311++G(d,p) calculations have shown (Jaeger et al., 2004) that indeed the $Ni^+(benzene)_2$ cluster does not present a D_{6h} structure but a C_1 geometry in which the metal ion is localized over a η^3 site on each benzene ring (see Figure 6). Also interestingly the monomer exhibits a C_{2v} geometry in which the benzene ring is distorted so that two *para* carbon atoms approach very slightly to the metal (see Figure 6). The good agreement between the corresponding calculated BDEs for both the monomer and the dimer (240 kJ/mol and 141 kJ/mol) and the experimental values (see Table 1) gives support to the aforementioned structures.

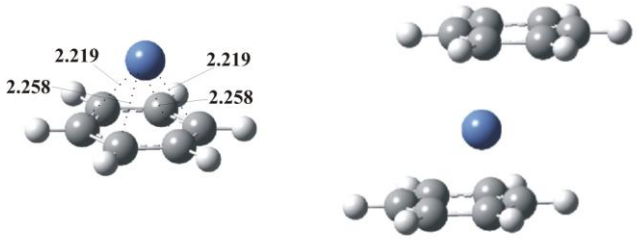

FIGURE 6. Structures of $Ni^+(benzene)_n$ (n = 1,2) cluster as reported by (Jaeger et al., 2004). Distances are in Å

$Ni^+(benzene)_n$ clusters (n =1-6) have been produced by laser vaporization, then mass selected and studied by infrared laser photodissociation spectroscopy in a reflectron time-of-flight mass spectrometer (Jaeger & Duncan, 2005b). Although clusters with a large number of ligands were detected, a significant drop in intensity occurs after n = 2 in the mass spectra, indicating that the n = 1, 2 clusters are more stable than the larger ones. As a matter of fact the easy dissociation of n = 3 and larger clusters suggest that the binding energy in these complexes is less than the photon energy of about 3100 cm^{-1} used in the photodissociation experiments. This seems to indicate that the third and subsequent benzene ligands are not bound directly to the metal cation. Although no BDEs can be extracted from these experiments, the significant frequency shifts

observed in the benzene vibrations within the n = 1 and 2 clusters with respect to the free molecule indicate that the ligands are strongly bound to the metal ion. In a subsequent study using the same experimental technique (Jaeger & Duncan, 2005a), it was found that clusters with more than two benzenes fragmented directly down to $Ni^+(benzene)_2$ with a small amount of Ni^+(benzene), what indicates that likely, the structure of clusters with $n \geq 3$ corresponds to a stable sandwich $Ni^+(benzene)_2$ core that is solvated by subsequent molecules of benzene.

The interactions of Ni^+ with pyrrole are qualitatively similar to those with benzene, but quantitatively stronger (Gapeev et al., 2000). The BDE in $Ni^+(pyrrole)_n$ (n = 1, 2) clusters (See Table 2) have been experimentally determined by the analysis of radiative association (RA) kinetics for the reaction:

$$Ni^+ + \text{pyrrole} \rightarrow Ni^+\text{-pyrrole} \qquad (9)$$

In the same work, B3LYP calculations showed the metal cation to be located more or less above the centre of the four carbon portion of the pyrrole ligand, in a ^{2}A" C_s-symmetry ground state, while the ^{2}A' state is only 18 kJ/mol higher. However, more recent calculations (Jarvis et al., 2003) found that the metal lies immediately above the C-C bond opposite to the nitrogen, although the calculated BDE is in good agreement with the previously reported value (Gapeev et al., 2000). The possibility that the metal binds to the p_z orbital of the N rather than to the π-system leads to a structure which is not a stationary point (Jarvis et al., 2003). A further possibility of binding is the Ni^+ attachment to pyrrolenine structures in which the N-hydrogen is shifted to one of the carbons. However, also in this case the most stable structures were found to be at least 8.4 kJ/mol less stable than the corresponding π-complex. For the $Ni^+(pyrrole)_2$ dimers a

C_{2h} and a C_2 symmetry structures were found as local minima of the PES, the latter (see Figure 7) being 1.3 kJ/mol more stable than the former. Hence, the $Ni^+(pyrrole)_2$ cluster exhibits a ^2B ground state. Also for the dimers new available calculations (Jarvis et al., 2003) found the Ni^+ ion to lie 0.08 Å inside the perimeter of the ring, instead of 0.06 Å outside it (Gapeev et al., 2000).

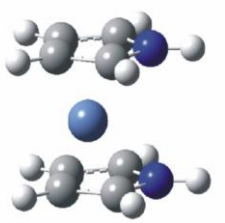

FIGURE 7. Structure of the $Ni^+(pyrrole)_2$ cluster obtained by means of B3LYP calculations (Gapeev et al., 2000)

Although the measured BDEs for Fe^+- and Co^+-pyrrole complexes (Gapeev et al., 2000) are rather similar to those obtained for the corresponding benzene complexes (Meyer et al., 1995), for Ni^+ the binding to pyrrole is predicted to be about 12 kJ/mol larger than that to benzene. This result is somewhat unexpected and also much higher than that obtained from the aforementioned DFT calculations, and may indicate (Gapeev et al., 2000) that these ions present a different structure, what needs further investigation. Also for the dimers the results obtained in these RA experiments are clearly in contrast with those reported for benzene dimers (Meyer et al., 1995). In the first place, for benzene complexes a steady decrease in the binding energy was observed in going from Cr^+ to Ni^+, whereas for pyrrole ligands there is a sharp increase in going from Mn^+ to Ni^+, with the result that while the BDE for the second benzene ligand in Ni^+ complexes is 146 kJ/mol, for pyrrole this value becomes 183 kJ/mol. Certainly, these dissimilarities between benzene and pyrrole when interacting with Ni^+ call for further investigations.

The interaction in $Ni^+(butadiene)_n$ (n = 1, 2) was theoretically investigated (Kandalam et al., 2004) by means of the BPW91 DFT method. Only three equilibrium structures were

found to be stable for the monomer, the ground state being a η^4-cis structure (see Figure 8). For $Ni^+(butadiene)_2$ the ground state corresponds to a sandwich-type arrangement in which Ni^+ interacts with two *cis*-isomers of butadiene, with the bottom butadiene rotated with respect to the top one (see Figure 8). The calculated BDEs for both the monomer and the dimer are much larger than those measured for benzene, or for other unsaturated systems such as pyrrole, or ethylene although, similarly to what was found for these ligands, the second BDE is significantly lower than the first one. Its experimental IRMPD spectrum was reported by (Surya et al., 1997), but no information on the bonding was provided.

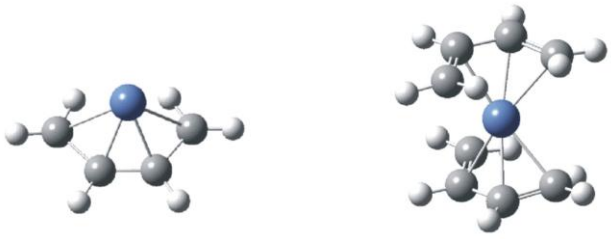

FIGURE 8. Optimized geometries of $Ni^+(butadiene)$ and $Ni^+(butadiene)_2$ clusters taken from (Kandalam et al., 2004)

Nickel cyanide ions $[Ni_n(CN)_{n-1}]^+$ (n = 1-3) have been generated in the gas phase by laser ablation of anhydrous $Ni(CN)_2$ at 1064 nm (Dance et al., 2002). When 532 nm radiation was used, the $[Ni_4(CN)_3]^+$ ion was observed but with a relative abundance of less than 1%. In the same experiments the $[Ni_n(CN)_{n+1}]^-$ (n = 1-3) were also produced and all of them investigated using Fourier Transform Ion Cyclotron Resonance (FT-ICR) mass spectrometry. Although no information about sequential BDEs was provided, the DFT calculations carried out indicate that $[Ni(CN)_2]^-$ anions exhibit a near-linear structure in which the metal is preferentially bound to the carbon atom of the cyanide. $[Ni(CN)_3]^-$, $[Ni_2(CN)_3]^-$ and $[Ni_3(CN)_4]^-$ exhibit, as the most stable

configuration, a nontrigonal planar (C_{2v}), a linear and a double-bridge arrangement, respectively (See scheme 4).

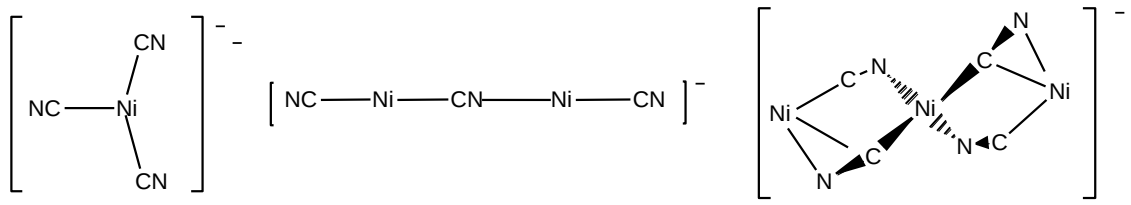

$[Ni(CN)_3]^-$ $[Ni_2(CN)_3]^-$ $[Ni_3(CN)_4]^-$

Scheme 4

Two different papers have been published devoted to the study of $Ni^+(CO_2)_n$ clusters (Walker et al., 2003; Walker et al., 2004). These clusters are produced by laser vaporization, then mass selected and studied with infrared photodissociation near the asymmetric stretch resonance in the CO_2 molecule. Although no BDEs could be measured some interesting information about the coordination within these clusters has been obtained. Dissociation was inefficient for clusters with $n \leq 3$, improved somewhat for $n = 4$ and increased dramatically for $n \geq 5$. This was taken as a first indication (Walker et al., 2003) that all clusters with $n \leq 4$ are more strongly bound than larger clusters, what suggests that the coordination of CO_2 around Ni^+ is complete with four ligands, as it has been found for the case of acetylene discussed above. Furthermore, all fragmentations of clusters with $n \geq 5$ terminated at a clusters size of n = 4, what confirmed that the binding energies of the clusters with $n = 4$ are significantly greater than those for larger clusters. Also consistently, clusters beyond this critical size exhibit in their infrared spectra bands at the free CO_2 resonance, indicating the existence of external ligands. The wavelength photodissociation spectra have blue shifted bands that indicate a linear Ni^+-OCO arrangement within the clusters.

Similar experimental techniques carried out in the O-H stretching region applied to the study of $Ni^+(H_2O)_n$ (n = 1-25) clusters (Walters et al., 2005a) showed that in the smallest clusters ($n \leq 4$), the water molecules are coordinated directly to Ni^+. However, for clusters with n = 4 evidences for hydrogen bonding were found, in agreement with B3LYP/6-311+G** calculations, which predict a C_{2v} $Ni^+(H_2O)$ complex with a $^2B_2$ ground state, while the dimer $Ni^+(H_2O)_2$ presents a C_2 ^2B ground state. Only one stable isomer was also found for n = 3, where all three water molecules are attached directly to Ni^+ in a C_{2v} arrangement (see Figure 9). For n = 4, two different arrangements were found to be stable. In one of them the four ligands are directly bonded to Ni^+ in a nearly square planar arrangement, whereas the second local minimum corresponds to 3+1 species, in which the external molecule behaves as a hydrogen bond acceptor (see Figure 9). The characteristics of the infrared spectrum provided good evidences for the presence of this 3+1 structure, even though calculations predict it to be slightly less stable than the four coordinated one. The situation for n = 5 is more complex. Two isomeric structures, 3 + 2 and 4 + 1, were located as local minima of the PES. In the 4 +1 structure the external molecule behaves as a double acceptor bridging two inner-sphere molecules (see Figure 9). In the two different 3 + 2 isomers located the two external water molecules behave as HB acceptors from two separate inner-shell molecules (C_1) or from the same inner-shell molecule (C_{2v}). The different bands observed in the infrared spectra seemed to indicate that both the 4+1 and the 3 + 2(C_1) isomers are present. From these calculations it was possible to estimate the sequential BDEs that are summarized in Table 3, which are not in very good agreement with the available experimental information. Only for the n = 1 complex the calculated BDE is close to two experimental values (see Table 3) but underestimates significantly the most recent one. Similarly to what has been experimentally found for H_2, CH_4 and NH_3 the

calculated BDE for n = 2 is significantly greater than that for n = 1, again in disagreement with the available experimental information which predicts a rather small increase (4 kJ/mol) (Marinelli & Squires, 1989), or a sizable decrease (14 kJ/mol) (Dalleska et al., 1994).

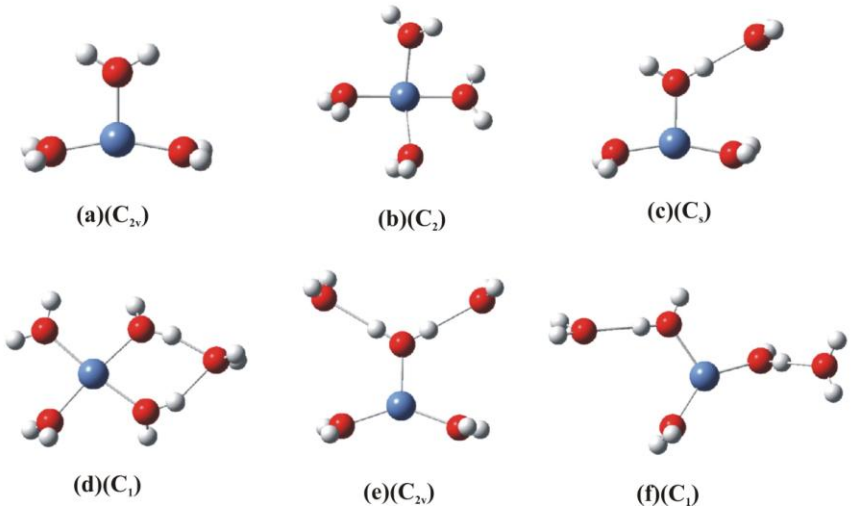

FIGURE 9. B3LYP optimized geometry for $Ni^+(H_2O)_3$ cluster (a), $Ni^+(H_2O)_4$ clusters (b) and (c) and $Ni^+(H_2O)_5$ clusters (d), (e) and (f) as reported by (Walters et al., 2005a).

The infrared spectra of $Ni^+(H_2O)_n$ clusters present strong similarities to those observed for protonated water clusters, although for clusters in the size range near n = 20, Ni^+ systems do not attain high symmetry structures like those found for protonated water clusters.

TABLE 3. Calculated sequential BDEs (kJ/mol) for $Ni^+(H_2O)_n$ (n = 1-5) clusters

Cluster	Structure	BDE
Ni^+-H_2O	$^2B_2$ (C_{2v})	163 (166[a]; 153[b]; 184 ± 3[c])
$Ni^+(H_2O)$-H_2O	^2B (C_s)	198 (168 ± 8[c] ; 170[a])
$Ni^+(H_2O)_2$-H_2O	$^2A_1$ (C_{2v})	92 (68 ± 6[c])
$Ni^+(H_2O)_3$-H_2O	^2B (C_2)	70 (52 ± 6[c])
$Ni^+(H_2O)_3$-H_2O	$^2A'$ (C_1) (3 + 1)	61
$Ni^+(H_2O)_4$-H_2O	^2A (C_1) (4 + 1)	67
$Ni^+(H_2O)_4$-H_2O	^2A (C_1) (3 + 2)	62
$Ni^+(H_2O)_4$-H_2O	$^2A_1$ (C_{2v}) (3 + 2)	51

[a](Marinelli & Squires, 1989). [b](Magnera et al., 1989). [c](Dalleska et al., 1994)

$Ni^+(H_2O)_6$ octahedral clusters have been also investigated by absorption spectroscopy (Landry-Hum et al., 2001) of the Tutton salt $(NH_4)_2Ni(SO_4)_2 \cdot 6H_2O$. Parallel CASPT2 calculations were used to obtain theoretical absorption spectra that were in good agreement with experimental data, and indicated that the two $^3T_{1g}$ excited states show strong configuration mixing.

The experimental techniques used for the study of benzene complexes have been also employed to obtain the sequential bond energies for $Ni^+(NH_3)_n$ (Walter & Armentrout, 1998), $Ni^+(CO)_n$, $Ni^+(N_2)$ (n = 1-4), and $Ni^+(NO)_n$ (n = 1-3) (Khan et al., 1995) clusters. Rate constants for reactions of Ni^+ with CO, O_2 (Jarvis et al., 2003), CO_2, D_2O, NH_3 and NO (Jarvis et al., 2004) obtained from Inductively Coupled Plasma/Selected-Ion Flow Tube (ICP/SIFT) tandem mass spectrometric techniques have been reported, but these experimental studies only provide qualitative information on the bonding.

Both the first and second ammonia BDEs to Ni^+ are relatively high (see Table 2). In general this has been explained as the result of two concurrent factors (Walter & Armentrout, 1998), on the one hand a strong electrostatic contribution to the bonding because the late first-row transition metal ions have small ionic radii, and on the other hand, the sd_σ hybridization already described when discussing the clusters between Ni^+ and H_2 (Kemper et al., 1998a). This latter effect would be consistent with the fact that the $Ni^+(NH_3)$-NH_3 BDE is greater than Ni^+-NH_3 BDE by 13 kJ/mol. Qualitatively, the situation is similar when the ligands are CO and N_2, although the absolute values of the BDEs are smaller, because the electrostatic interactions are smaller (small or null dipole moment) and N_2 is both a weak σ-donor and weak π-acceptor. Conversely, the BDE of the first NO molecule is rather similar to the BDE of the first NH_3 molecule, which has been considered (Khan et al., 1995) an indication that while CO and N_2 have a dative

interaction with Ni^+, NO can form a covalent bond with this metal ion, because both are doublets in their ground states. High-level *ab initio* calculations (Thomas et al., 1997) showed, two years later, that in the $^1\Sigma^+$ ground state Ni^+ binds NO in a linear structure by coupling its unpaired electron with the unpaired NO π^* electron. The fact that Ni^+NO has a shorter N-O distance relative to other metal complexes indicates that there is a large contribution to the bonding from Ni^0 and NO^+ (Thomas et al., 1997). This picture is ratified by the NBO analysis we have performed at the B3LYP/6-311+G(3df,2p) level, which indicates that the Ni^+-NO complex can be viewed as the interaction between Ni and NO^+ (isoelectronic with N_2) which exhibits a N≡O triple bond, which is reflected in the shortening of the NO bond distance in the Ni^+-NO complex (by 0.03 Å) with respect to the NO distance in the isolated molecule. This NO distance is however larger (by 0.06 Å) than that predicted for the NO^+ molecular ion, because there is a strong donation from the occupied *d* orbitals of Ni to the π^* antibonding MO of the NO moiety, followed by a back-donation from the N lone pair to the 4*s* empty orbital of the metal. Consistently, when an atoms in molecules (AIM) (Bader, 1990) analysis is carried out a bond critical point (bcp) between Ni and N is found, and the charge density at the bcp between N and O in the Ni^+-NO complex (0.647 a.u.) is smaller than in the NO^+ cations (0.745 a.u.).

In contrast to what has been found for ammonia, as well as for other ligands such as H_2 and CH_4 discussed above, the BDE of $Ni(NO)^+$-NO is significantly lower (by 105 kJ/mol) than the BDE of the singly coordinated complex (Khan et al., 1995). This behavior is also at variance with that of N_2 and CO for which the second BDE is equal or only slightly smaller (7 kJ/mol), respectively than the first one, or with respect to O_2 for which the computed theoretical value of the BDE of $(O_2)Ni^+$-O_2 is only 10 kJ/mol smaller than the BDE of the Ni^+-O_2 complex. For the particular case of CO, this

experimental gap is in nice agreement with recent calculated values (Jarvis et al., 2003) obtained at the B3LYP level and that correct previous theoretical estimates (Barnes et al., 1990) by more than 42 kJ/mol. In this study both, the $Ni^{+}CO$ and the $Ni^{+}(CO)_2$ complexes, are predicted to be linear in their ground states, the Ni^{+}-C interaction being thermodynamically favored over the Ni^{+}-O interaction. As shown in Figure 10, the addition of a second CO molecule leads to a weakening of the Ni-C bond that lengthens by 0.05 Å and the calculated binding energy decreases from 185 kJ/mol to 171.5 kJ/mol.

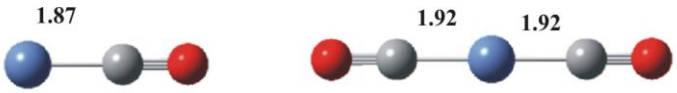

FIGURE 10. Optimized geometries of $Ni^{+}(CO)$ and $Ni^{+}(CO)_2$ complexes reported by (Jarvis et al., 2003). Bond lengths are in Å

Quite interestingly, the Ni^{+}-O_2 complexes were found (Jarvis et al., 2003) to be bent, the angle between the O_2 molecule and the Ni-O bond being 126.8º and 127.5º for the monomer and the dimer, respectively (See Figure 11). This particular conformation was explained as the result of the depletion of charge density along the bond axis behind each O atom that renders the linear Ni^{+}-O_2 arrangement highly unlikely, while favors the interaction with the π-orbital.

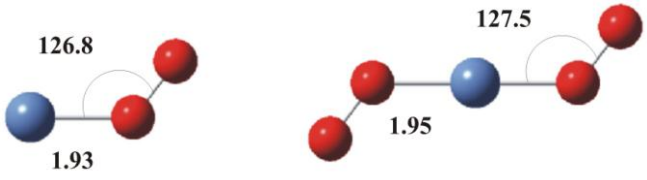

FIGURE 11. Optimized geometries of $Ni^{+}(O_2)$ and $Ni^{+}(O_2)_2$ complexes reported by (Jarvis et al., 2003). Bond lengths are in Å and bond angles in degrees.

To gain some insight on the peculiar behavior of Ni^+-NO complexes when a second NO molecule is added, we have carried out calculations at the B3LYP/6-311+G(3df,2p) level which indicate that, in contrast with the $Ni^+(CO)_2$ complex (Jarvis et al., 2003), the $Ni^+(NO)_2$ cluster is a $^2B_1$ bent structure in the ground state (see Figure 12), in agreement with previous theoretical calculations carried out with a smaller basis set (Zhou & Andrews, 2000). An interesting discussion on the type of orbital interactions that stabilized bent M^+L_2 configurations respect to the linear ones can be found in a review on the nature of the bonding in transition metal compounds (Frenking & Fröhlich, 2000).

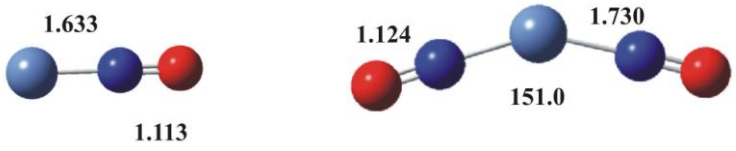

FIGURE 12. B3LYP/6-311+G(3df,2p) optimized geometry of the $^2B_1$ ground state of $Ni(NO)_2^+$ cluster. Bond lengths are in Å and bond angles in degrees.

In accordance with the experimental evidence the addition of the second NO molecule weakens the Ni-NO bonds that lengthen by 0.1 Å, while the charge density at the corresponding bcp decreases by 0.045 a.u. A NBO description envisages the $Ni^+(NO)_2$ cluster as the result of the interaction of the singlet Ni^+NO ion with the second NO molecule through charge donations from the nitrogen lone pair of the second NO molecule into the 4*s* orbital of Ni and into the Ni-N antibonding MO of the Ni^+-NO moiety, which is responsible for the observed weakening of this bond. However, these calculations should be taken with caution because they show a quite high spin contamination, with an expectation value for $S^2 = 1.00$, likely due to the fact that the $^4B_1$ state is only ca. 80 kJ/mol higher in energy.

There is another peculiarity of NO that deserves to be commented. As mentioned in previous sections of this review, as a general rule for triply and quadruply ligated systems there is typically a decrease in BDE relative to singly and doubly ligated counterparts, mainly due to an increase of the ligand-ligand repulsions, and because the alleviation of Pauli repulsion through the formation of sd_σ hybrids is effective for only two ligands on opposite sides of the metal. This is indeed observed for H_2, CH_4, NH_3, CO, N_2, but not for NO where the addition of a third ligand to the $Ni(NO)_2^+$ systems does not cause a decrease in bond energy, likely due to the fact that $Ni(NO)_3^+$ is an 18-electron species (Khan et al., 1995).

As we have discussed in preceding sections, first and also second BDEs should vary following the trend $Co^+ > Ni^+ > Cu^+$, which is indeed the one observed for CO, NO, H_2, C_2H_4, and C_6H_6. However, this is not the case, neither for ammonia nor for N_2. For ammonia the first BDE follows the trend $Co^+ < Ni^+ \approx Cu^+$ while the second BDEs are rather similar for the three cations. For N_2 only the BDE of the Co^+-N_2 is known to the best of our knowledge, but this value is slightly smaller than that for Ni^+ (Freiser, 1996). Ni^+ exhibits also an anomalous behavior as far as the BDEs for the third and fourth ammonia ligands are concerned. As expected, the BDEs for the third and fourth ammonia molecules are 145 and 203 kJ/mol smaller, respectively than the BDE of the first one. What it is surprising, however, is the BDE for the third ammonia molecule in $Ni(NH_3)_2^+$-NH_3 complex to be 20-50 kJ/mol greater than for the other late first-row transition metals. An explanation of this enhanced BDE requires a careful and systematic study of the bonding in these clusters that has not been carried out so far.

H. Ni^+ mixed dimers and trimers

Particular attention deserve the clusters in which Ni^+ is bound to two or more different ligands. Paradigmatic examples are those complexes in which one of the ligands is cyclopentadienyl (Wong et al., 1997a) or pyrrole (Jarvis et al., 2003; Jarvis et al., 2004). Mixed clusters involving cyclopentadienyl(Cp) and pyridine and its mono-, bi- and tri-substituted methyl derivatives have been investigated by the kinetic method. These clusters were generated by electron ionization of nickelocene, which produces Ni^+ and $CpNi^+$ ion currents that are allowed to react with a mixture of two pyridines (Py). In this way it is possible to compare relative magnitudes for the $CpNi^+$ cation affinities using the quantity $\ln\{[Py_1(CpNi^+)]/[Py(CpNi^+)]\}$, which is directly proportional to the $CpNi^+$ affinity difference. As it was found when dealing with the bare metal cation, the $CpNi^+$ affinities are linearly correlated with the corresponding proton affinities of *meta*- and *para*-substituted pyridines. Nevertheless, the slope of the correlation for $CpNi^+$ affinities (0.49) is larger than that obtained for Ni^+ (0.41) affinities, indicating that the bonding is weaker in the former. As a matter of fact fragmentations of MePy-($NiCp^+$)-Py dimers occur much more readily than those of MePy-Ni^+-Py, indicating that the $CpNi^+$-Py bond is weaker than the Ni^+-Py bond, very likely due to steric repulsions between the bulky Cp group and the pyridines. It is worth noting that these steric interactions are larger for Ni^+ than for the Co^+ and Fe^+, presumably due to a higher occupancy of the 3*d* orbitals.

Mixed clusters involving pyrrole with other ligands such as O_2, CO (Jarvis et al., 2003), CO_2, D_2O, NH_3 and NO (Jarvis et al., 2004) were investigated by means of ICP/SIFT tandem mass spectrometry, and for the particular case of O_2 and CO containing clusters a parallel theoretical study using the B3LYP method was also carried out.

It was found that Ni^+(pyrrole) ligates only one molecule of O_2 (Jarvis et al., 2003), CO_2, D_2O and NO (Jarvis et al., 2004) while under the same experimental conditions it

ligates up to two molecules of CO (Jarvis et al., 2003) or NH_3 (Jarvis et al., 2004). No ligand-switching reactions:

$$Ni^+(pyrrole) + L \rightarrow Ni^+L + pyrrole \quad L = O_2, CO \qquad (10)$$

were observed for any of these ligands, what implies that O_2, CO, CO_2, D_2O, NH_3 and NO ligate less strongly to Ni^+ than pyrrole, The B3LYP calculated structures for the Ni^+(pyrrole)(CO) clusters indicate that the addition of a CO ligand skew the symmetry of the Ni^+-pyrrole complex by shifting the metal ion from the midline of the pyrrole molecule, but when a second ligand is added to the system the symmetry is restored. These effects are however negligible when the ligand is O_2 (See Figure 13).

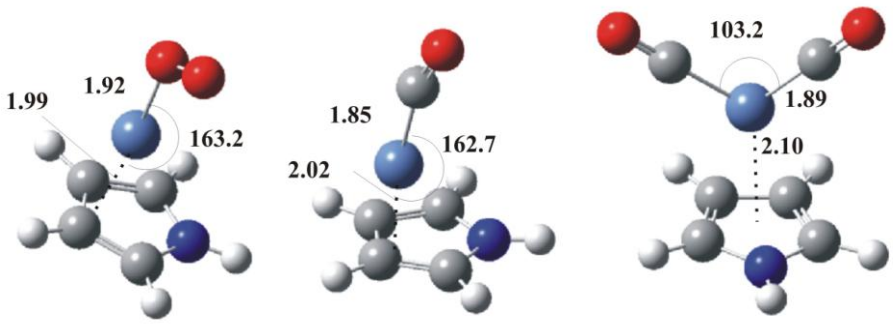

FIGURE 13. Optimized geometries of Ni^+(pyrrole)(O_2), Ni^+(pyrrole)(CO) and Ni^+(pyrrole)$(CO)_2$ complexes reported by (Jarvis et al., 2003). Bond lengths are in Å and bond angles in degrees.

Addition of a single molecule of CO, NH_3 and NO was the only reaction observed with $Ni^+(pyrrole)_2$ clusters, which are unreactive with respect to O_2, D_2O and CO_2. The failure to observe ligand-switching reactions for CO and NH_3 suggest that $D_0(Ni^+(pyrrole)\text{-}L) < D_0(Ni^+(pyrrole)\text{-}pyrrole)$ (L = CO, NH_3). Conversely, displacement of a pyrrole ligand by a NO molecule has been observed when $Ni^+(pyrrole)_2$ interacts with nitrogen monoxide, suggesting that $D_0(Ni^+(pyrrole)\text{-}NO) > D_0(Ni^+(pyrrole)\text{-}pyrrole)$. For the particular case of NH_3-containing complexes, it has

been proposed that the formation of $Ni^+(pyrrole)(NH_3)_2$ clusters can proceed by addition of a second molecule of NH_3 to the $Ni^+(pyrrole)(NH_3)$ complex, or by the switching reaction of $Ni^+(pyrrole)_2(NH_3)$ with ammonia.

Mixed $Ni^+O_2(CO_2)_n$ clusters have been also investigated (Walker et al., 2003; Walker et al., 2004) using the same photodissociation techniques mentioned above when discussing $Ni^+(CO_2)_n$ clusters. These mixed clusters exhibit a similar behavior than $Ni^+(CO_2)_n$ species, in the sense that dissociation is inefficient for clusters with $n \leq 2$, so that assuming that the two oxygen atoms are individually bounded to nickel, the total coordination around nickel would be four. The infrared spectra measured for the critical size cluster suggest that it has C_{2v} symmetry with a cyclic NiO_2^+ moiety.

The IRMPD of $Ni^+(C_2H_2)(C_2H_4)$ mixed clusters showed them to be photoinactive under the experimental conditions (Surya et al., 1997). An estimate for the BDEs of Ni^+-C_2H_2 and Ni^+-C_2H_4 of 188 ± 8 kJ/mol and 184 ± 8 kJ/mol, respectively was provided assuming that Ni^+ binding energies are about 8 kJ/mol higher than Co^+ binding energies.

Finally, it must be mentioned that some mixed clusters are produced by complexation of Ni^{2+} when electrospray mass spectrometry techniques are used. This is the case of mixed complexes involving ethylenediamine and Cl (Tsierkezos et al., 2004), dimethylformamide and Cl, or Br (Tsierkezos et al., 2003), L-histidine and CO_2, or different aminoacids (Zhang et al., 2001a). However in these articles no information about the bonding is provided and only reactivity patterns are discussed (see section V.D).

III. BONDING IN Ni^+ CONTAINING SYSTEMS

The basic ideas regarding the bonding in complexes involving transition metal cations can be extracted from a previous review (Frenking & Fröhlich, 2000), that can be nicely complemented with the discussions on the bonding between transition metals and carbenes (Frenking et al., 2005) and with another recent analysis of bonding and bonding perturbations in ion-molecule interactions (Corral et al., 2004b).

A. General features and illustrative examples

As mentioned in the introduction, it is well established that bonding involving transition metal cations cannot be understood by simply considering electrostatic interactions. The significant role of covalent components are reflected in binding energies that are systematically higher than those found for alkali or alkaline-earth metal cations, and because, quite often the structures of complexes involving transition metal monocations resemble closely those of the corresponding protonated species (Luna et al., 2000b; Luna et al., 2002), where covalent interactions are a dominant ingredient of the bonding. As a consequence, also good linear correlations between transition metal ion affinities and proton affinities are often found. The presence of covalent forces in the bonding is normally associated to four different factors. a) a charge donation from occupied MOs of the ligand into the 4s empty orbital of the metal ion (with some minor participation of 3dσ orbital if available, as it is the case in Ni^+); b) a backdonation from the occupied 3d orbitals of the metal ion into some antibonding empty orbital of the ligand; c) a hybridization between the $3d_z^2$ and the 4s orbitals in order to reduce Pauli repulsion along the axes in which the metal approach to the ligand; d) in some specific cases, mainly for singly ligated systems, the polarization of 4s orbitals by mixing with the 4p orbitals that, although higher in energy, can be used to polarize the electron density to

the opposite side of the metal, what contributes to decrease the repulsion between the metal and the ligand.

For the particular case of Ni^+ complexes the three factors a), b) and c) are commonly present. Ni^+ has a d^9 configuration and therefore a $^2D_{5/2}$ ground state. This implies that the 4*s* orbital as well as one of the 3*d* orbitals are empty and propitiate both the donation from occupied orbitals of the ligands and the $sd\sigma$ hybridization. An almost general characteristic of Ni^+ complexes is that a great majority are low-spin systems, in which the metal retains the original d^9 configuration. NiO^+ and NiS^+ complexes are clear exceptions, since as we have indicated earlier they are quartets in their ground state. Another general characteristic of Ni^+ containing systems is the existence of several states very close in energy, what sometimes hinders the unambiguous assignment of the ground state, and very often is the origin of dramatic failures of DFT or single-reference *ab initio* calculations.

The interaction of Ni^+ with the simplest ligand, H_2, clearly illustrates the existence of factors a), b) and c) mentioned above. In this interaction electron donation from the H_2 σ orbital into the 4*s* of the metal ion (with a very minor contribution from the $3d_\sigma$ orbital) is followed by a back-donation from filled $3d\pi$ orbitals of the metal into the H_2 σ^* antibonding orbital. Simultaneously, a hybridization between the $3d_z^2$ and the 4*s* orbital may help to reduce on-axis repulsion. The first two mechanisms, which imply a decrease in the population of the H_2 bonding orbital and a concomitant increase of the population of the antibonding orbital, leads to a lengthening of the H-H distance in the complex with respect to that in the isolated molecule. Ni^+-H_2 complexes are also a paradigmatic example of systems that illustrates the existence of several states very closed in energy. Calculations carried out at the MP2 level (Kemper et al., 1998b) indicate that the $Ni^+(H_2)$ complex has C_{2v} symmetry with a $^2A_1$ ground state (see Figure

14). Importantly, the first three excited states $^2A_2$, $^2B_2$, and $^2B_1$ are only 5.9 kJ/mol 20 and 32 kJ/mol higher in energy, respectively. Similarly, for the $Ni^+(H_2)_2$ cluster the D_{2h} ground state (see Figure 14) is predicted to be only 3.3 kJ/mol more stable than the D_{2d} configuration, at the MP2 level.

Another example is provided by NiS^+ complex, which at the B3LYP/6-311+G* level of theory (Husband et al., 2001) presents two near degenerate states, $^4\Sigma$ and $^4\Delta$, or when dealing with Ni^+(pyrrole) and $Ni^+(pyrrole)_2$ complexes (Gapeev et al., 2000). For the former, as it was already discussed in previous sections, the energy gap between the C_s ^2A" ground state and the ^2A' is only 18 kJ/mol. For $Ni^+(pyrrole)_2$ the C_2 ^2A ground state lies only 1.2 kJ/mol below the ^2B_g in C_{2h} symmetry and 31.8 kJ/mol below the ^2A_g.

The optimized structure for $Ni^+(H_2)_3$ has D_{3h} symmetry with all atoms in the same plane. This configuration is stabilized through a "push-pull" effect, that enhances the back donations already seen in the smaller clusters and reduces at the same time the repulsive interaction of the H_2 σ orbitals with the 3*d* shell of Ni^+. The enhancement in the back-donation is reflected in a further elongation of the H-H bonds (see Figure 14).

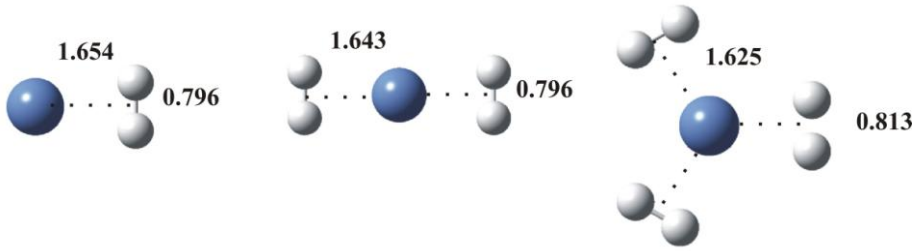

FIGURE 14. MP2 optimized geometries of $Ni^+(H_2)_n$ (n = 1-3) clusters reported by (Kemper et al., 1998b). Bond lengths are in Å and bond angles in degrees.

Some particular attention deserve also the clusters in which Ni^+ interacts with radicals such as OH, because the existence of an unpaired electron in both the metal cation and the ligand opens new bonding possibilities (Ricca & Bauschlicher, 1997). In Ni^+-OH

one possibility is the formation of a Ni-OH covalent bond to yield a singlet state if Ni^+ retains its d^9 configuration or a triplet state if Ni^+ behaves as a $3d^8 4s^1$ system. The second possibility is to have a dominant ionic interaction, in which the open shell on OH is high spin coupled with the Ni^+ open shell. In this case a $3d^9$ configuration would yield a triplet state and a $3d^8 4s^1$ would yield a quintet state. At the B3LYP level, the ground state was found to be (Ricca & Bauschlicher, 1997) a triplet state, with the singlet almost 167 kJ/mol higher in energy. An analysis of the bonding indicated that it arises from a mixture of $3d^9$ and $3d^8 4s^1$ configurations, as reflected in a population of the 3*d* orbitals lower than 9. The bonding in $Ni(OH)_2^+$ is very similar to that in $NiOH^+$. The ground state is a quartet that arises again from a mixture of $3d^9$ and $3d^8 4s^1$ configurations.

For $Ni^+(CH_4)$ complexes, which have a C_{2v} $^2A_2$ ground state, the primary covalent interactions (Zhang et al., 2001b) are rather similar to those described for H_2 complexes, that is, the donation from the a_1 symmetry orbital on CH_4 into the vacant 4*s* and into (very small) the singly occupied d_{xy} orbitals of Ni^+, which result in a small elongation of the C-H bond and in a red shifting of the corresponding stretching frequencies. For $Ni^+(CH_4)_2$ a D_{2h} $^2B_{1g}$ ground state is predicted. For $Ni^+(CH_4)_3$ two configurations almost degenerate in energy were found. In one of them the complex has a near T-shape structure, which corresponds to a C_{2v} $^2A_1$ state (see Figure 15), while the other is a trigonal C_{2v} $^2A_2$ state. For $Ni^+(CH_4)_4$ the B3LYP calculations predict a $^2B_{2g}$ ground state with D_{4h} symmetry.

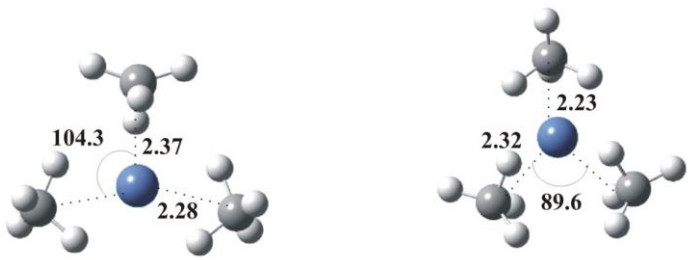

FIGURE 15. Optimized geometries of $Ni^+(CH_4)_3$ clusters reported by (Zhang et al., 2001b). Bond lengths are in Å and bond angles in degrees.

The interactions of Ni^+ with other alkanes such as propane involve similar donations, but the electron donation comes preferentially from C-H bonds of the terminal methyl groups. Accordingly, in the global minimum, Ni^+ bridges between these two groups (Yi et al., 1998; Corral et al., 2003c) (see Figure 16).

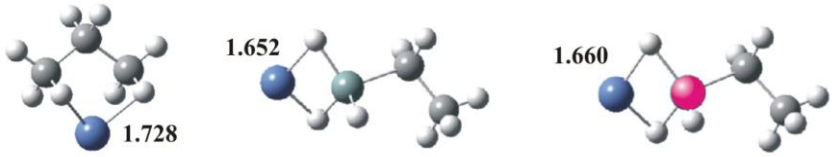

FIGURE 16. B3LYP/6-311G(d,p) optimized geometry for the Ni^+-propane, Ni^+-ethylsilane and Ni^+-ethylgermane complexes reported by (Corral et al., 2003c). Bond lengths are in Å

B. Agostic-type interactions

The interactions between transition metal cations and X-H bonds, when X is less electronegative than carbon, have been found to be particularly strong (Corral et al., 2003c; Corral et al., 2003a; Corral et al., 2003b; Corral et al., 2004a). This is indeed the case, as we have mentioned in preceding sections, for silanes and germanes. The fact that both Si and Ge are electropositive atoms results in a $X^{+\delta}$- $H^{-\delta}$ polarity of the XH bonds, which become better electron donors. On the other hand, the larger participation of the H atomic orbitals on the corresponding bonding molecular orbital facilitates the overlap with the *d* orbitals of the metal. The obvious consequence is an enhancement of both the electron donation from the σ_{XH} bonding MO into the 4*s* orbital of the metal, and the back donation from the occupied 3*d* orbitals of the metal into the σ_{XH^*} antibonding MO of the silane or germane. Both interactions are reflected in a much greater lengthening of the X-H (X = Si, Ge) bonds in ethylsilane and ethylgermane

(0.112 and 0.139 Å, respectively) than that observed in the propane (0.048 Å) upon Ni^+ association. This causes also significant dissimilarities between the most stable structures of Ni^+-alkanes and those found for the silicon and germanium containing analogues. While for Ni^+-propane, the metal cation bridges between the two terminal methyl groups, for both ethylsilane and ethylgermane, in the most stable Ni^+-complex, the metal cation interacts exclusively with the SiH_3 or the GeH_3 group (see Figure 16). These dissimilarities between carbon and silicon or germanium derivatives are even more significant for unsaturated systems. As we have already shown at the beginning of this review (see Figure 1) while Ni^+-propene is a conventional π-complex, the most stable structure for Si- and Ge-containing compounds corresponds to a non-conventional one in which the Ni^+ bridges between the C of the vinyl moiety and one of the hydrogens of the XH_3 (X = Si, Ge) group For the alkene, the interaction with Ni^+ implies exclusively donations and backdonations from the bonding and antibonding π orbitals, respectively, while the interaction with vinylsilane or vinylgermane involves also electron donations from the X-H σ bonding orbital and backdonations to the corresponding σ* antibonding orbital. These orbital interactions are clearly reflected in the molecular graph which shows the existence of a bond path between Ni^+ and one of the carbon atoms and between Ni^+ and one of the hydrogen atoms of the XH_3 (X = Si, Ge) group (See Figure 17).

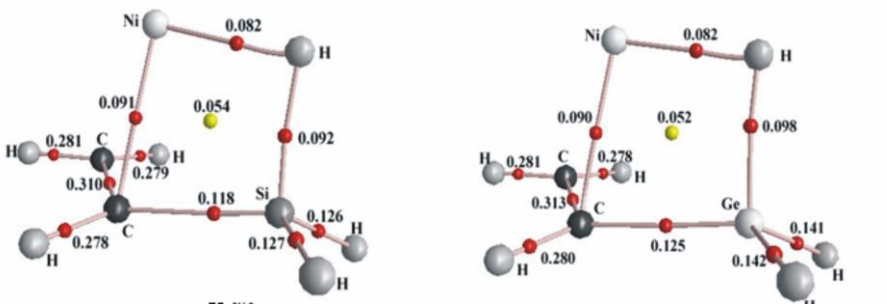

FIGURE 17. Molecular graphs of the most stable Ni^+ complexes of vinylsilane and vinylgermane reported by (Corral et al., 2003c) Red dots are bond critical points and yellow dots ring critical points. Electron densities are in a.u.

These non-conventional bonds have been named as agostic-type interactions (Corral et al., 2003c) since they are rather similar to those between neutral transition metals and C-H bonds which lead to unusual low field shifts in the ^{1}H-NMR spectrum (Trofimenko, 1967), C-H bond lengthening (Trofimenko, 1968), reduced C-H stretching frequencies (Trofimenko, 1968), and remarkably short metal-hydrogen distances (Cotton et al., 1974), and which have been named agostic bonds after (Brookhart & Green, 1983).

C. The performance of different theoretical models

Although a general overview on the use of computational techniques in the realm of mass spectrometry studies has been reported before (Alcamí et al., 2001) and another interesting review on the use of theoretical methods for the understanding of the structure and reactivity of gas-phase ions has been published recently (Mercero et al., 2005), we have considered it of interest to finish this section by making some comments on the performance of ab initio and DFT calculations to reproduce the thermochemistry of transition metal cations in general, and of Ni^+ in particular. We have already mentioned that one of the difficulties inherent to the theoretical treatment of Ni^+ containing complexes is the existence of different states close in energy. An added difficulty is the fact that for transition metal ions some times more than one solution is obtained in the Hartree-Fock (HF) calculations. This has been shown to occur already in very simple systems such as CuH^+ (Ghanty & Davidson, 2000); but the most dramatic consequence is that when more than one HF solution exist neither solution is a good representation of the wave function, and even high-correlated methods based on them become no reliable. Some of these solutions can be discarded “a priori” because they

present some instability (Luna et al., 2000a) and therefore obtaining the right orbitals to start with in the HF calculation becomes sometimes critical (Lynch & Truhlar, 2002). Quite interestingly, in many cases in which several HF solutions exist, only a unique solution is obtained when the density functional theory is used (Ghanty & Davidson, 2000). For example, in $NiOH^+$, there were two ^3A" states that differ by only 0.8 kJ/mol, which arose from the two ways in which three electrons can be put in the two orbitals of a" symmetry (Ricca & Bauschlicher, 1997). Since these orbitals are very different they lead to very different solutions when electron correlation is taken into account, and at the CCSD(T) level of theory the energy gap between them becomes 20.5 kJ/mol (Ricca & Bauschlicher, 1997). Similarly to the CuH^+ case mentioned above (Ghanty & Davidson, 2000), only one solution is found when the B3LYP approach is used. The situation is even worse when dealing with $Ni(OH)_2^+$ for which four different HF solutions within 10.5 kJ/mol are found, while again the B3LYP solution is unique, and may help to ensure that the ground state has been correctly found in the HF calculations. Some word of warning is, however, necessary when DFT methods are used. As indicated several times along this review, in Ni^+ complexes doublet and quartet states are sometimes very close in energy and high spin contamination in the corresponding unrestricted treatment cannot be avoided, that may render DFT calculations completely unreliable (Alcamí et al., 2000).

Some other pathological behaviors can be found when dealing with Ni^+-containing systems related to the slow convergency of the Moller-Plesset (MP) series on which several high-level ab initio models are based. It has been shown indeed (Luna et al., 2002) that already for the bare Ni^+ ion the MP series up to fifth order presents significant oscillations, and that these oscillations increase appreciably when the basis set includes diffuse components and high angular momentum polarization functions.

These oscillations are typically associated with systems which present a significant electron clustering (Cremer & He, 1996).

IV. Ni^{2+}-COMPLEXES

The number of studies involving multiply charged species in the gas phase, and in particular dications of transition metal ions has increased significantly in the last decade due to the availability of electrospray ionization (ESI) (Yamashita & Fenn, 1984) which permits the transfer of solvated ions from solution to the gas phase. ESI is indeed very important in trying to understand the solvation mechanisms at the molecular level involving the first solvation shells and has been used in combination with laser photofragment spectroscopy to investigate $Ni^{2+}(H_2O)_n$ (n = 4-7) clusters (Thompson et al., 2000). Although no information on the corresponding BDEs was obtained in these studies, it was possible to establish that the most abundant aqueous species, $Ni^{2+}(H_2O)_6$ dissociate by loss of either one or two water molecules. The same behavior was observed for the cluster containing seven ligands. In contrast, for the pentahydrate no dissociation was observed over the visible and near-UV, due to limited absorption by the chromophore. The minor $Ni^{2+}(H_2O)_4$ dissociates via charge reduction, producing $H_3O^+ + NiOH^+(H_2O)_2$.

The information on enthalpies of hydration of divalent ions is very scarce and refers essentially to water molecules in the second solvation shell. To the best of our knowledge the first experimental value on the enthalpy of hydration of a water molecule belonging to the first solvation shell was obtained by using blackbody infrared radiative dissociation (BIRD) on $Ni^{2+}(H_2O)_n$ (n = 6-8) clusters (Rodríguez-Cruz et al., 1998). For $Ni^{2+}(H_2O)_8$ the BDE (71 ± 3 kJ/mol) was slightly higher than the value measured using high-pressure mass spectrometry (HPMS) techniques (63 kJ/mol) (Blades et al., 1990).

The value obtained for n = 7 was rather similar (74 ± 3 kJ/mol), but that obtained for n = 6 was significantly higher (101 ± 4 kJ/mol), what is consistent with the well known fact that in aqueous-solution, first-row transition metal dications are surrounded by an inner solvation shell of six water molecules. It is worth noting that this value is between the two theoretical estimates published four years later (92 kJ/mol at the B3LYP/6-31G level and 116 kJ/mol at the B3LYP/6-311++G** level) (Ricca & Bauschlicher, 2002)

ESI-MS techniques have been also used to study the solvation of Ni^{2+} in water/dimethylformamide (DMF) mixtures (Tsierkezos et al., 2003). Although no BDEs could be measured, the absence of signals of hydrated nickel ions, even in water-rich mixtures, indicated that DMF-solvated nickel ions are more stable than water-solvated ions, what is in agreement with condensed-phase data (Gritzner & Horzenberger, 1992). The complexation of Ni^{2+} by ethylenediamine (en) in water/methanol solution of $NiCl_2$, both in the presence and absence of DMF was reported one year later (Tsierkezos et al., 2004). The formation of doubly charged $[Ni(en)_n]^{2+}$ with n = 2-5 solvated ions was detected. In complexes with a large number of n, ethylenediamine seems to form a second solvation shell through the formation of hydrogen bonds between the molecules in the first and second shell. Some mixed-ligand Ni^{2+} complexes such as $[Ni(en)_3(DMF)_n]^{2+}$ (n = 0-4), $[Ni(en)_2(DMF)_n]^{2+}$ (n = 0-2), $[Ni(en)_2(DMF)Cl]^{+}$ and $[Ni(en)_n(DMF)Cl_3]^{+}$ (n = 2-4) were generated from solutions of $NiCl_2$ which contain ethylenediamine and DMF.

Dissociation kinetics of Ni^{2+}-bound trimeric complexes of amino acids, generated by ESI, was used to distinguish the enantiomers of all nineteen chiral aminoacids (Zhang et al., 2001a). These complexes are formed from aqueous mixtures of $NiCl_2$, the analyte amino acid and a chiral reference L-amino acid. For the chirality analysis the most interesting clusters are the singly charged Ni(II)-bound amino acid dimers and trimers

formed by way of deprotonation of one of the constituent aminoacids, while the remaining aminoacids bind to Ni(II). The mass-selected trimeric clusters dissociate to form two dimeric clusters exclusively,

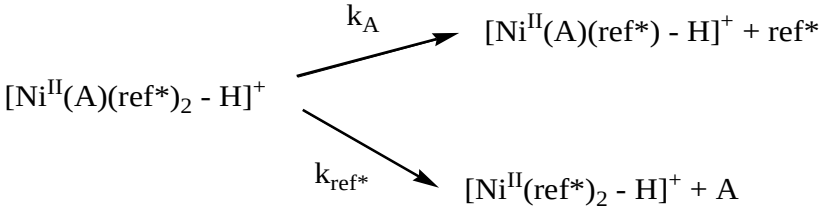

(11)

without other competitive or consecutive fragmentations. Then for a pair of enantiomers A_D and A_L, the chiral resolution factor is given by

$$R_{chiral} = R_D / R_L \quad (12)$$

where R_D and R_L are the corresponding branching ratios,

$$R_D = [[Ni^{II}(A_D)(ref^*)\text{-}H]/[[Ni^{II}(ref^*)_2\text{-}H]^+] \quad (13)$$

$$R_L = [[Ni^{II}(A_L)(ref^*)\text{-}H]/[[Ni^{II}(ref^*)_2\text{-}H]^+] \quad (14)$$

which are, in turn related to the difference between the formation enthalpies of the two dimeric clusters,

$$\Delta(\Delta Ni^{II}BDE) = \Delta Ni^{II}BDE(A_D)(ref^*) - \Delta Ni^{II}BDE(A_L)(ref^*) \quad (15)$$

indicating that chiral resolution of A_D and A_L is directly correlated with the relative stabilities of the two diastomeric clusters formed by the dissociation of the Ni(II)-bound trimeric clusters. The same approach has been adopted recently by Speranza and co-

workers in their study of diastereoselective fragmentation of α-aminoacidphosphonic acids/Ni(II) aggregates (Filippi et al., 2006).

Complexation with Ni^{2+} and other divalent transition metal cations generated by ESI, was used also as an alternative to protonation or deprotonation for the analysis of a series of flavonoids (Satterfield & Brodbelt, 2000), pharmaceutical compounds (Alvarez & Brodbelt, 1998) or aza-crown ether macrocycles (Williams et al., 2003).

Several papers have been devoted to the synthesis and characterization of Ni^{2+} complexes with a series of aminopyridine ligands range from tri- to heptadentate (Hartman et al., 2000; Vachet et al., 2001; Hartman et al., 2004). The coordination number of the various complexes was determined by means of gas-phase ion-molecule reactions that will be described in detail in section V.D. In all these studies it was found that Ni^{2+} forms 6-coordinated complexes both in solution and in the solid state. However, this is not always true as far as complexes in the gas phase are concerned. For example, hexadentate ligands such as 1,12-bis(2-pyridyl)-2,5,8,11-tetraazadodecane or 1,14-bis(2-pyridyl)-2,6,9,13-tetraazadodecane showed less than 6-coordination (Hartman et al., 2004). In the same study it was also concluded that the stability of Ni(**II**) complexes in the gas phase increases as more 5-membered chelate rings are replaced by 6-membered rings.

Several theoretical studies on Ni^{2+} complexes have been published during the period of time under scrutiny in this review. Using a constrained space orbital variation (CSOV) technique it has been shown that in $[Ni(H_2O)_n(imidazole)_m]^{2+}$ the bonding is mostly electrostatic. Accordingly, imidazole binds Ni^{2+} more strongly than water because its larger dipole moment and polarizability.

The geometry and electronic structure of $[Ni(CO)_n]^{2+}$ (n = 1-4) clusters were examined by using B3LYP and CCSD(T) approaches. $[Ni(CO)]^{2+}$ and $[Ni(CO)_2]^{2+}$ complexes

were found to be linear species with $C_{\infty v}$ and $D_{\infty h}$ symmetry, respectively. The $[Ni(CO)_3]^{2+}$ trimer was a T-shape C_{2v} structure and the tetramer $[Ni(CO)_4]^{2+}$ a square planar D_{4h} complex. Also in this case, it has been found that coulombic interactions are the dominant contributors for the bonding, although covalent interactions through σ-donation and π-back-donation are not negligible. The calculated sequential BDEs ((*n* = 1) 387 kJ/mol; (*n* = 2) 291 kJ/mol); (*n* = 3) 257 kJ/mol); (*n* = 4) 241 kJ/mol) show a steady decrease, that is more pronounced in going from the monomer to the dimer, in clear contrast with the behavior of the clusters involving the Ni^+ monocation (see Table 2), where the largest decrease is observed in going from the dimer to the trimer.

Theoretical studies on Ni^{2+} complexes with ethene (Alexander & Dines, 2004) and butadiene (Bögel et al., 1998) concluded that the high positive charge on the metal reduces significantly backdonation interactions from the metal to the neutral base, and this diminishes also the donation from the carbon atoms since its positive charge is not compensated through the backdonation. Consistently, the geometry distortions in both ethane and butadiene are smaller in Ni^{2+} than in Ni^0 complexes. $Ni^{2+}(C_2H_4)$ is predicted to be a C_s structure (Alexander & Dines, 2004). For Ni^{2+}-butadiene complexes, the η^4-structure, in which the metal interacts with the four carbon atoms was the only local minimum found, for both the *cis* and the *trans* isomers, the former being 22 kJ/mol more stable (Bögel et al., 1998) than the latter.

The interaction energies of functional groups representing the side chains of amino acid residues with Ni^{2+} were calculated at the B3LYP level of theory (Rulísek & Havlas, 2000) in order to investigate the specific coordination arrangement of ligands, that turn out to be octahedral. Also the different affinity of Ni^{2+} for a particular donor atom or ligand was analyzed, as well as the optimum size of the metal-binding site.

Finally, two other theoretical papers dealing with the stability of $Ni^{2+}(H_2O)$ (El-Nahas, 2001) and Ni_2^{2+} (Pis Diez & Alonso, 2000) should be mentioned.

V. UNI- AND BIMOLECULAR REACTIVITY OF BARE OR LIGATED NI(I) AND N(II) IONS

Notably thanks to the advent of the electrospray ionization, the gas-phase ion chemistry of nickel has been extensively studied during this last decade. Part of the interest in the gas-phase chemistry of metal ions arises from the fact that a detailed description of the reactivity of bare or ligated transition-metal ions can give precious insights on the mechanisms occurring in the condensed phase. As already mentioned in the introduction, two particular fields have been the subject of numerous publications. This first one concerns the activation of chemical bonds within hydrocarbons. The basic understanding of metal/hydrocarbons interactions is indeed of fundamental importance as it may give valuable insight into the possibility of catalytic reactions. The second one deals with the interaction of Ni(I) and Ni(II) species with molecules of biological interest, because transition metals play a role in many biological processes. This section is divided in four subtopics, followed by several concluding remarks. The first one summarizes the extensive work published during the last ten years about the reactivity of cationized nickel with hydrocarbons. The second one reports the results obtained when nickel was put in presence of small polyatomic molecules (up to four atoms). Reactions observed with molecules of biological interest (mainly aminoacids and saccharides) are discussed in a third subtopic. Finally, systems that could not be classified in the three first subtopics are gathered in the last section.

A. Reactivity towards hydrocarbons (alkanes, alkenes, alkynes and aromatics)

The transition-metal-mediated functionalization of methane constitutes an important topic of research stimulated by both the challenging inertness of this molecule and the economic interest. Mechanistic details of the activation process can be assessed by studies of mass-selected metal ions in the gas phase and not surprisingly, methane activation by bare transition-metal ions M^+ has been the subject of several studies (Weisshaar, 1993; Schwarz & Schröder, 2000). In the gas phase, the activation of methane by atomic platinum ions is among the best studied reactions of this type. It has been shown that the Pt^+ ion is capable of dehydrogenating methane at thermal energies to yield the methylidene complex (Irikura & Beauchamp, 1991). To further appreciate the differences between the reactions of Pt^+ and its lighter congener Ni^+, Armentrout and co-workers reinvestigated more thoroughly the reaction of methane with atomic Ni^+ ions using a guided ion beam tandem mass spectrometer (GIBMS) (Liu et al., 2005). In addition to the reaction of Ni^+ with CH_4 or CD_4 previously investigated, they also considered the reverse reactions $NiCH_2^+ + H_2$ and D_2, and performed CID studies on $NiCH_2^+$ and $NiCH_4^+$. They also described the potential energy surfaces involved, including full characterization of all products, intermediates and transition states on both doublet and quartet spin surfaces.

Reactions of Ni^+ with methane yielded the following products :

$$Ni^+ + CH_4 \longrightarrow \begin{cases} NiH^+ + CH_3 \\ NiC^+ + 2\,H_2 \\ NiCH^+ + H_2 + H \\ NiCH_2^+ + H_2 \\ NiCH_3^+ + H \end{cases} \qquad (16)$$

The dominant reaction at all energies is formation of NiH^+, while an energy threshold of near 2.1-2.2 eV was found for formation of $NiCH_2^+$ (dehydrogenation). The thermodynamical threshold for this process being 1.54±0.04 eV, indicates that there is a barrier to this reaction of 0.58 eV in excess of the endothermicity. The mechanism proposed is given in Figure 18.

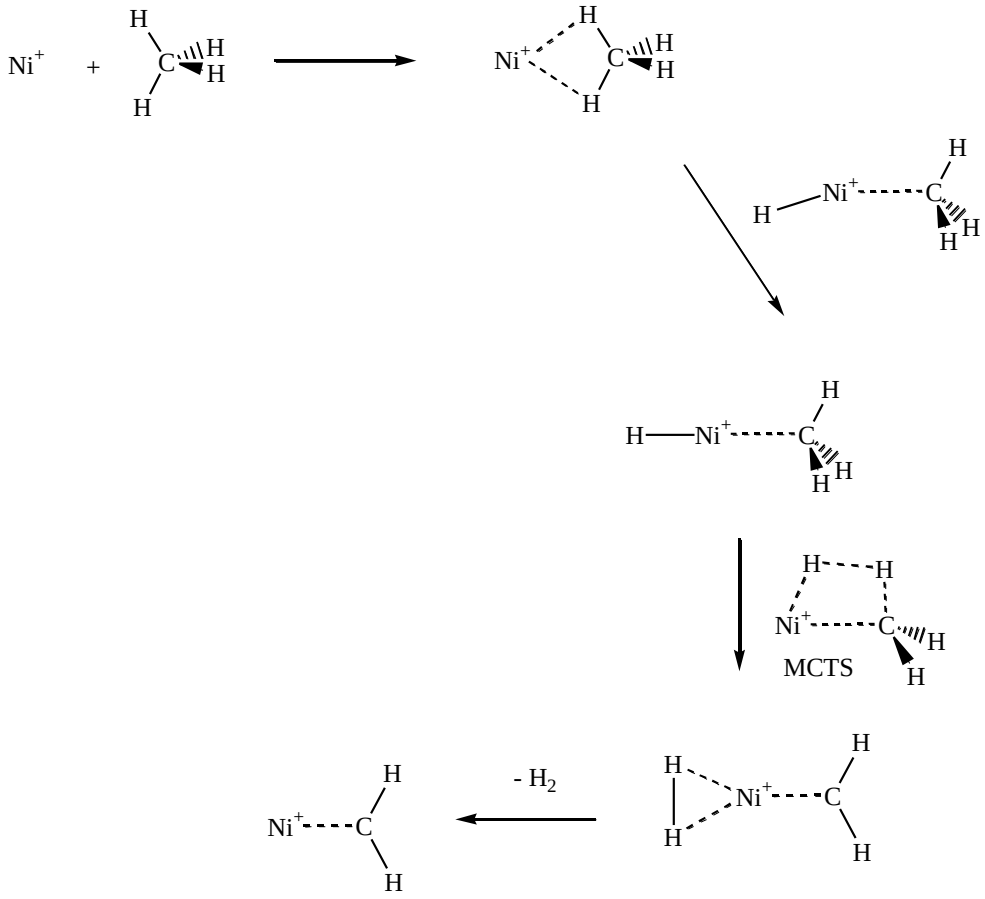

FIGURE 18. Mechanism associated with the formation of the nickel/methylidene complex

The initial interaction of Ni^+ and CH_4 is attractive because of a long-range ion-induced dipole interaction. Therefore the $Ni(CH_4)^+$ lies in a potential well and is the global minimum on both surfaces. The calculations clearly identified the $Ni(CH_4)^+$ species as a simple electrostatic adduct between Ni^+ and CH_4. After formation of the encounter

complex, the activation process starts by an oxidative addition mechanism in which Ni^+ inserts into a C-H bond to form the $H\text{-}Ni^+\text{-}CH_3$ intermediate. Once this intermediate is formed, all subsequent rearrangements and formation of all products can evolve along the doublet surface. The $H\text{-}Ni^+\text{-}CH_3$ species then evolves into the $(H_2)Ni^+CH_2$ intermediate by a transition state that can be viewed as a four-centered TS, consistent with the multi-center transition states (MCTS) proposed for reactions of hydrocarbons with first-row transition metal ions (Holthausen et al., 1996; Holthausen & Koch, 1996b; Holthausen & Koch, 1996a). This TS is different from that calculated with Pt^+ ion and corresponds to an α-shift to form a dihydride carbene intermediate $(H)_2Pt(CH_2)^+$. The MCTS is 0.46 eV above the $NiCH_2^+ + H_2$ products. This is therefore consistent with the threshold observed experimentally for the dehydrogenation process. The intermediate $(H_2)NiCH_2^+$ then easily loses the dihydrogen ligand. The H-H bond distance was found close to that of free H_2. This clearly suggests that this last step can occur with no barrier. The authors also noticed that the energy of the MCTS was close to the energy of the $NiH^{+\cdots}CH_3$ and $NiCH_3^+ + H$ products. These are kinetically more favorable as they involve only simple bond cleavage from the common $H\text{-}Ni^+\text{-}CH_3$ intermediate. Thus, the cross section for dehydrogenation never becomes large. This study showed that the efficiency of the dehydrogenation process differs dramatically between Ni^+ and Pt^+. For Ni^+, the reaction is endothermic while the analogous reaction for Pt^+ is very efficient and occurs with no barrier. Moreover, platinum forms much stronger bonds with H and CH_x than nickel, and the multiply bonding ligands C, CH and CH_2 are particularly strongly bound to Pt^+ compared to Ni^+. The authors interpreted these differences in term of sd hybridization and relativistic effects. For Pt^+, because of relativistic effects, sd-hybridization, which is required to form multiple bonds, is efficient and energetically accessible. Formation of multiple bonds helps to explain the

large difference in thermochemistry. This sd-hybridization leads to stabilization of the various intermediates and transition state along the dehydrogenation pathway for Pt^+, enabling this reaction to occur efficiently at room temperature. In the Nickel (and Pd) system, the difficulty in forming multiple bonds leads to an unstable $(H)_2Ni^+CH_2$, thus the reaction has to proceed through a four center TS (MCTS), which has an energy in excess of the endothermicity for dehydrogenation. The reactions of bare Fe^+, Co^+ and Ni^+ with CH_4 have been reported to be exothermic (Armentrout & Beauchamp, 1989; Eller & Schwarz, 1991), but the ion beam experiments suggest a threshold indicating a barrier to reaction. Comparison between these three metal ions has emphasized the importance of the effect of the electronic state and spin state upon the metal ion reactivity.

Recently, Ekeberg and Uggerud have studied the reactions between ethane and $Ni(Cp)^+$ ions (Cp=cyclopentadienyl) (Ekeberg et al., 1999). Experiments were carried out in a dual-cell Fourier transform ion cyclotron resonance mass spectrometer. Reactivity with $Fe(Cp)^+$ and $Co(Cp)^+$ has been also considered. After 0.2 second of reaction time, an ion appeared according to the following dehydrogenation reaction :

$$Ni(Cp)^+ + C_2H_6 \longrightarrow (Cp)Ni(C_2H_4)^+ + H_2 \qquad (17)$$

With higher reactant pressure and longer reaction times the $NiCp^+$ was totally consumed, suggesting that the observed chemistry was characteristic of ground state species and not just of excited states formed during the ionization process. A parallel reaction is observed for $Co(Cp)^+$, while this reaction does not occur with $Fe(Cp)^+$. There is also a substantial difference in reaction rates. (k_{Fe}:k_{Co}:k_{Ni} = <0.01:1.00:0.40). To understand these differences, the authors examined the electronic structures for the

series $M(Cp)^+$. $Ni(Cp)^+$ has 14 valence electrons and therefore an open shell structure. Occupation of antibonding orbitals weakens the metal-ligand interaction and the molecule will be more open for reaction. The metal d orbitals are more weakly perturbed by the presence of the ligand, and a high-spin configuration is expected. The resulting LUMO is 4s in its character and available for ethane dehydrogenation. Consequently, the authors suggested that $Co(Cp)^+$ and $Ni(Cp)^+$ with their a_1 predominantly metal 4s LUMOS could react by an "oxidative addition mechanism" comparable to those commonly proposed for M^+ + alkane reactions and known to be facilitated by a metal LUMO with 4s character.

The oxidative addition mechanism invoked initial, rate limiting (high activation barriers) C-H or C-C bond insertions by the metallic center , followed by facile β-H or β-alkyl migration to the metal atom to form stable intermediates of the form $M^+(H)_2$-(alkene) or $M^+(H)(R)$(alkene), and subsequent elimination of H_2 or of a smaller alkane RH (Hanratty et al., 1988; van Koppen et al., 1991; van Koppen et al., 1994; Eller & Schwarz, 1991; Armentrout & Beauchamp, 1989).

For the $Fe(Cp)^+$ complex, the 12 valence electrons of the complex fill all the bonding MOs, forming a stable closed shell. The LUMO has metal d and carbon 2p character, which is not particularly conductive to oxidative addition of C-H bonds to the metal. Accordingly, no reaction is observed experimentally.

A particularly well-studied set of reactions involves the dehydrogenation and demethanation of propane in collisions with the late-3d series cations Fe^+, Co^+ and Ni^+. A series of studies employing various experimental setups (Armentrout & Beauchamp, 1981a; Halle et al., 1982a; Schultz & Armentrout, 1991; van Koppen et al., 1994; Haynes et al., 1996) (Tonkyn et al., 1988) (Jacobson & Freiser, 1983b; Jacobson & Freiser, 1983a) (van Koppen et al., 1990; van Koppen et al., 1991; van Koppen et al.,

1994), have been aimed at determining the energetics of the different reaction steps, the nature of important pathways to H_2 and CH_4 elimination, and the effects of kinetic energy, initial M^+ electron configuration and spin. It is likely that initial insertion of M^+ into a C-H bond leads to H_2 elimination, but it was still not certain whether CH_4 elimination occurs via initial C-H or C-C bond insertion. The reaction of the ground state Ni^+ ($^2D_{5/2}$) with propane at collision energies of formally 0.01 eV and 0.21 eV under carefully controlled single-collision cross-beam conditions was studied (Noll et al., 1998). A beam of Ni^+ ions ($^2D_{5/2}$) was formed at a sharp zero of time by resonant two-photon ionization with a nanosecond dye laser pulse and crossed with a beam of propane. The resonant ionization process ensured that the Ni^+ reactant was formed exclusively in the lowest energy spin-orbit level. In contrast with many earlier studies of this reaction under more energetic conditions, they found that at 0.01 eV collision energy, ground state Ni^+ reacts with propane to form long-lived complexes almost exclusively. They also observed 3 % of CH_4 elimination product $Ni(C_2H_4)^+$ and roughly 1% of H_2 elimination product, $Ni(C_3H_6)^+$. At 0.21 eV collision energy, the same products were observed but with different branching ratios: 23±4 % $Ni(C_2H_4)^+$, 4±2 % of $Ni(C_3H_6)^+$ and 73± 4 % of $Ni(C_3H_8)^+$. Consequently, the apparent cross section for elimination products rose dramatically from nominal 0.01 to 0.21 eV collision energy. Their cross-beam study strongly suggested that one of the potential energy barriers along the reaction path lies very near the energy of Ni^+ ($^2D_{5/2}$) + C_3H_8 reactants. These results differ from those reported by Van Koppen et al. (van Koppen et al., 1994), who found that the barrier to C-H insertion was rate limiting and was located 0.10±0.03 eV below the reactants.

To complete their experimental findings, Weisshaar and co-workers used the B3LYP functional in order to explore in detail the potential energy surface leading from the Ni^+

($^2D_{5/2}$) + C_3H_8 reactants to the products corresponding to H_2 and CH_4 elimination (Yi et al., 1998). They considered mechanisms involving the so-called multicenter transition states (MCTSs, see Figure 18) as already proposed for reactions of hydrocarbons with first-row transition metal ions. (Holthausen et al., 1996; Holthausen & Koch, 1996a; Holthausen & Koch, 1996b). These transition states involve concerted motion of many atoms along a segment of the reaction path connecting each insertion intermediate to the corresponding exit channel ion-induced dipole complex. The proposed mechanism included dissociation back to the reactants and two parallel elimination paths: one involving C-C insertion and subsequent CH_4 elimination, and the other involving secondary C-H insertion and subsequent H_2 elimination. The authors also explored pathways beginning with either primary or secondary C-H insertion and found that the energy difference between the MCTSs involving secondary and primary C-H insertion was sufficiently large to render primary C-H insertion unimportant at low collision energy. In their kinetic model, the energies of the MCTS determine the product branching fractions, since they are by far the highest potential energy points on each reaction path. The MCTS energies are similar to those found for the $Fe^+ + C_3H_8$ reaction (Holthausen & Koch, 1996a). However, it was found that lowering the MCTS energies by 21-29 kJ/mol from the B3LYP value was necessary to account for the observed branching ratios and to fit the Armentrout's absolute cross section for CH_4 elimination. Without adjustment, the model predicted only 0.012 % CH_4 elimination and no H_2 elimination at 0.21eV, in sharp contrast with experiments.

Their theoretical study also called into question the very existence of stable minima of the form $M^+(H)_2$-(alkene) or $M^+(H)(CH_3)$(alkene) that should be produced via an oxidative addition mechanism, and instead demonstrated that the highest potential energies along the paths to H_2 and CH_4 elimination correspond to multicenter transition

states (MCTS) connecting the C-H insertion intermediate directly to the exit channel complex of the form $M^+(H_2)$(alkene), and the C-C insertion intermediate directly to $M^+(CH_4)$(alkene). Finally, their study also predicted that for the $Ni^+ + C_3H_8$ system at low energy, CH_4 elimination occurs exclusively by initial C-C bond insertion and H_2 elimination occurs exclusively by initial secondary C-H bond insertion.

The authors then extended this approach to the reaction of ground state Ni^+ cation with n-C_4H_{10} at the same collision energies. (Blomberg et al., 1999). At 0.01 eV, product branching fractions were 63±5 % $Ni(C_2H_4)^+$ (C_2H_6 elimination), <1 % of $NiC_3H_6^+$ (CH_4 elimination), and 26± 2 % of $Ni(C_4H_8)^+$ (H_2 elimination) and 11±4 % intact $NiC_4H_{10}^+$ complex. At 0.21 eV, $Ni(C_2H_4)^+$ was again prominent, while there was still virtually no methane elimination. This result differed from that reported by Armentrout (Halle et al., 1982a).

The authors have also used DFT in its B3LYP variant to construct a detailed rate model of the reaction. As for the reaction with n-propane, the highest potential energy points along pathways leading to dissociation products were multi-center transition states. According to their model, essentially all the C_2H_6 and H_2 products come from initial insertion into the central C-C bond, the weakest bond in the alkane. The alternative pathway to ethane elimination, which involves initial insertion into a primary C-H bond followed by β-ethyl migration, occurs through a MCTS lying 42 kJ/mol higher in energy. For methane elimination, the lowest energy pathway involved initial insertion into a terminal C-C bond. This route is analogous to that described with propane. Finally, the lowest energy path to H_2 elimination was completely novel, involving initial insertion into the central C-C bond followed by simultaneous migration of two β-hydrogens toward each other while being stabilized by the metal cation center. Insertion into a terminal C-C bond, or into either type of C-H bond lead to less favorable

fragmentation pathways. Note that like for propane, energetics of the MCTS had to be modified to match the product branching ratio obtained at 0.21 eV.

Besides the interest of the reactions of bare metal ions with small alkanes, understanding metal ion interactions with long-chain alkanes not only is of fundamental importance in the areas of organometallic chemistry, surface chemistry, and catalysis, but also has significant implication in mass spectrometry method development for the analysis of polyethylenes. In this context, Chen and Li studied the reactions of several transition-metal cations (including Ni^+) with long-chain alkanes, $C_{28}H_{58}$ and $C_{36}H_{74}$ (Chen & Li, 2001). This laser desorption study showed that in all cases metal ion/alkane adducts are observed as the base peak in the spectra. In addition, dehydrogenation products are detected. In-source fragmentation products corresponding to loss of alkyl groups from the adduct ions were observed for Fe^+, Co^+ and Ni^+. Furthermore, PSD spectra of these adducts are characterized by dominant ions associated with dealkylation. The appearance of these products was found independent of laser power used. Nevertheless, their intensities generally increased as laser power increased.

The type of reaction products for Fe^+, Co^+ or Ni^+ interaction with long-chain alkanes was similar in conventional spectra and PSD spectra. It had been shown previously (Halle et al., 1982a) that exothermic reactions of Fe^+, Co^+ and Ni^+ with linear alkanes up to heptane produced ions of general formula $MC_nH_{2n}^+$.The same type of product ions are observed in this work. However, the loss of methane from $M(alkane)^+$ was not found for the long chain alkanes. This is consistent with the notion that the metal insertion into a terminal C-CH_3 bond is the least preferred reaction (Halle et al., 1982a; Blomberg et al., 1999). Results also indicated that alkane elimination is strongly favored for the long-chain alkanes over H_2 elimination. In addition, among the alkane elimination products, a strong propensity for the loss of larger alkanes was found.

During the last decade, the reactivity of Ni(I) complexes with unsaturated hydrocarbons (alkenes, alkynes and aromatics) has also been investigated. Besides the study (section II.G) of Walters et al. (Walters et al., 2002) on $Ni^+(C_2H_2)_n$ complexes, IRMPD has also been used to examine the unimolecular reactivity of transition metal ion complexes $M(C_nH_{2n})^+$ (n=2-5) containing alkenes (M=Fe, Co, Ni) (Surya et al., 1996). In addition to IRMPD experiments, the authors also applied the sustained off-resonance irradiation (SORI) activation and showed that these two techniques yield similar product distribution. $M(C_2H_2)^+$, $M(C_2H_4)^+$, $M(C_3H_6)^+$ were found to undergo photodissociation by loss of the whole ligand. SORI of these ions also produced the metal cation M^+. Infrared activation of $NiC_4H_8^+$ generated by the well characterized reaction between Ni^+ and *n*-butane (Halle et al., 1982b), only yielded loss of C_2H_4, consistent with the $Ni(C_2H_4)_2^+$ structure. Loss of H_2 was not observed, indicating that no ligand coupling occurred between the two ethenes upon activation. $NiC_4H_8^+$ complexes have also been generated by reaction with *n*-heptane, isobutane and cyclopentanone. Their IRMPD spectra are summarized in Table 4.

TABLE 4. IRMPD spectra of $Ni(C_4H_8)^+$ ions generated from reactions of Ni^+ with various organic compounds.

Organic compounds	Product ions (%)		Attributed structure
	$Ni(C_4H_6)^+$	$Ni(C_2H_4)^+$	
n-butane		100	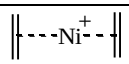
n-heptane	100		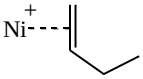
Isobutane	92	8	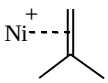
Cyclopentanone	< 62	> 38	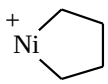

These data demonstrated that isomeric $NiC_4H_8^+$ species could be differentiated thanks to their IRMPD spectra. In the case of cyclopentanone, a small amount of Ni(1- or 2-butene)$^+$ should be formed (Larsen & Ridge, 1984; Peake et al., 1984) and should contribute to the loss of H_2. Note that the product ions observed with cyclopentanone and acetone are different, the latter reacting with Ni^+ under resonant laser ablation conditions by addition of up to two intact molecules (Gill et al., 1996).

Transition metals have been found to facilitate cycloadditions and cyclooligomerization reactions in the condensed phase (Lautens et al., 1996; Ojima et al., 1996). Mass spectrometric studies revealed that certain bare transition-metal cations lead to cyclization reactions of unsaturated hydrocarbons in the gas phase too (Bakhtiar et al., 1992). As many bare transition metal cations are able to couple cyclization reactions with CH bond activation in the gas phase, M^+-mediated cyclization reactions in the gas phase are often accompanied by one or several dehydrogenation steps to eventually form stable aromatic complexes. In this context, Wesendrup and Schwarz studied in a FT-ICR instrument, the catalytic benzene formation in the gas-phase reactions of $MC_4H_4^+$ with ethyne (M=Fe, Co, Ni). The bis(ethene) complexes $M(C_2H_4)_2^+$ were generated in a first step by reaction of the bare metal ions with pulsed-in propane , followed by a consecutive pulse of ethane (reaction 18).

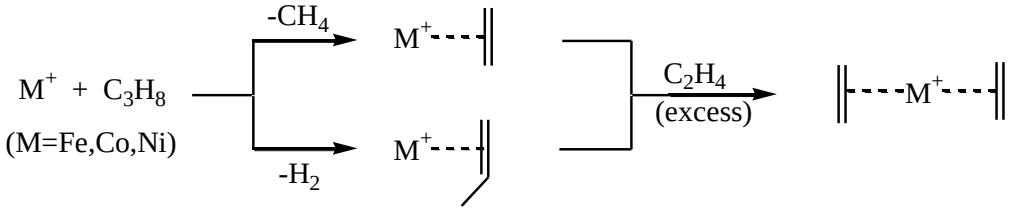

(18)

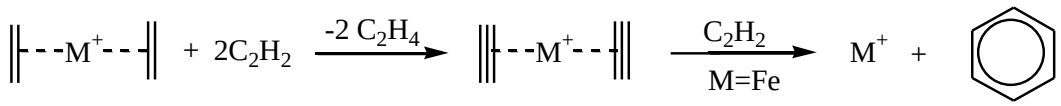

The resulting $M(C_2H_4)_2^+$ complexes then served subsequently as precursors in ligand exchange with residual ethyne. For all the three metals, the stepwise displacement of C_2H_4 by C_2H_2 was observed. CID of the obtained $MC_4H_4^+$ units products showed consecutive losses of two C_2H_2 units which suggests that the complexes retained their bis(ligated) structure $M(C_2H_2)_2^+$. Further evidence for a bis(ethyne) structure was also provided by the reversible ligand exchange reaction of $M(C_4H_4)^+$ with background water which results in $(H_2O)M(C_2H_2)^+$.

The reactivity of the three $M(C_2H_2)_2^+$ complexes toward ethyne differed remarkably: only $Fe(C_2H_2)_2^+$ underwent an efficient reaction with ethyne to yield bare Fe^+ and neutral C_6H_6. According to thermochemical considerations, the liberated C_6H_6 molecule must correspond to benzene. In contrast, $Co(C_2H_2)_2^+$ and $Ni(C_2H_2)_2^+$ were totally unreactive toward ethyne and neither adduct formation nor generation of bare metal cations was observed. Finally, note that this study also included a comparison with second- and third-row transition metal ions. The catalytic benzene formation has been observed for Ru^+ and Rh^+, while Pd^+ was unreactive. The C_4H_4 complexes of Os^+, Ir^+ and Pt^+ and ethyne gave rise to $M(C_6H_4)^+$ ions probably corresponding to the benzyne complexes of these cations.

Finally, completing our survey about the reactivity of Ni^+ with alkynes, the gas phase reaction with propargyl alcohol (PPA) of all the singly charged ions of the first-row transition metals was studied by laser ablation/FTICR mass spectrometry (Zhao et al., 2001). Ni^+ ions reacted to give rise to numerous product ions, the most abundant being $[C_3H_3O]^+$, $[C_3H_5O]^+$, $[MC_3H_2]^+$, $[MC_3H_4]^+$, $[M+PPA]^+$ whose formation involve C-C, C-O (dehydration), C-H or O-H (dehydrogenation) insertion mechanisms. Ni^+ exhibits a reactivity similar to Fe^+ or Co^+ and was found less reactive than Sc^+, Ti^+ and V^+. The difference in reactivity seemed to be partly correlated with the Metal-O bond strength

and the electronic configuration of the ions, the less reactive ions having half and completed occupied valence electronic configurations.

We have already mentioned in section II.F of this review the FTICR investigations on the reactivity of 25 metal ions M^+ towards coronene (COR) and the isomeric molecule tribenzocycline (TBC) (see scheme 1) (Pozniak & Dunbar, 1997), in relation with the cavity effect in the bonding of M^+ with TBC. From the reactivity point of view, it was observed that when a laser-ablated atomic ion M^+ is trapped in the presence of a background pressure of coronene, the reaction sequence leading to ion/coronene complexes can be summarized as follows:

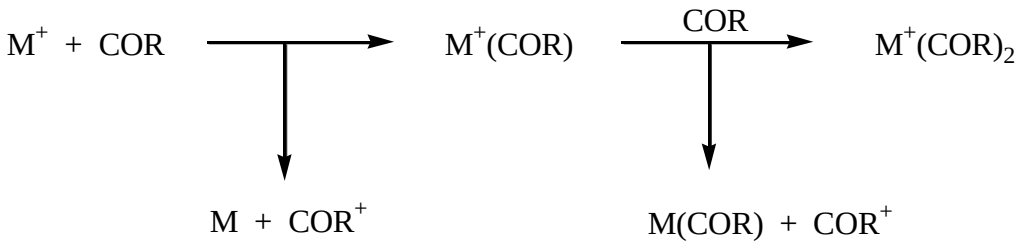

(19)

In the case of nickel the charge transfer reaction is exothermic by 0.35 eV and therefore is significant. All of the first transition series formed dimer complexes $M(COR)_2^+$ readily, except Zn^+, which was dominated by charge transfer (exothermic by 2.1 eV).

In the SIMS studies of the interaction with cyclophanes (See Scheme 2 in section II.F) (Grutzmacher et al., 2001), a significant signal of $M(cyclophane)^+$ was observed, ions being formed in SIMS ion source, by ion/molecule reaction between the sputtered metal ion M^+ and the neutral cyclophane evaporating from the heated target holder. All SIMS spectra also contained a distinct peak of the molecular ion $(cyclophane)^+$, produced by charge transfer occurring in the vapor plume. Experiments in which two metal cations compete for the same host were performed in order to get information about the ability of the different transition metal ions to complex with a given ligand. The following

order $Fe^+ < Co^+ \approx Ni^+ < Cu^+ < Ag^+$ was obtained for the ability to generate adducts with cyclophanes.

If one excepts the biggest metal ions Ag^+ and Co^+ and the cyclophane **1** (with the smallest cavity size), formation of dimeric $M(cyclophane)_2^+$ complexes is not observed. This was attributed to a cavity effect, as supported by the structural information deduced from the CID spectra of the $M(cyclophane)^+$ ions. These spectra indeed did not exhibit any. As mentioned before, this is a clear indication that the metal is strongly bonded in these adduct as expected for an "inside-cavity" structure with the metal buried in the cavity of cyclophane.

An inductively coupled plasma (ICP) selected-ion flow tube tandem mass spectrometer has been employed in a systematic survey of room-temperature reactions of C_6F_6 with all the transition metals but the radioactive Tc^+ (Caraiman et al., 2004). Marked differences were observed for reactivities of early and late transition metal cations with regard to both the reaction efficiency and the type of dissociation pathway. While remarkable multiple fluorine atom abstraction dominated the chemistry of early transition metals, the chemistry of late transition-metal cations is dominated by simple association reactions. In the particular case of Ni^+ two processes were observed:

$$Ni^+ + C_6F_6 \xrightarrow{\text{85 \%}} Ni^+C_6F_6 \qquad (20)$$
$$\xrightarrow{\text{15 \%}} NiF^+ + C_6F_5$$

The efficiency of the C_6F_6 addition process was found to vary across the periodic table, and followed the variation of the bond energy associated with the formation of the adduct.

Single fluorine atom transfer implies that the bond M-F is stronger than the C_6F_5-F bond being dissociated, unless of course some internal excitation energy resides in the metal

ion. The authors estimated that the fluorine atom transfer was exothermic by 29±25 kJ/mol. Furthermore, an analysis of the internal energy population distribution at 5500 K (temperature of the plasma) indicated that the ^4F excited state of Ni^+ should account for 16% of the population and should have more than 100 kJ/mol of energy. Consequently, the possibility that incomplete relaxation of excited stated could be responsible for this process could not be ruled out.

B. Reactivity towards small polyatomic molecules (O_2, CO, CO_2, COS, CS_2, D_2O, NH_3, NO, PH_3)

The study of reactions of coordinatively unsaturated transition metal ions with dioxygen is useful since such processes are often essential in the activation of molecular oxygen for its subsequent utilization in oxidation reactions. The reactivity with O_2 of coordinatively unsaturated ions $[M(bpy)_2]^{2+}$ (M=Cr, Ru, Os) and $[M(bpy)]^+$ (M=Co, Ni, Cu) was investigated using ESI techniques (Molina-Svendsen et al., 1998). Complexes were allowed to react with dioxygen (in multiple-collision conditions) in the collision cell. The interpretation of the spectra was confirmed through reactions with ^{18}O-labeled molecular oxygen. The reactions observed are summarized below:

$$[M(bpy)_2]^{2+} \xrightarrow{O_2} [M(bpy)_2O_2]^{2+} \xrightarrow{CID} \begin{array}{l} [M(bpy)O_2]^+ + bpy^{+\cdot} \quad M=Os \\ \text{or} \\ [M(bpy)_2]^{2+} + O_2 \quad M=Ru, Cr \end{array} \qquad (21)$$

$$[M(bpy)]^+ \xrightarrow{O_2} [M(bpy)O_2]^+ \xrightarrow{CID} [M(bpy)]^+ + O_2 \quad M=Co, Ni$$

The doubly charged unsaturated complexes were not detected for Cu, Co and Ni. Only the Ni- and Co- containing complexes gave detectable dioxygen adducts with the

composition $[M(bpy)O_2]^+$. If their composition is unequivocal, their structure remained speculative because two binding modes (end-on or side-on) are known for O_2. A formal inner-sphere electron transfer may occur so that the dioxygen can be formally reduced and the metal formally oxidized, possibly involving O-O bond cleavage. The authors also recorded the CID spectra of the $[M(bpy)O_2]^+$ ions. For the $[Ni(bpy)O_2]^+$ complex, the loss of a mass equivalent to two oxygen atoms was the predominant process, suggesting that nickel does not activate the molecular oxygen under these conditions.

The rate and equilibrium kinetics of the reactions of O_2 and CO (Jarvis et al., 2003), and CO_2, D_2O, NH_3 and NO (Jarvis et al., 2004) with M^+, $M(pyrrole)^+$ and $M(pyrrole)_2^+$ (M=Ni, Cu) have been investigated in the gas phase at 295±2 K in helium buffer gas. The measurements were obtained with an inductively coupled plasma/selected ion flow tube tandem mass spectrometer. The reactions of bare Ni^+ and Cu^+ ions with O_2, CO, CO_2, NH_3 and D_2O were found to proceed by sequential addition of ligand molecules, the maximum number of ligands added being 3, except for D_2O (2). These reactions were assumed to be termolecular, facilitated by collision stabilization with helium atoms.

$$M(L)_n^+ + L + He \longrightarrow M(L)_{n+1}^+ + He \qquad (22)$$

When measurable, the rate coefficients for the addition of the second ligand were significantly larger than those reported for the first addition. The enhanced reactivity was attributed to the increased lifetime of the intermediate collision complex. The presence of the first molecule of ligand substantially increases the degrees of freedom and therefore the lifetime of the collision complex involving a second molecule of ligand, thus allowing for more effective collisional stabilization by the buffer gas (He).

As we have already mentioned in section II.H, $Ni(pyrrole)^+$ ions were also observed to be reactive with these ligands. Only one addition of a ligand was observed with O_2, CO_2, D_2O. The ion $M(L)^+$ ($L=O_2$, CO_2, CO, D_2O) were not detected. Failure to observe ligand-switching reaction implies that these ligands bind less strongly to the metal ions than pyrrole. Note that $Ni(pyrrole)(CO)^+$ can add a second CO molecule. In contrast, higher-order NH_3 chemistry has been observed with $Ni(pyrrole)^+$. $Ni(pyrrole)(NH_3)^+$ appeared to react both by switching and by addition, leading to $Ni(NH_3)_2^+$ and $Ni(pyrrole)(NH_3)_2^+$ complexes, respectively. The presence of one molecule of pyrrole significantly increases the lifetime of the intermediate collision complex and subsequently the gas-phase rate of metal-ion ligation.

The pyrrole bis-adduct of Ni^+ was reactive only with CO and NH_3. The former ligand reacts exclusively by addition while reactions with ammonia may proceed by either addition or switching of one pyrrole ligand. Finally, theoretical calculation have also been performed to characterize the complexes (structure, energetics) observed with CO and O_2 (Jarvis et al., 2003). See section II.H of the present review for more details.

Bohme and co-workers also examined the reactivity with nitrogen monoxide (NO) (Jarvis et al., 2004). Its reactivity differed remarkably from the other ligands investigated. The effective reaction efficiency with Ni^+ ions is small (2.9 %). The reaction exhibits multiple reaction channels leading to NO^+, $Ni(NO)^+$ and NiO^+. Again, the $Ni(NO)^+$ ion can be formed by a ternary addition (reaction 22). The authors interpreted the formation of both NO^+ and NiO^+ in terms of a second-order reaction mechanism in which a $Ni(NO)^+$* collision intermediate (or alternatively the $Ni(NO)^+$ adduct, if stabilization has already occurred) reacts with a second molecule of NO according the following sequence:

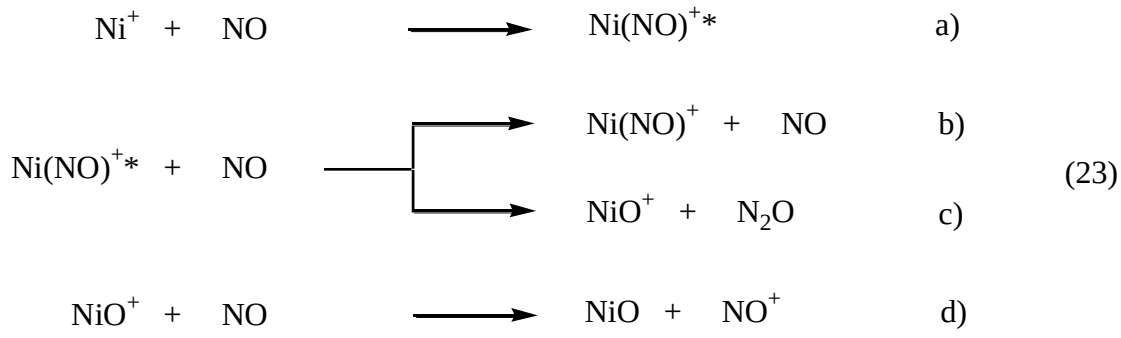

(23)

NO second-order chemistry is supported by their thermodynamic calculations and is facilitated by the radical nature of this ligand. Finally, the Ni(pyrrole)$^+$ complex was found to react by addition of a single ligand while the reaction with Ni(pyrrole)$_2^+$ proceed either by addition or by displacement of one pyrrole unit.

Armentrout and co-workers used guided-ion beam techniques to study the reactivity of late first-row transition metal cations towards CS_2 and COS. (Rue et al., 2002) Measurable quantities of the $Ni^+(^4P)$ third excited state were produced in the DC discharge/flow tube (DC/FT) ion source, but could be seriously limited by adding a cooling gas (O_2). Three primary product ions were formed according to the following endothermic reactions :

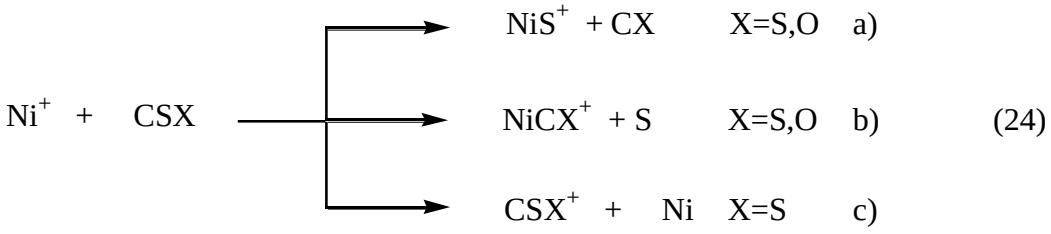

(24)

In the particular case of COS, product ions like COS^+, NiO^+ and $NiCS^+$ were looked for and not observed. The overall behavior of the Ni^+/CS_2 and Ni^+/COS systems, suggests that Ni^+ ions activate CXS by inserting into the C-S bond to form the corresponding S-

Ni^+-CX intermediates. All of the observed products can be formed by cleavage of specific bonds of this intermediate. Thus cleavage of the SNi^+-CS and S-$NiCS^+$ bonds provide low-energy route to formation of NiS^+ and $NiCS^+$ according to reactions 24a and 24b, respectively. Likewise, involvement of S-M^+-CO can account for the experimental observations in the COS system. Insertion of the C-S bond is more facile than in CS_2, because the bond is weaker. There is a reduced probability of inserting into the C-O bond to form the O-M^+-CS intermediate, due to the large difference in the C-O and C-S bond energies. Accordingly, NiS^+ and $NiCO^+$ dominate as products, while their NiO^+ and $NiCS^+$ counterparts are not observed.

Schwarz and co-workers have also studied the reactions of group 8, 9, and 10 laser-ablated monocations (Fe^+, Co^+, Ni^+, Ru^+, Rh^+, Pd^+, Od^+, Ir^+, Pt^+) with phosphane (PH_3), under single-collision conditions in a Fourier transform ion cyclotron resonance (FT-ICR) mass spectrometer (Mazurek & Schwarz, 2002). While Fe^+ cation was found completely unreactive (Bronstrup et al., 1999), Ni^+ only reacts slowly to form the $Ni(PH_3)^+$ and $NiP_2H_6^+$ adducts. Double resonance experiments revealed that the species $NiPH^+$, though not observed in kinetic measurements, seemed to be involved to a certain extent in the generation of these two adducts. Furthermore, $NiP_2H_6^+$ is only to a small extent formed from $NiPH_3^+$. Consequently, C5-C8 hydrocarbons, present in the background of the mass spectrometer were suspected to play a role in the formation of the heaviest adduct.

C. Reactivity with molecules of biological interest

The cationization of relevant organic molecules by transition metals is one of the major topics in the gas-phase chemistry (Eller & Schwarz, 1991; Freiser, 1996) due to the important role that transition metals play in many biological processes. Gas-phase

studies on the interaction of transition metals with small model molecules is of great interest because the knowledge of their intrinsic properties can provide important clues to understand the behavior of more complicated systems of biological importance. A typical example is formamide, the simplest amide containing a prototype NH-CO peptide linkage. Thus, it can be used as a model for the study of the hydrolysis of peptide bonds in living systems. It is also one of the building blocks that can be used to model the cationization of larger bases like uracil, cytosine or thymine. Within this context, Rodríguez-Santiago and Tortajada (Rodríguez-Santiago & Tortajada, 2002) have investigated the reactions between Ni^+ and formamide. As mentioned by Schwarz and co-workers (Hornung et al., 1995), due to the relatively high pressure in a FAB ion source, efficient collisional cooling of the ions takes place and therefore excited states of Ni^+ ions are not likely to participate in the observed reactivity. Under FAB conditions, the Ni^+ cation reacts with neutral formamide to produce mainly $Ni(formamide)^+$ adduct ion at m/z 103 (for ^{58}Ni). The unimolecular reactivity of this complex has been investigated by means of the MIKES analysis. The $Ni(formamide)^+$ ion undergoes several fragmentations. The main one corresponds to its dissociation to produce Ni^+. Other losses, namely that of H_2, NH_3 and H_2O were observed in significant abundance. Finally small peaks at m/z 75 and 74 that could correspond to elimination of CO and (H,N,C), respectively, were also detected. In comparison, the loss of carbon monoxide was not observed in the case of the $Cu(formamide)^+$ system (Luna et al., 1998b).

The authors also studied this system under electrospray conditions. The electrospray spectrum appeared to vary significantly with the cone voltage. At low cone voltage, the spectra of the formamide/$NiSO_4$ solution showed different Ni^+ and Ni^{2+} hydrated complexes. A reduction of the metal occurred under electrospray conditions, leading at

high cone voltage (70 V and above) to the formation of the Ni(formamide)$^+$ ion. Its low energy CID spectrum is mainly characterized by the elimination of the formamide moiety. The second most important ion is attributed to the elimination of CO, while it was a minor process under FAB-MIKE conditions.

In order to rationalize these results, the authors explored in detail the potential energy surface associated. They found that the most stable structure corresponds to the metal ion interacting with the oxygen atom of the most stable conformer (monodentate), in the direction of the dipole moment. Stating from this species, several mechanisms have been proposed to account for the elimination of CO, H_2O, NH_3 and (C,H,N) from Ni(formamide)$^+$. It turned out that the most energetically favorable pathway leading to CO elimination implies in a first step insertion of the metal into the C-N bond. In contrast with the case of the Cu(formamide)$^+$ system, all the inserted structures were found to lie below the energy of the reactants. This finding may account for the absence of CO loss in the case of the Cu(formamide)$^+$ system. Remarkably, the most favorable route was found to correspond to the loss of intact formamide, in agreement with the experimental observations.

The same approach was adopted to study the Ni(urea)$^+$ system (Rodríguez-Santiago et al., 2003). Under FAB-MIKE conditions, the main fragmentation of the Ni(urea)$^+$ ion corresponds to the loss of CO giving rise to the Ni(N_2H_4)$^+$ ion (m/z 90). A very strong signal is also observed for the loss of ammonia (m/z 101). Moreover, two small peaks attributed to Ni$^+$ and elimination of HNCO, were detected at m/z 58 and 75, respectively. These results were somewhat different from those obtained by FAB for the Cu(urea)$^+$ system, for which the base peak of the spectrum corresponded to the loss of NH_3 whereas loss of CO was not detected (Luna et al., 2000c).

Under electrospray conditions, the $Ni(urea)^+$ MS/MS spectrum is qualitatively comparable to that obtained under FAB conditions, because elimination of ammonia, carbon monoxide, and urea are also observed. However, an additional peak associated with elimination of water is detected at m/z 100. As already proposed by Schröder during the study of unimolecular reactivity of the $Cu(urea)^+$ complex generated by electrospray (Schröder et al., 2002), this fragmentation could be attributed to a partial collision-induced isomerization of the $Ni(urea)^+$ complex in the cone region prior to mass selection by the first quadrupole.

B3LYP calculations indicated that like for copper (Luna et al., 2000c), the most stable structure **Ni1** (Scheme 5), corresponds to the attachment of the metal cation to the oxygen atom.

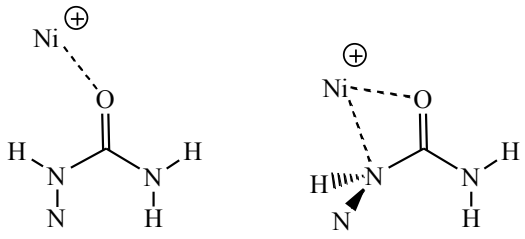

Ni1 **Ni2**

Scheme 5

The second most stable structure, **Ni2**, is only 10.0 kJ/mol less stable than **Ni1** and corresponds to the Ni^+ cation bridging between the O and N atoms. These two structures were considered as starting points for the potential energy surfaces associated with the different dissociation channels. Calculations have demonstrated that elimination of CO, NH_3, and HNCO arise from C-N insertion mechanisms concomitant with hydrogen migration. In addition, loss of ammonia may also occur from a non insertion mechanism (by transfer of a hydrogen from one NH_2 group to the other one). The most stable

structures along the C-N insertion potential energy surface are bisligated intermediates H_3N-Ni^+-ONCH and H_3N-Ni^+-N(H)CO, which can further dissociate to produce complementary Ni-NH_3^+ and Ni^+(HNCO) ions without any barrier in excess. As the computed Ni^+-NH_3 binding energy is larger than the Ni^+-ONCH and Ni^+-N(H)CO ones, the m/z 101 ion (ammonia loss) should be less intense than the m/z 75 ion. However experimentally, the m/z 101 is found to predominate, regardless of the ionization method used to generate the initial adduct. Moreover all the barriers associated with these two mechanisms were found roughly of the same magnitude and close or sometimes above the energy of the dissociation channels. In this particular case, as noticed by Schröder et al. during their electrospray study of the $Cu(urea)^+$ system (Schröder et al., 2002), energized $Ni(urea)^+$ complexes can lead to fragmentations with branching ratios that do not correlate with reaction thermochemistry. If the activation barriers for isomerization were well below the thresholds for dissociation, then isomerization should be rapid compared to dissociation, and CID of a mass-selected ion would yield correct thermochemical thresholds and branching ratios. Clearly, according to the calculated potential energy surfaces, such a situation is not encountered neither with the $Ni(urea)^+$ system nor with the $Ni(formamide)^+$ complex.

The reactivity of Ni(I) and Ni(II) ions towards amino acids (AA) has been extensively studied during the last decade. These studies can be divided in two categories: those involving ternary complexes and those examining the reactivity of bare nickel ions.

In the gas phase, metal proteins interactions have been modeled by ternary complexes of the type $[M(II)(AA-H)(L)]^+$, involving an amino acid and an additional bidentate ligand (Wilson et al., 1992). The role of this ligand is to occupy two coordination sites at the metal cation and thus block coordination of a second amino acid carboxylate that would lead to neutral $[M(II)(AA-H)_2]$ complex. Gatlin and Tureček (Gatlin & Turecek, 1995)

reported preliminary results on the formation of ternary amino acid complexes of late transition-metal cations, Fe^{2+}, Fe^{3+}, Co^{2+}, $Ni^{2+}$and Zn^{2+}, under electrospray conditions. The 2,2'-bipyridyl (bpy) and 1,10-phenantroline (phen) compounds were used as auxiliary ligands. While no cationic aminoacid complexes could be detected with iron, a variety of gas-phase Co^{2+}, Ni^{2+} and Zn^{2+} ternary complexes were produced. With bpy, five complexes were detected with Ni(II): $[Ni(II)(bpy)_n]^{2+}$ (n=2,3), $[Ni(II)(AA-H)(bpy)]^+$, $[Ni(II)(AA-H)(bpy)_2]^+$ and $[Ni(II)(AA-H)(AA)(bpy)]^+$, but their unimolecular reactivity has not been explored. Kückelmann and Müller applied this method to LSIMS by using 1,10 phenantroline (Kückelmann & Müller, 1998). A $[Ni(II)(AA-H)(phen)]^+$ complex could be detected but its intensity was very weak compared to the complexes formed with Cr(II) or Co(II).

The interaction between amino acids and bare nickel ions has been examined in more detail. In 1995, Bouchonnet and co-workers reported some Plasma Desorption Mass Spectrometer (PDMS) results about the interaction of several first-row transition metal cations with six aliphatic AA: glycine, alanine, valine, leucine, isoleucine, and proline (Bouchonnet et al., 1995). For Ni, Cu and Co, the organometallic species observed were the pseudomolecular ion $M(AA)^+$ and its fragment ions, the immonium species being the base peak almost systematically. The abundance of this $M(AA)^+$ ion seemed to be linked to the length of the amino acid side chain. Two other abundant species were detected: $[M(AA)-CH_2O_2]^+$ and $[M(AA)-CH_4O_2]^+$. $[M(AA)-CH_2O_2]^+$ ions are formally analogous to the immonium ion $[MH-CH_2O_2]^+$. Based on the use of deuterated amino acids, the authors proposed that the elimination of CH_2O_2 could be interpreted by initial insertion of the metal into the C-COOH (Figure 19).

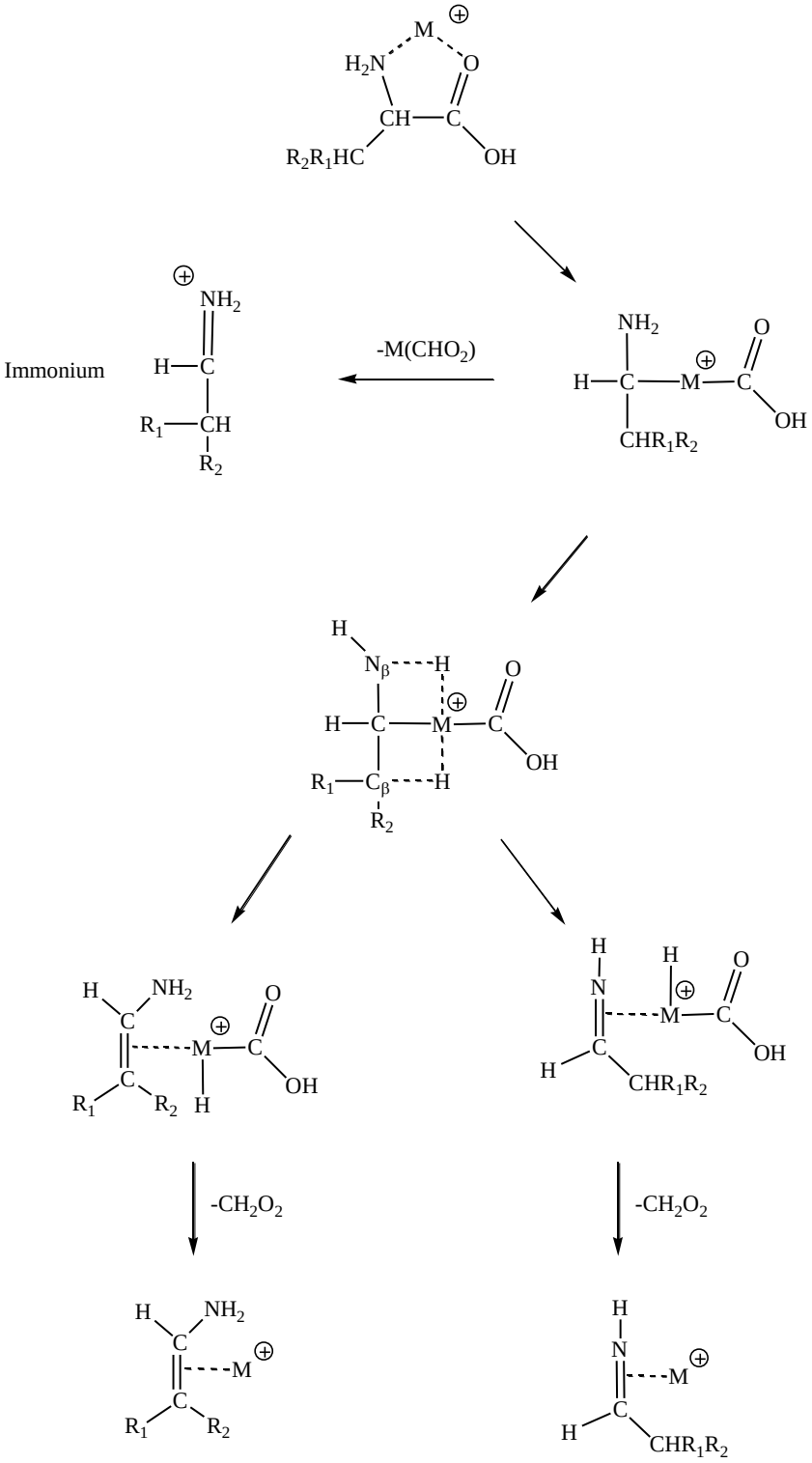

FIGURE 19. Mechanism proposed by (Bouchonnet et al., 1995) to explain the formation of $[M(AA)\text{-}CH_2O_2]^+$ and immonium ions.

A hydrogen atom located on an atom in the β position relative to the transition metal can then easily migrate onto the metal center. The final step consists in the reductive elimination of CH_2O_2. This ion may further lose H_2 to give rise to the $[M(AA)\text{-}CH_4O_2]^+$ complex. For amino acids with a side chain long enough, elimination of a small alkane may compete with the loss of dihydrogen. The formation of the immonium ions was also postulated to arise from the initial insertion of the metal into the C-COOH bond (Figure 19). The authors concluded that the reactivity observed with these amino acids did not correspond to the superposition of the reactivity observed with amines (Karrass & Schwarz, 1990) and carboxylic acids (Schröder et al., 1994).

Several years later, the same group published an electrospray study of the 1:1 complexes of L-histidine (His) with a series of divalent transition metal cations Fe^{2+}, Co^{2+}, Ni^{2+}, Cu^{2+} and Zn^{2+} (Lavanant et al., 1999). At low cone voltage (10 V) all the metals lead to a series of $[M(II)(His\text{-}H)(CH_3OH)_n]^+$ ions (n=1-3). As the cone voltage was increased, labile ligands (solvent) were lost and $[M(II)(His\text{-}H)]^+$ ions were detected. Note doubly charged $[M(His)_2]^{2+}$ complexes have been observed, but their reactivity upon collision has not been further explored.

MS/MS experiments have shown that $[Ni(II)(His\text{-}H)]^+$ ions lose in a first step a molecule of CO_2. Based on previous reports on copper (Gatlin et al., 1995a; Gatlin et al., 1995b), the authors have proposed a radical-like process to account for the decarboxylation process. This mechanism is reproduced in Figure 20.

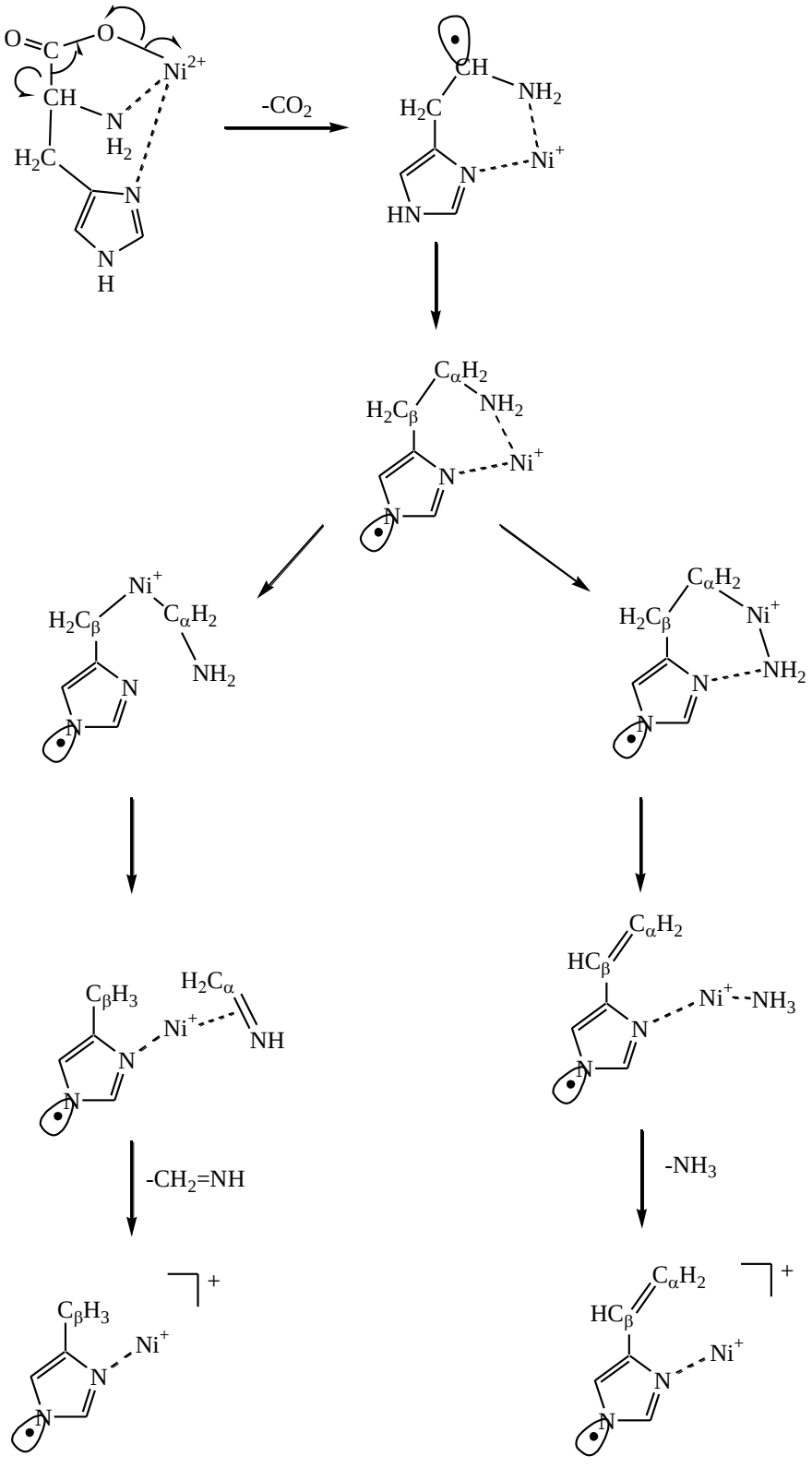

FIGURE 20. Mechanism for the decomposition of $[Ni(II)(His)-H]^+$ ion.

This hypothesis of a reduction taking place is supported by the fact that a loss of a neutral metal is observed in further fragmentations. The $[Ni(II)(His-H)-CO_2]^+$ species

then decomposes in several fragment ions corresponding to loss of ammonia, cyanic acid and formaldimine. To be consistent with deuterium labeling experiments, the authors proposed in a first step the migration of the labile pyrrole hydrogen to the radical site, followed by a classical insertion/β-hydrogen migration/decoordination mechanism, with an insertion in the C_α-N bond for ammonia loss, and an insertion in the C_α-C_β bond for imine loss (see Figure 20). Elimination of HCN was supposed to occur within the imidazole ring. Like for Cu^+ and Zn^+, the immonium ion was detected on the MS/MS spectrum of the $[Ni(II)(His\text{-}H)\text{-}CO_2]^+$ complex, through elimination of Ni(0) from the $[(His\text{-}H)\text{-}Ni(II)\text{-}CO_2]$ intermediate. Finally, note that the gas-phase coordination of Ni^{2+} ion by histidine-containing peptides has also been studied by electrospray ionization and it was observed that the histidine residue was the preferred anchor for the metal cation (Hu & Loo, 1995).

FAB and electrospray experiments have also been used to explore the interaction between nickel metal ions and a series of aliphatic and nonaliphatic amino acids, and their methyl esters (Yalcin et al., 1997). Under electrospray, the major-nickel containing species correspond to $[Ni(AA\text{-}H)(AA)]^+$. Interestingly, the methyl esters did not form any adduct under electrospray conditions, suggesting that the (AA-H) species is the carboxylate anion and that nickel is formally in the +2 oxidation state.

The major metal-containing species formed upon FAB is the $Ni(AA)^+$ adduct, but with a very weak intensity compared to the signal detected for the protonated amino acids. As for Cu^+ (Lei & Amster, 1996; Wen et al., 1995), the main fragmentation of the $Ni(AA)^+$ ions generated with nonaliphatic amino acids (such as phenylalanine) are elimination of H_2O, $CO+H_2O$, and CO_2. Like with PDMS, the spectra also exhibit an abundant immonium ion, generated by the elimination of an entity that could correspond to (CO)NiOH. In the case of phenylalanine, elimination of a neutral of mass 92 was

observed and attributed to toluene on the base of deuterium labeling experiments. Furthermore, no elimination of C-bonded deuterium was observed in the elimination of water or of water + CO. This finding supports the postulate that the structure of $[Ni(AA) -H_2O -CO]^+$ ion is an imine coordinated to Ni^+. Adducts with valine and norvaline fragment in a fashion similar to the adduct with phenylalanine.

With the three isomeric leucine, isoleucine and norleucine (aliphatic amino acids), the metastable fragmentation spectra obtained are sensibly different and therefore provide a clear identification of the amino acid. Furthermore, they also differ from those obtained with the nonaliphatic amino acids. They are indeed characterized by intense peaks corresponding to the loss of H_2, CH_4, and, according to the length of the side chain, of the following alkenes : C_2H_4 (as determined by ^{18}O labeling), C_3H_6 an C_4H_8. These processes clearly indicate C-C and C-H activations of the hydrocarbon side chain by the transition metal. Such dissociation channels had been already observed by Karass and Schwarz (Karrass & Schwarz, 1989) with aliphatic amines, and mechanisms were proposed to account for those fragmentations. These mechanisms assume that the reactive species initially involve a Ni^+ bonded solely to the amino function. However, according to the study of Rodríguez-Santiago and Tortajada (Rodríguez-Santiago et al., 2001) about the $Ni(glycine)^+$ system, this configuration does not correspond to the most stable structure. The global minimum corresponds to the bidentate interaction of the metallic center with the nitrogen atom and with the carbonyl oxygen. This structure is almost planar and implies a cis carboxyl group and the formation of a five-membered ring. The same structure was found to be the most stable in the case of Cu^+ (Hoyau & Ohanessian, 1997a; Bertrán et al., 1999) and in the case of alkali cations Li^+ and Na^+ (Hoyau & Ohanessian, 1998). Coordination to the zwitterionic form of glycine was also considered, since it had been established that the interaction of Ni^+ with the negatively

charged end of the zwitterion not only stabilizes this form but also greatly facilitate the intramolecular proton transfer between the neutral and the zwitterionic form (Pulkkinen et al., 2000). The resulting structure is indeed a minimum, lying 58 kJ/mol higher in energy than the most stable form. The FAB/MIKE dissociation spectrum of the complex has also been recorded. Different fragmentations were observed. The base peak corresponds to the loss of water. The same experiment repeated with deuterated glycine-2,2-d_2 demonstrated that the hydrogen atoms involved in this fragmentation are those of OH and NH_2 groups. Besides this fragmentation, the Ni(glycine)$^+$ ion shows remarkable losses, namely that of CO and CH_2O_2.

In order to rationalize these experimental findings, Rodríguez-Santiago and Tortajada, also studied the potential energy surfaces associated with the loss of H_2O, CO and CH_2O_2. To obtain the elimination of a water molecule, a hydrogen atom of the amino group has to be transferred onto the hydroxyl group. The authors considered that the reaction could start by the insertion of the metal in either a C-C or a C-O bond, as reported in Figure 21. These two insertion processes finally lead to a common intermediate corresponding to the interaction of the metal with three ligands, namely CO, H_2O and CH_2NH. This intermediate may then expel either CO or H_2O. Note that all the fragmentations studied are exothermic with respect to the entrance channel. In addition to the sequential loss of H_2O and CO, the authors considered that the loss the CH_2O_2 could also correspond to the elimination of the formic acid molecule, as suggested by Bouchonnet et al. (Bouchonnet et al., 1995). The associated mechanism appears kinetically unfavorable as characterized by a very high energy barrier and may therefore account for the small abundance of the Ni^+-$NHCH_2$ ion.

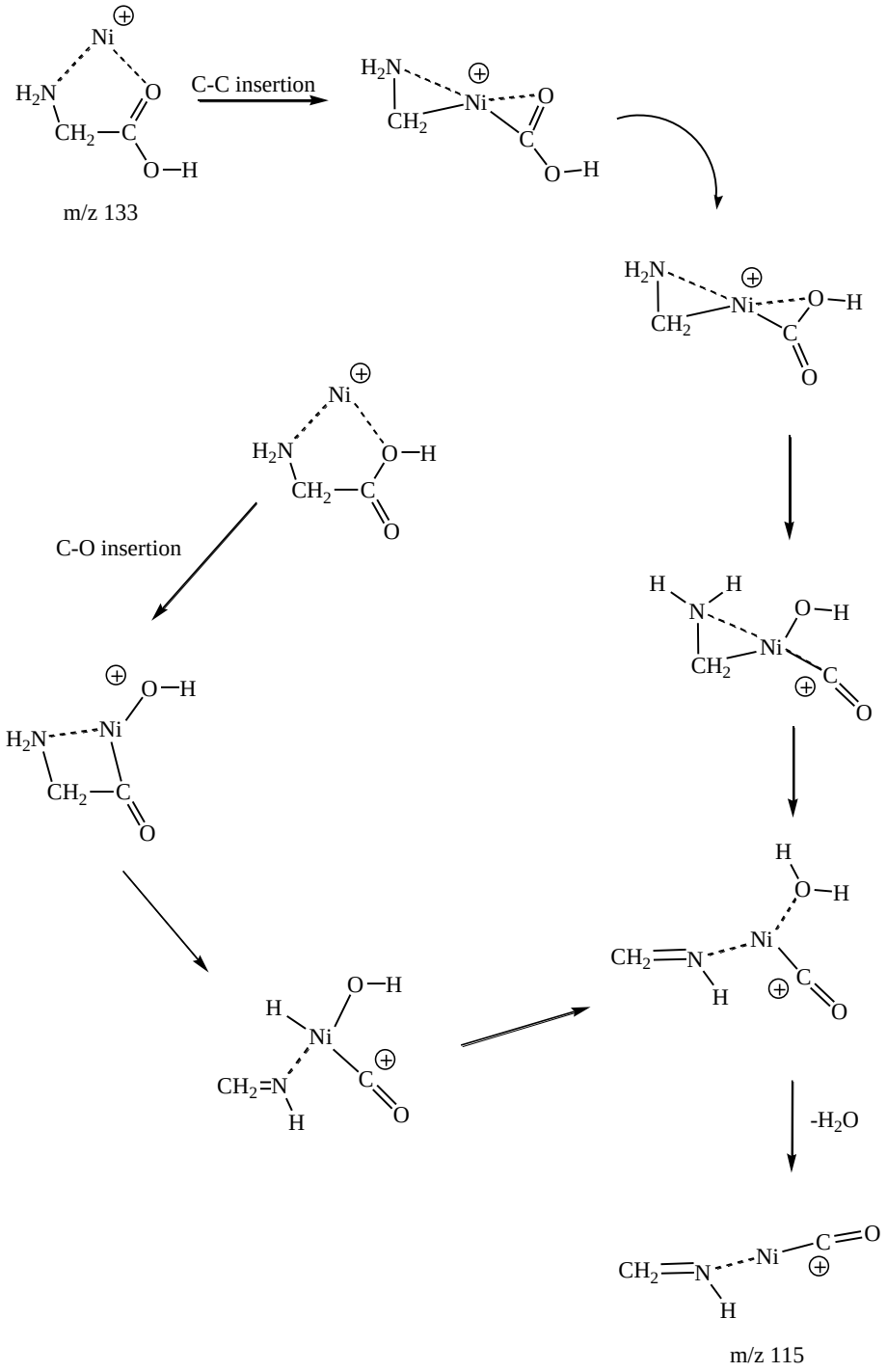

FIGURE 21. Elimination of water from the Ni(glycine)$^+$ complex as proposed by Rodríguez-Santiago and Tortajada (Rodríguez-Santiago et al., 2001).

Finally, to conclude this discussion about the reactivity of amino acids, Williams and Brodbelt (Williams & Brodbelt, 2004) reported the use of metal complexes to the characterization of cyclic peptides, which constitute an important class of antibiotics. In

their study, Williams and Brodbelt used CAD and MS^n experiments of protonated and metal-cationized cyclic peptides generated by electrospray and analyzed in a quadrupole ion trap. The cyclic peptides ranged from six to twelve residues. Two types of complexes were observed with nickel: $[Ni(CP-H)]^+$ and $[Ni(CP)]^{2+}$. Complexation with nickel proved to be particularly helpful for the characterization of cyclosporin A (used to prevent rejection of transplanted organs) and surfactin. The complexes were found more intense relative to protonation and nickel complexes gave for cyclosporine A additional sequence information compared with the protonated peptide.

Carbohydrates are the second family of biomolecules extensively studied during the last decade. Oligosaccharide analysis is a challenging task for mass spectrometry. With the advent of soft ionization techniques, the use of metallic salts as ionization agent has been greatly simplified, and it has been shown that isomeric carbohydrates can be differentiated when coordinated to alkali, alkali-earth or transition metal ions. In this context, Leary et al. published very extensive work about the use of transition metals complexes, and notably Ni(II) species, to distinguish diastereomeric isomers of mono- or oligosaccharides. This group first studied the unimolecular reactivity of tri-coordinate diastereomeric $|Ni(II)(N\text{-glycoside})\text{-}H]^+$ complexes (m/z 293, Scheme 6) produced by FAB analysis of crude reaction mixtures $Ni(DAP)_3Cl_2$ (DAP= $NH_2(CH_2)_3NH_2$, diaminopropane) with four isomeric hexopyranoses : *D*-glucose, *D*-mannose, *D*-talose, *D*-galactose (Smith & Leary, 1996).

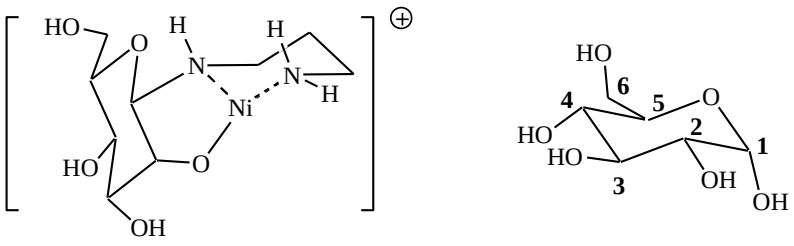

Scheme 6

The metastable spectrum of these four isomeric complexes present a common fragmentation (m/z 233) corresponding to the elimination of a $C_2H_4O_2$ moiety through a cross-ring cleavage. It was observed that the kinetic energy released associated with this particular fragmentation was particularly large for diastereomers whose C-2 hydroxyl of the monosaccharide was in axial position (*D*-mannose and *D*-talose). This was not surprising because the structure of these two particular tri-coordinate complexes was known to involve a direct coordination of this hydroxyl to metallic center. Additional labeling experiments further demonstrated that the loss of $C_2H_4O_2$ arise from cross-ring cleavages occurring at different locations (Smith & Leary, 1998).

The same complexes were also generated under electrospray conditions and subjected to collision-induced dissociation (CID) (Smith et al., 1997). A more straightforward distinction between isomers was obtained by the direct comparison of the MS/MS spectra. Of the four complexes examined, the m/z 201 ion was only detected for the two aldohexoses possessing equatorial C-2 hydroxyl groups, namely *D*-glucose and *D*-galactose. This loss of 92 Da was proposed to be a combination of H_2 and $C_3H_6O_3$ losses. ^{13}C labeling experiments demonstrated that the $C_3H_6O_3$ neutral loss was a contiguous three-carbon fragment containing C-4, C-5 and C-6. The origin of the dehydrogenation was determined by use of glucose-1-*d* and glucose-2-*d* and replacement of all the exchangeable protons by deuteriums. These experiments showed that the H_2 loss involved one exchangeable hydrogen and the hydrogen bond to C-2. A mechanism involving a β-hydrogen elimination has been proposed to account for these experimental findings (Figure 22).

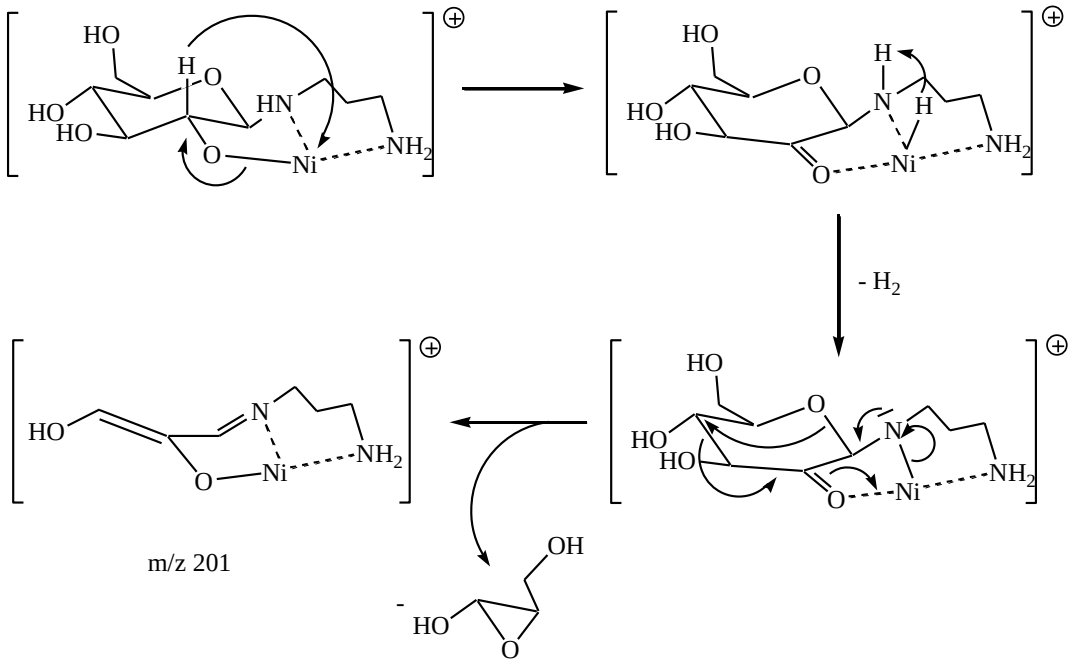

FIGURE 22. Mechanism proposed by Smith et al. (Smith et al., 1997) to account for the loss of 92 Da from the [Ni(II)(*N*-glycoside)-H]$^+$ complex

Using the same ligand, this group has also studied the fragmentation of the five-coordinate complexes |Ni(II)(*N*-glycoside)(DAP)-H]$^+$ generated in the gas phase by electrospray ionization (Smith & Leary, 1999). Following excitation of these precursor ions in a quadrupole ion trap, reproducibly distinct product ion spectra were obtained for each of the diastereomeric complexes.

Distinction between *D*-glucose and *D*-galactose has been also achieved by using diethylenetriamine (dien) as ligand, exclusive loss of formaldehyde from the [Ni(II)(*N*-glycoside)(dien)-H]$^+$ ion being only observed for the former (Gaucher & Leary, 2000).

Leary et al. also applied the transition metal ion chemistry to the analysis of sialic acid-containing oligosaccharides (Leavell & Leary, 2001a). These molecules are difficult to analyze because they contain a labile glycosidic bond between the sialic acid moiety and the remaining carbohydrate portion of the oligosaccharide. Metal-ligand derivatization of the sialic acids with the dien ligand and one of the four transition

metals Co(II), Ni(II), Cu(II) and Zn(II) suppressed sialic acid loss in the collision induced dissociation process by deprotonation of the carboxylic acid and subsequent coordination of the carboxylate to the metal ion. Suppression of sialic acid loss allows sialic acid linkage information to be obtained. Indeed, analysis of the product ion spectra showed a clear distinction between two different positions of the sialic linkage. Finally, use of Ni(II) complexes to the analysis of neuraminic acids was also reported (Leavell & Leary, 2001b).

A slightly different approach was adopted by Davis ad Brodbelt during their analysis of flavonoid monoglucosides (Davis & Brodbelt, 2004). Thousands of flavonoids have been discovered, differing by the location of hydroxy and methoxy groups and by the placement, number and identity of the saccharide moiety. As an example, the structure of apigenine-7-O-glucoside is given in scheme 7.

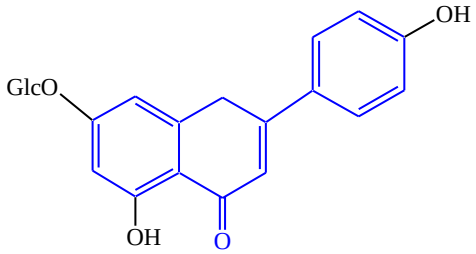

apigenine-7-O-glucoside

Scheme 7

The goal of this study was to develop a simple but robust method based on metal-complexation, but without the addition of a ternary ligand. Five metals were considered: Ca(II), Mg(II), Co(II), Ni(II) and Cu(II). Under electrospray conditions, the flavonoid glycosides (L) formed 1:1 and 2:1 analyte/metal complexes of the type $[M(II)(L-H)]^+$ and $[M(II)(L)(L-H)]^+$. CID of the $[Mg(L)(L-H)]^+$ ions resulted in diagnostic mass

spectra, five different sites of glycosylation being characterized. In contrast, cobalt, nickel and copper complexation had only limited success in this application.

D. Reactivity with other systems

Vachet and co-workers have explored new ways to obtain the coordination structure of metal complexes by mass spectrometry. Given the fact that for metal-ligand complexes structural information may sometimes be difficult to obtain unambiguously from routine CID MS/MS experiments due to rearrangements around the metal center prior to dissociation, this group developed an alternate approach based on the use of ion/molecule reactions of metal complex ions with neutral reagents at thermal energies (Combariza et al., 2005). They demonstrated that ion/molecule reactions carried out in a modified quadrupole ion trap can provide varying degrees of detail about the divalent metal complex's coordination structure by choosing the appropriate reagents. Two different approaches were developed. The first one involves reagent gases that are selectively reactive with complexes exhibiting a given coordination number. Four different reagent gases were generally used to assess the coordination chemistry of the metal complexes : pyridine, water, methanol and ammonia. The following trend allowed the coordination number of metal complexes to be determined: six-coordinate complexes are unreactive, five-coordinate complexes are reactive only with pyridine, four-coordinate complexes are reactive with ammonia and pyridine, and three-coordinate complexes are reactive with all the reagents including water and methanol. They used this technique in order to characterize the structure of ion pairs (Vachet & Callahan, 2000), species that are not normally abundant in solution but can be readily produced in the gas phase owing to the complicated nature of the electrospray process. The ion pairs studied were of the type $[M(phen)_2X]^+$, where M was among others

Co(II), Zn(II) and Ni(II), phen was 1,10 –phenantroline, and X is Cl^-, NO_3^-, acetylacetate, ClO_4^-, acetate or SCN^-. This study showed a number of unexpected results. For example, ClO_4^- was almost exclusively found to be a unidentate ligand in all complexes except when Ni(II) was the metal. In that case, ClO_4^- is found to be bidentate, presumably coordinated through two oxygens. The same was found as far SCN^- is concerned, indicating that either the bonding occurs side-on, i.e. involving the π-system or the thiocyanate ligand is bent within the complex. Some suitable theoretical calculations would be necessary to confirm which of these two possibilities is the most favorable one. These authors have also applied this approach to the characterization of doubly charged complexes $Ni(L_n)^{2+}$ (n=1,2) with a series of aminopyridine ligands (Vachet et al., 1998) (Hartman et al., 2000; Vachet et al., 2001). The majority of the gas-phase structures of these complexes were found to agree with the results deduced from condensed phase investigations.

The second approach for determining the coordination number consists in using a single reagent (acetonitrile) that is capable of titrating the unoccupied coordination sites in a complex. In this approach, sequential increase of 41 Daltons (or the absence of a mass increase) after the ion/molecule reaction indicates the initial coordination number of the complex. Reactions with acetonitrile were used to characterize the coordination scheme within M(II) complexes (M=Cu, Co, Ni) of homodisubstituted diethylenetriamines (DIEN) (Combariza & Vachet, 2003). In this paper, the experimental parameters suspected to have an effect on the reproducibility of the results, notably the temperature and the pressure of both the buffer gas and acetonitrile, were examined in detail. The authors concluded that with a careful control of the temperature and reagent gas pressure, ion/molecule reaction with acetonitrile can provide a rapid and sensitive analysis of the functional groups bound to a metal in a given complex. This approach

has been recently applied to characterize the coordination environments for the Ni(II) complexes of a series of linear penta- and hexadentate aminopyridine ligands (Hartman et al., 2004). Finally, kinetic and thermodynamical data deduced from these ion-molecule reactions appear to be sensitive to the geometry of the complexes studied (Combariza & Vachet, 2004b) and to the chelate ring size (Combariza & Vachet, 2004a). To conclude, in comparison to threshold CID measurements, which are currently limited to monovalent metal ion complexes, ion/molecule reactions in a QITMS may not provide as detailed and precise thermodynamic information, but do provide access to coordination structure information using less-specialized equipment.

Tsierkesos et al. have used electrospray ionization (ESI) mass spectrometry to investigate the complexation of Ni(II) by ethylenediamine (en) in water/methanol solution of $NiCl_2$, both in the presence and the absence of N,N-dimethylformamide (DMF) (Tsierkezos et al., 2004). Three aspects have been addressed : (i) at which number of ligand n, bond activations or electron transfer reactions occur in the dissociation of Ni(II) complexes, (ii) what are the bonding patterns of those multiply ligated species which formally exceed the hexafold coordination of nickel, that was already discussed in section IV, and (iii) to which extent can DMF compete with ethylenediamine as a ligand. The ESI spectra present numerous nickel-containing cations and notably the dications $[Ni(en)_n]^{2+}$ with n=2-5, and the monocations $[Ni(en)_nCl]^{+}$ with n=1-3.

The CID spectra of $[Ni(en)_n]^{2+}$ with n=3-5 ions are characteristic of metal dication complexes with more than two ligands. Two main dissociation pathways were indeed observed. The first one corresponds to sequential elimination of neutral ethylenediamine units:

$$[Ni(en)_n]^{2+} \longrightarrow [Ni(en)_{n-x}]^{2+} + x\text{en} \qquad (25)$$

In the particular case of the $[Ni(en)_2]^{2+}$ species, the ethylenediamine elimination decreased sharply and intracomplex electron transfer followed by charge separation according the following reaction prevailed.

$$[Ni(en)_2]^{2+} \longrightarrow [Ni(en)]^{+} + en^{+} \qquad (26)$$

According to the authors, the failure to observe the monoligated dication $[Ni(en)]^{2+}$ under these conditions, does not mean this species is unstable with respect to the charge separation asymptote $Ni^{+} + (en)^{+}$. As the ionization potential of the ligand (7.6 eV) is much lower than the ionization energy of Ni^{+} (18.2eV), efficient and facile electron transfer from the neutral ligand to the metal dication is likely to suppress the formation of the monoligated dication in favor of the corresponding monocation.

The second dissociation pathway corresponds to dissociative proton transfer. For the dication with n=3-5, proton transfer between ethylenediamine ligands is observed as well :

$$[Ni(en)_n]^{2+} \longrightarrow [Ni(en\text{-}H)(en)_{n-1}]^{+} + (en)H^{+} \qquad (27)$$

Use of deuterated ethylenediamine revealed that the proton loss originates from one of the amino groups.

The authors focused their attention to the ligated dications $[Ni(en)_n]^{2+}$ with n>3 since these ions are known not to be present in solution because they formally exceed the hexafold coordination of nickel. They concluded that the formation of multiply ligated

dications which exceed the formal coordination number of six critically depended on the ability of the bifunctional ligand to form hydrogen bonds. Consequently, the possibility that ethylenediamine could act as a monodentate ligand in $[Ni(en)_n]^{2+}$ with n>3 was discarded in favor of hydrogen bonding between ethylenediamine units belonging to different solvation shells.

The authors have also carefully examined the unimolecular reactivity of $[Ni(en)_nCl]^+$ monocations. Much like for the dications, the dominant process observed when n=2 and 3 upon CID corresponds to elimination of neutral ligand. Elimination of HCl is also a dominant process for n=2 and 3, a hydrogen of the amino groups being involved in the process. The $[Ni(en)Cl]^+$ is particularly stable and exhibits a specific dissociation, namely elimination of ammonia through insertion of the metallic center in a C-N bond.

This group also used electrospray ionization to explore in detail the unimolecular reactivity of Ni(II) ions towards DMF (Tsierkezos et al., 2003). Globally, the results are similar to those obtained with ethylenediamine. At low cone voltages, gas-phase ions are observed which also exist in solution (Elias et al., 2000), e.g. $[Ni(DMF)_n]^{2+}$ (n=2-6) and $[Ni(DMF)_nX]^+$ (n=1-4; X=Cl, Br, NO_3). Enhanced cone voltage affords coordinatively unsaturated complexes to be formed via consecutive loss of DMF units. (e.g. $[Ni(DMF)_2]^{2+}$ and [Ni(DMF)Cl]+). Applying high cone voltage (> 60 V) results in reduction of the metal and both Ni^+ and $Ni(DMF)^+$ ions were detected.

Upon CID, for $[Ni(DMF)_n]^{2+}$ (with $n \geq 3$), only sequential losses of neutral DMF ligand are observed, which become more difficult as the number of ligands decrease. When n=2, the ligand loss is associated with an electron transfer giving rise to two singly charged ions through a Coulomb explosion :

$$[Ni(DMF)_2]^{2+} \longrightarrow [Ni(DMF)]^+ + DMF^+ \qquad (28)$$

While this fragmentation should yield equal amounts of both product ions, the authors noticed that there was a clear preference for the $[Ni(DMF)]^+$ ion. We made the same observation for the Coulomb explosions arising from the $[Ca(urea)]^{2+}$ complex (Corral et al., 2004c). This phenomenon is attributed to increased scattering of the lightest ion due to the energy released in coulomb explosion. The authors further explored the $[Ni(DMF)_n]^{2+}$ ions (n=1-2) by means of charge-stripping experiments. They failed to observe the monoligated cation. Like for ethylenediamine, the difference in ionization energies is so large that any transiently formed complex cannot prevent charge separation leading to Ni^+ and DMF^+.

Finally, mixed complexes of Ni(II) with both ethylenediamine and DMF were studied. The MS/MS spectrum obtained for the $[Ni(en)_3(DMF)_n]^{2+}$ ion (n=1-4) are characterized by sequential losses of DMF. This demonstrates that Ni(II) has a significantly large affinity for the amino group of ethylenediamine than for the carbonyl oxygen of DMF, as already mentioned in section IV.

As shown by Palii et al. during their electron impact study (Palii et al., 1999), tetradentate quasimacrocyclic ligands (scheme 8) may constitute convenient precursors for a variety of relatively simple nickel-containing ions. Structure of these ions were assigned based on their metastable (MI) and collision induced dissociation (CID) spectra.

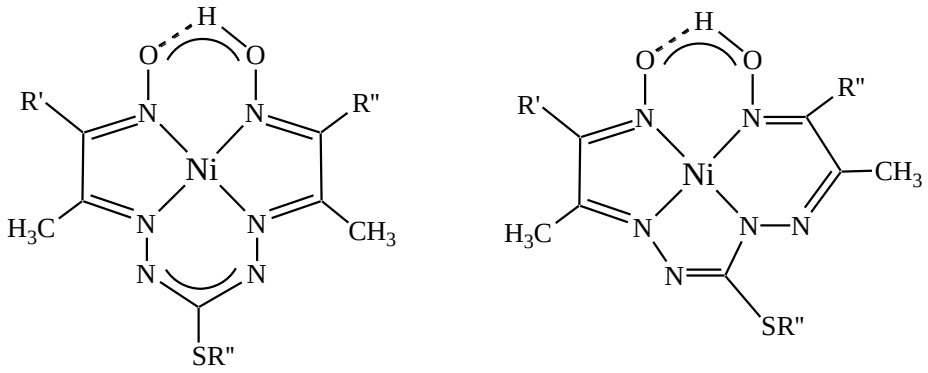

Scheme 8

Hence, the MI spectrum of $Ni^+(NCCH_3)$ is very simple, showing only a peak for the Ni^+ ion. Its CID spectrum results in three additional products, and notably a methyl loss involving the metal atom insertion into the C-C bond. The MI spectrum of $Ni^+(NCCH_3)_2$ displayed only one peak corresponding to the loss of acetonitrile while bare Ni^+ ion is observed under collision. The metastable $HONi^+NCCH_3$ ions loses mainly water, which unambiguously involves a irreversible H-atom shift from the methyl group to the hydroxyl group. The other metastable dissociation corresponds to loss of acetonitrile. The absence of $HO^{\cdot}$ was consistent with a stronger Ni^+OH bond relative to Ni^+-$NCCH_3$. On the other hand, the dissociation of $HONi^+(NCCH_3)_2$ is significantly different, the most favorable process being elimination of a hydroxyl radical. This observation, in contradiction with the known thermochemistry, might be consistent with the cyclic structure presented below (scheme 9), although other possibilities cannot be completely discarded.

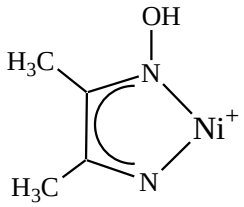

Scheme 9

Most of the investigations concerning the properties and reactivity of nickel ions in the gas phase refer to cationic species. However, in the last years a few studies dealt with nickel-involving anions. Oliveira et al. studied with an FTICR instrument the formation and the reactivity with methanol of negative cluster ions of transition metal oxides $[M_xO_y]^-$. (M=Mn, Fe, Co, Ni, Cu) (Oliveira et al., 1999) generated by laser desorption. With nickel, the following clusters anions were detected: $[NiO_2]^-$ (the most intense), $[Ni_2O_3]^-$, $[Ni_3O_3]^-$, $[Ni_4O_4]^-$, and $[Ni_5O_5]^-$. Collision-induced dissociation experiments with argon were performed for the lightest ion. No dissociation products were detected but a decrease of the intensity of the parent ion was observed. The authors assumed that the excited anions could undergo a collision-induced electron detachment to form neutral species with the same formula. $[NiO_2]^-$ were allowed to react with methanol. The reaction was characterized by a very low efficiency (10^{-4}), and gave rise to $[NiO_2H_2]^-$ and a molecule of formaldehyde. Interestingly, it is worth mentioning that dehydrogenation of methanol into formaldehyde without metal is endothermic by 86 kJ/mol. The same process has been observed with the $[Ni_2O_3]^-$ anion but the reaction was 300 times more efficient. Experiments carried out with deuterated methanol indicated that the elimination of hydrogen atoms involves both the hydroxyl and the methyl group of methanol. For longer reaction times, the primary product $[M_2O_3H_2]^-$ in turn reacts with methanol according to reactions 29b and 29c.

$$[M_2O_3]^- + CH_3OH \longrightarrow [M_2O_3H_2]^- + CH_2O \quad a)$$

$$[M_2O_3H_2]^- + CH_3OH \longrightarrow [M_2O_3CH_4]^- + H_2O \quad b) \qquad (29)$$

$$[M_2O_3CH_4]^- + CH_3OH \longrightarrow [M_2O_3C_2H_6]^- + H_2O \quad c)$$

Finally, formation of metal cyanide ions in the gas phase has been also reported (Dance et al., 2002) (see section II.G for more details).

VI. CONCLUDING REMARKS

It seems clear from the preceding compilation that a much larger amount of accurate Ni^+ BDEs and, in particular, Ni^{2+} BDEs are needed in order to have enough data to extract general trends. On the other hand, many questions on the nature of the bonding between transition metal cations and the different ligands are still open. For example, the Ni^+ binding preference to pyrrole with respect to benzene. Also, for most ligands (H_2, C_2H_4, C_6H_6, S, CS and CH_2) the observed trend in BDEs is $Co^+ > Ni^+ > Cu^+$, but there are significant exceptions. For instance, for CO the BDE of Co^+ and Ni^+ are essentially equal, while for NH_3 the sequence is $Co^+ < Ni^+ \approx Cu^+$ and for pyridine $Co^+ < Ni^+ > Cu^+$. In contrast, for pyrimidine the trend is $Co^+ \approx Ni^+ < Cu^+$. Probably one of the most surprising cases is imidazole for which a $Co^+ < Ni^+ < Cu^+$ trend was determined. These exceptions likely arise from subtle differences in covalent interactions that need to be fully understood. In this respect it is worth noting that, as it has been shown recently (Corral et al., 2005), although the neutral-ion interaction energy for alkali monocations and alkaline-earth metal dications is dominated by electrostatic contributions, in many cases the correct basicity trends are only attained when the energy associated with covalent interactions are taken into account.

As far as sequential BDEs are concerned it is often found (H_2, CH_4, NH_3) that the second ligand is bound more strongly than the first one what has been rationalized in terms of $sd\sigma$ hybridization that alleviates Pauli repulsion, whose energetic cost in essentially paid by the first ligand. But again the existence of significant exceptions

(CO, C_2H_4, C_6H_6, NO) seem to indicate that the aforementioned model is likely incomplete.

Our survey of the reactivity observed in the gas phase clearly illustrates the importance of the reactivity of nickel ions in numerous fields of research. Note however, that we have deliberately not examined in detail the particular case of spin-forbidden reactions. Several spin-forbidden processes were reported by Rue et al. during their study of the reactions of Ni^+ with COS and CS_2 (Rue et al., 2002). Another example has been given by Irigoras et al. (Irigoras et al., 2000) when examining the potential energy surface associated with the formation of NiO^+ and H_2 from the reaction between Ni^+ and water. Consequently, spin-forbidden reactions are likely to play an important role in the gas-phase reactivity of nickel ions and could undoubtedly constitute the subject of a dedicated review like those reported recently for other metals (Carreón-Macedo & Harvey, 2004; Schwarz, 2004).

REFERENCES

Alcamí M, Mó O, Yáñez M. 2001. Computational Chemistry. A useful (some times mandatory) tool in mass spectrometry studies. Mass Spectrom. Rev. 20:195-245.

Alcamí M, Mó O, Yáñez M, Cooper I L. 2000. The performance of density-functional theory in challenging cases: Halogen oxides. J. Chem. Phys. 112:6131-6140.

Alexander B D, Dines T J. 2004. Ab initio calculations of the structure and vibrational spectra of ethane complexes. J. Phys. Chem. A. 108:146-156.

Alvarez E J, Brodbelt J S. 1998. Evaluation of metal complexation as an alternative to protonation for electrospray ionization of pharmaceutical compounds. J. Am. Soc. Mass Spectrom. 9:463-472.

Amunugama R, Rodgers M T. 2001. Periodic trends in the binding of metal ions to pyrimidine studied by threshold collision-induced dissociation and density functional theory. J. Phys. Chem. A. 105:9883-9892.

Armentrout P B, Beauchamp J L. 1981a. Ion-Beam Studies Of The Reactions Of Atomic Cobalt Ions With Alkanes - Determination Of Metal-Hydrogen And Metal-Carbon Bond-Energies And An Examination Of The Mechanism By

Which Transition-Metals Cleave Carbon-Carbon Bonds. J. Am. Chem. Soc. 103:784-791.

Armentrout P B, Beauchamp J L. 1981b. Ion-beam studies of the reactions of atomic cobalt ions with cycloalkanes in the gas-phase - formation and decomposition of chemically activated metallacycles. J. Am. Chem. Soc. 103:6628-6632.

Armentrout P B, Beauchamp J L. 1989. The Chemistry of atomic transition-metal ions: Insight into fundamental aspects of organometallic chemistry. Acc. Chem. Res. 22:315-321.

Armentrout P B, Kickel B L. 1996. Gas-phase thermochemistry of transition metal ligand systems: Reassessment of values and periodic trends. In: B. S. Freiser. Edit. Organometallic ion chemistry Dordrecht: Kluwer Academic.p. 1-45.

Bader R F W. 1990. Atoms in Molecules. A Quantum Theory. Oxford: Clarendon Press.

Bakhtiar R, Drader J J, Jacobson D B. 1992. Iron-Mediated [4+2] Cycloaddition Of 1,3-Butadiene With Ethyne And Propyne In The Gas-Phase. J. Am. Chem. Soc. 114:8304-8306.

Barnes L A, Rozi M, Bauschlicher J C W. 1990. Theoretical-studies of the 1st-row and 2nd-row transition-metal monocarbonyl and dicarbonyl positive-ions. J. Chem. Phys. 93:609-624.

Bartlett R J. 1981. Many-body perturbation-theory and coupled cluster theory for electron correlation in molecules. Ann. Rev. Phys. Chem. 32:359-401.

Bauschlicher C W, Jr. 1995. A comparison of the accuracy of different functionals. Chem. Phys. Lett. 246:40-44.

Bauschlicher C W, Jr., Partridge H. 1995. A modification of the Gaussian-2 approach using density functional theory. J. Chem. Phys. 103:1788-1791.

Bauschlicher J C W, Partridge H, Langhoff S R. 1992a. Theoretical study of transition-metal ions bound to benzene. J. Phys. Chem. 96:3273-3278.

Bauschlicher J C W, Partridge H, Sheehy J A, Langhoff S R, Rosi M. 1992b. Theoretical-study of the bonding of the 1st-row and 2nd-row transition-metal positive-ions to methylene. J. Phys. Chem. 96:6969-6973.

Becke A D. 1988. Density-functional exchange-energy approximation with correct asymptotic behavior. Phys. Rev. A. 38:3098-3100.

Becke A D. 1993. A new mixing of Hartree-Fock and local-density-functional theories. J. Chem. Phys. 98:1372-1377.

Bertrán J, Rodríguez-Santiago L, Sodupe M. 1999. The different nature of bonding in Cu^{+}-glycine and Cu^{2+}-glycine. J. Phys. Chem. B. 103:2310-2317.

Blades A T, Jayaweera P, Ikonomou M G, Kebarle P. 1990. Ion-molecule clusters involving doubly charged metal-ions (M^{2+}). Int. J. Mass Spectrom. Ion Process. 102:251-267.

Blomberg M, Yi S S, Noll R J, Weisshaar J C. 1999. Gas-phase $Ni^{+}(^{2}D_{5/2})$+*n*-C_4H_{10} reaction dynamics in real time: Experiment and statistical modeling based on density functional theory. J. Phys. Chem. A. 103:7254-7267.

Bögel H, Tobisch S, Nowak T. 1998. DFT investigations of the structure and bonding between transition metals and olefins. Int. J. Quant. Chem. 69:387-396.

Bouchonnet S, Hoppilliard Y, Ohanessian G. 1995. Formation And Fragmentations Of Organometallic Complexes Involving Aliphatic Alpha-Amino-Acids And Transition-Metal Cations - A Plasma Desorption Mass-Spectrometry Study. J. Mass Spectrom. 30:172-179.

Bronstrup M, Schroder D, Schwarz H. 1999. Reactions of bare FeO+ with element hydrides EHn (E = C, N, O, F, Si, P, S, Cl). Chemistry-A European Journal. 5:1176-1185.

Brookhart M, Green M L H. 1983. Carbon-hydrogen-transition metal bonds. J. Organomet. Chem. 250:395-408.

Caraiman D, Koyanagi G K, Bohme D K. 2004. Gas-phase reactions of transition-metal ions with hexafluorobenzene: Room-temperature kinetics and periodicities in reactivity. J. Phys. Chem. A. 108:978-986.

Carreón-Macedo J L, Harvey J N. 2004. Do spin state changes matter in organometallic chemistry? A computational study. J. Am. Chem. Soc. 126:5789-5797.

Chen R, Li L. 2001. Reactions of atomic transition-metal ions with long-chain alkanes. J. Am. Soc. Mass Spectrom. 12:367-375.

Combariza M Y, Vachet R W. 2003. The utility of ion-molecule reactions in a quadrupole ion trap mass spectrometer for analyzing metal complex coordination structure. Analytica Chimica Acta. 496:233-248.

Combariza M Y, Vachet R W. 2004a. Gas-phase reactions of divalent Ni complex ions with acetonitrile: Chelate ring size, inductive, and steric effects. J. Am. Soc. Mass Spectrom. 15:1128-1135.

Combariza M Y, Vachet R W. 2004b. Effect of coordination geometry on the gas-phase reactivity of four-coordinate divalent metal ion complexes. J. Phys. Chem. A. 108:1757-1763.

Combariza M Y, Fahey A M, Milshteyn A, Vachet R W. 2005. Gas-phase ion-molecule reactions of divalent metal complex ions: Toward coordination structure analysis by mass spectrometry and some intrinsic coordination chemistry along the way. Int. J. Mass Spectrom. 244:109.

Corral I, Mó O, Yáñez M. 2003a. The importance of agostic-type interactions for the binidng energies of Ni^+ to saturated and α,β-unsaturated alkanes, silanes and germanes. New J. Chem. 27:1657-1664.

Corral I, Mó O, Yáñez M. 2003b. Agostic vs. pi-interactions in complexes of ethynyl-silanes and ethynyl-germanes with Cu^+ in the gas phase. J. Phys. Chem. A. 107:1370-1376.

Corral I, Mó O, Yáñez M. 2003c. Binding energies of Cu^+ to saturated and a,b-unsaturated alkanes, silanes and germanes. The role of agostic interactions. Int. J. Mass Spectrom. 107:1370-1376.

Corral I, Mó O, Yáñez M. 2004a. Li^+ vs. Cu^+ association to toluene, phenyl-silane and phenyl-germane. Conventional vs. non-conventional -π complexes. Eur. J. Mass Spectrom. 10:921-930.

Corral I, Mó O, Yáñez M. 2004b. Bonding and Bonding Perturbation in Ion-Molecule Interactions in the Gas Phase. In: Edit. Encyclopedia of Computational Chemistry. URL: http/www.mrw.interscience.wiley.com/eccarticles/cn0062/frame.html

Corral I, Mó O, Yáñez M, Radom L. 2005. Why are the Ca^{2+} and K^+ binding energies of formaldehyde and ammonia reversed with respect to their proton affinities? J. Phys. Chem. A. 109:6735-6742.

Corral I, Mó O, Yáñez M, Salpin J Y, Tortajada J, Radom L. 2004c. Gas-phase reactions between urea and Ca^{2+}: The importance of Coulomb explosions. J. Phys. Chem. A. 108:10080-10088.

Cotton F A, LaCour T, Stanislowski A G. 1974. Interaction of an aliphatic carbon-hydrogen bond with a metal atom - structure of (diethyldi-1-pyrazolylborato)-(trihapto-2-phenylallyl) (dicarbonyl)molybdenum. J. Am. Chem. Soc. 96:754-760.

Cremer D, He Z. 1996. Sixth-Order Moller-Plesset Perturbation Theory-On the Convergence of the MPn Series. J. Phys. Chem. 100:6173-6188.

Csaszar P, Goggin P L, Mink J, Spencer J L. 1988. The vibrational-spectra and structure of tris(ethylene)metals. J. Organomet. Chem. 379:337-349.

Curtiss L A, Redfern P C, Raghavachari K, Pople J A. 2001. Gaussian-3X (G3X) theory: Use of improved geometries, zero-point energies, and Hartree-Fock basis sets. J. Chem. Phys. 114:108-117.

Dalleska N F, Honma K, Sunderlin L S, Armentrout P B. 1994. Solvation of transition metal ions with water. Sequential binding energies of $M_+(H_2O)_x$ (x = 1-4) for M = Ti-Cu. J. Am. Chem. Soc. 116:3519-3528.

Dance I G, Dean P A W, Fisher K J, Harris H H. 2002. Metal cyanide ions $[M_x(CN)_y]^{+,-}$ in the gas phase: M = Fe, Co, Ni, Zn, Cd, Hg, Fe + Ag, Co + Ag. Inorg. Chem. 41:3560-3569.

Davis B D, Brodbelt J S. 2004. Determination of the glycosylation site of flavonoid monoglucosides by metal complexation and tandem mass spectrometry. J. Am. Soc. Mass Spectrom. 15:1287-1299.

Dougherty D A. 1996. Cation-pi interactions in chemistry and biology: A new view of benzene, Phe, Tyr, and Trp. Science. 271:163-168.

Drohat A C, Stivers J T. 2000. NMR evidence for an unusually low N1 pK(a) for uracil bound to uracil DNA glycosylase: Implications for catalysis. J. Am. Chem. Soc. 122:1840-1841.

Duncan M A. 1997. Spectroscopy of metal ion complexes: Gas-phase models for solvation. Annu. Rev. Phys. Chem. 48:69-93.

Eberlin M N, Kotiaho T, Shay B J, Yang S S, Cooks R G. 1994. Gas-phase Cl^+ affinities of pyridines determined by the kinetic method using multiple-stage [ms(3)] mass-spectrometry. J. Am. Chem. Soc. 116:2457-2465.

Ekeberg D, Uggerud E, Lin H Y, Sohlberg K, Chen H L, Ridge D P. 1999. Dehydrogenation of ethane by CpM+ (M = Fe, Co, Ni) in the gas phase. An FT-ICR-MS study. Organometallics. 18:40-44.

El-Nahas A M. 2001. Thermochemically stable $M^{2+}OH_2$ complexes in the gas phase: M= Mn, Fe, Co, Ni, and Cu. Chem. Phys. Lett. 345:325-330.

Elias H, Schumacher R, Schwamberger J, Wittekopf T, Helm L, Merbach A E, Ulrich S. 2000. Kinetics and mechanism of complex formation of nickel(II) with tetra-N-alkylated cyclam in N,N-dimethylformamide (DMF): Comparative study on the reactivity and solvent exchange of the species $Ni(DMF)_6^{2+}$ and $Ni(DMF)_5Cl^+$. Inorg. Chem. 39:1721-1727.

Eller K, Schwarz H. 1991. Organometallic chemistry in the gas phase. Chem. Rev. 91:1121-1177.

Filippi A, Speranza M, Paladini A, De Carolis R, Guidoni A G, Lagana A, Satta M. 2006. Diastereoselective fragmentation of chiral alpha-aminophosphonic acids/metal ion aggregates. J. Mass Spectrom. 41:98-102.

Freiser B S. 1996. Organometallic Ion Chemistry. Understanding Chemical Reactivity. Dordrecht: Kluwer Academic.

Frenking G, Fröhlich N. 2000. The nature of the bonding in the transitin-metal compounds. Chem. Rev. 100:717-774.

Frenking G, Sola M, Vyboishchikov S F. 2005. Chemical Bonding in transition metal complexes. J. Organom. Chem. 690:6178-6204.

Gapeev A, Yang C N, Klippenstein S J, Dunbar R C. 2000. Binding energies of gas-phase metal ions with pyrrole: Experimental and quantum chemical results. J. Phys. Chem. A. 104:3246-3256.

Gatlin C L, Turecek F. 1995. Ternary Complexes Of Amino-Acids With Late Transition-Metals Cations And Diimine Ligands In The Gas-Phase. J. Mass Spectrom. 30:1636-1637.

Gatlin C L, Turecek F, Vaisar T. 1995a. Gas-Phase Complexes Of Amino-Acids With Cu(II) And Diimine Ligands .2. Amino-Acids With O, N And S Functional-Groups In The Side-Chain. J. Mass Spectrom. 30:1617-1627.

Gatlin C L, Turecek F, Vaisar T. 1995b. Gas-Phase Complexes Of Amino-Acids With Cu(II) And Diimine Ligands .1. Aliphatic And Aromatic-Amino-Acids. J. Mass Spectrom. 30:1605-1616.

Gaucher S P, Leary J A. 2000. Influence of metal ion and coordination geometry on the gas phase dissociation and stereochemical differentiation of N-glycosides. Int. J. Mass Spectrom. 197:139-148.

Ghanty T K, Davidson E R. 2000. Theoretical Investigation of Electronic Structure and ESR Hyperfine Parameters for the CuH^+ Molecule. Int. J. Quant. Chem. 77:291-300.

Gill C G, Garrett A W, Hemberger P H, Nogar N S. 1996. Resonant laser ablation as a selective metal ion source for gas-phase ion molecule reactions. J. Am. Soc. Mass Spectrom. 7:664-667.

Gritzner G, Horzenberger F. 1992. Gibbs energies, enthalpies and entropies of transfer of cations from acetonitrile and n,n-dimethylformamide into water. J. Chem. Soc., Faraday Trans. 88:3013-3017.

Grutzmacher H F, Zoric S, Wellbrock C. 2001. Complexation of transition metal ions M^+ (M = Fe, Co, Ni, Cu, Zn, Ag) by [2.n] paracyclophane-enes (n = 3, 4, 5, 6) in the gas phase: effect of the molecular cavity on the complexation capability. Int. J. Mass Spectrom. 210:311-325.

Halle L F, Armentrout P B, Beauchamp J L. 1982a. Ion-Beam Studies Of The Reactions Of Group-8 Metal-Ions With Alkanes - Correlation Of Thermochemical Properties And Reactivity. Organometallics. 1:963-968.

Halle L F, Houriet R, Kappes M M, Staley R H, Beauchamp J L. 1982b. Nickel Ions Effect A Highly Specific 1,4-Dehydrogenation Of Hydrocarbons In The Gas-Phase - Metallacycles Are Not Involved. J. Am. Chem. Soc. 104:6293-6297.

Hanratty M A, Beauchamp J L, Illies A J, van Koppen P A M, Bowers M T. 1988. Kinetic-energy release distributions as a probe of transition-metal-mediated H-H, C-H, and C-C bond formation processes - reactions of cobalt and nickel ions with alkanes. J. Am. Chem. Soc. 110:1-14.

Hartman J R, Vachet R W, Callahan J H. 2000. Gas, solution, and solid state coordination environments for the nickel(II) complexes of a series of aminopyridine ligands of varying coordination number. Inorg. Chim. Acta. 297:79-87.

Hartman J R, Combariza M Y, Vachet R W. 2004. A comparison of the gas, solution, and solid state coordination environments for the Ni(II) complexes of a series of linear penta- and hexadentate aminopyridine ligands with accessible Ni(III) oxidation states. Inorg. Chim. Acta. 357:51-58.

Haynes C L, Fisher E R, Armentrout P B. 1996. Probing the $[CoC_3H_8]^+$ potential energy surface: A detailed guided-ion beam study. J. Phys. Chem. 100:18300-18316.

Heck R F. 1974. Organotransition Metal Chemistry. New York: Academic Press.

Hettich R L, Jackson T C, Stanko E M, Freiser B S. 1986. Gas-phase photodissociation of organometallic ions - bond-energy and structure determinations. J. Am. Chem. Soc. 108:5086-5093.

Holthausen M C, Koch W. 1996a. Mechanistic details of the Fe^+-mediated C-C and C-H bond activations in propane: A theoretical investigation. Helv. Chim. Acta. 79:1939-1956.

Holthausen M C, Koch W. 1996b. A theoretical view on Co^+-mediated C-C and C-H bond activations in ethane. J. Am. Chem. Soc. 118:9932-9940.

Holthausen M C, Mohr M, W. K. 1995. The performance of density functional/Hartree-Fock hybrid methods: the bonding in cationic first-row trnsition metal methylene complexes. Chem. Phys. Lett. 240:245-252.

Holthausen M C, Fiedler A, Schwarz H, Koch W. 1996. How does Fe^+ activate C-C and C-H bonds in ethane? A theoretical investigation using density functional theory. J. Phys. Chem. 100:6236-6242.

Hornung G, Schroder D, Schwarz H. 1995. Diastereoselective Gas-Phase Carbon-Carbon Bond Activation Mediated by Bare Co^+ Cations. J. Am. Chem. Soc. 117:8192-8196.

Hoyau S, Ohanessian G. 1997a. Absolute affinities of alpha-amino acids for Cu^+ in the gas phase. A theoretical study. J. Am. Chem. Soc. 119:2016-2024.

Hoyau S, Ohanessian G. 1997b. Complexation of small organic molecules by Cu^+. Chem. Phys. Lett. 280:266-272.

Hoyau S, Ohanessian G. 1998. Interaction of alkali metal cations (Li^+-Cs^+) with glycine in the gas phase: A theoretical study. Chemistry-A European Journal. 4:1561-1569.

Hu P F, Loo J A. 1995. Gas-Phase Coordination Properties Of Zn^{2+}, Cu^{2+}, Ni^{2+}, And Co^{2+} With Histidine-Containing Peptides. J. Am. Chem. Soc. 117:11314-11319.

Husband J, Aguirre F, Thompson C J, Metz R B. 2001. Photodissociation spectra of transition metal sulfides: spin-orbit structure in charge transfer bands of FeS^+ and NiS^+. Chem. Phys. Lett. 342:75-84.

Husband J, Aguirre F, Thompson C J, Laperle C M, Metz R B. 2000. Photofragment spectroscopy of $FeCH_2^+$, $CoCH_2^+$, and $NiCH_2^+$ near the M^+-CH2 dissociation threshold. J. phys. Chem. A. 104:2020-2024.

Irigoras A, Elizalde O, Silanes I, Fowler J E, Ugalde J M. 2000. Reactivity of Co^+ (^{3}F, ^{5}F), Ni^+(^{2}D,^{4}F), and Cu^+(^{1}S,^{3}D): Reaction of Co^+, Ni^+, and Cu^+ with water. J. Am. Chem. Soc. 122:114-122.

Irikura K K, Beauchamp J L. 1991. Electronic-Structure Considerations For Methane Activation By 3rd-Row Transition-Metal Ions. J. Phys. Chem. 95:8344-8351.

Jackson T C, Carlin T J, Freiser B S. 1986. Gas-phase reactions of MS^+ ions (M=Fe, Co, Ni) with alkanes - An FTMS study. Int. J. Mass Spectrom. Ion Process. 72:169-185.

Jacobson D B, Freiser B S. 1983a. Studies Of The Reactions Of Group-8 Transition-Metal Ions Fe^+, Co^+, And Ni^+ With Linear Alkanes - Determination Of Reaction-Mechanisms And $NiC_nH_{2n}^+$ Ion Structures Using Fourier-Transform Mass-Spectrometry Collision-Induced Dissociation. J. Am. Chem. Soc. 105:5197-5206.

Jacobson D B, Freiser B S. 1983b. Structural Determination Of $NiC_nH_{2n}^+$ Ions In The Gas-Phase Using Fourier-Transform Mass-Spectrometry Collision-Induced Dissociation. J. Am. Chem. Soc. 105:736-742.

Jacobson D B, Freiser B S. 1983c. Reactions of group 8 transition-metal ions (Fe^+, Co^+, and Ni^+) with cyclic hydrocarbons in the gas-phase. J. Am. Chem. Soc. 105:7492-7500.

Jaeger T D, Duncan M A. 2005a. Photodissociation of $M^+(benzene)_x$ complexes (M = Ti, V, Ni) at 355 nm. Int. J. Mass Spectrom. 241:165-171.

Jaeger T D, Duncan M A. 2005b. Vibrational spectrocopy of $Ni^+(benzene)_n$ complexes in the gas phase. J. Phys. Chem. A. 109:3311-3317.

Jaeger T D, van Heijnsbergen D, Klippenstein S J, von Helden G, Meijer G, Duncan M A. 2004. Vibrational spectroscopy and density functional theory of transition metal ion-benzene and dibenzene complexes in the gas phase. J. Am. Chem. Soc. 126:10981-10991.

Jarvis L M, Blagojevic V, Koyanagi G K, Bohme D K. 2004. Gas-phase kinetic measurements of the ligation of Ni^+,Cu^+, $Ni(pyrrole)_{1,2}^+$ and $Cu(pyrrole)_{1,2}^+$ with CO_2, D_2O, NH_3 and NO. Eur. J. Mass Spectrom. 10:949-961.

Jarvis M J Y, Pisterzi L F, Blagojevic V, Koyanagi G K, Bohme D K. 2003. Gas-phase kinetic measurements and uantum chemical calculations of the ligation of Ni^+, Cu^+, $Ni^+(pyrrole)_{1,2}$ and $Cu^+(pyrrole)_{1,2}$ with O_2 and CO. Int. J. Mass Spectrom. 227:161-173.

Kandalam A K, Rao B K, jena P, Lilly A C. 2004. Binding of butadiene molecules mediated by Ni atom and Ni^+ ion. J. Phys. Chem. A. 108:5234-5241.

Karrass S, Schwarz H. 1989. Site-Specific, Oxidative Addition Of C-C Bonds By Anchored Bare Fe(I) Cations Prior To C-H Bond Activation - Preliminary Communication. Helv. Chim. Acta. 72:633-637.

Karrass S, Schwarz H. 1990. Evidence For The Activation Of Unstrained Carbon Carbon Bonds By Bare Transition-Metal Ions Fe^+, Co^+ Without Prior C-H Bond Activation. Organometallics. 9:2034-2040.

Kemper P R, P. W, Bowers M T. 1998a. $Ni^+(H_2)_n$: Ligand bond energies for the ground state ions. Chem. Phys. Lett. 293:503-510.

Kemper P R, Weis P, Bowers M T, Maitre P. 1998b. Origin of bonding interactions in $Cu^+(H_2)_n$ clusters: An experimental and theoretical investigation. J. Am. Chem. Soc. 120:13494-13502.

Khan F A, Steele D L, Armentrout P B. 1995. Ligand effects in orgametallic thermochemistry: The sequential bond energies of $Ni(CO)_x^+$ and $Ni(N_2)_x^+$ (x = 1-4) and $Ni(NO)_x^+$ (x = 1-3). J. Phys. Chem. 99:7819-7828.

Kim K, Jordan K D. 1994. Comparison of density-functional and MP2 calculations on the water monomer and dimer. J. Phys. Chem. 98:10089-10094.

Klippenstein S J, Yang C-N. 2000. Density functional theory predictions for the binding of transition metal cations to pi systems: from acetylene to coronene and tribenzocyclyne. Int. J. Mass Spectrom. 201:253.

Kretzschmar I, Schröder D, Schwarz H, Armentrout P B. 2001. Advances in metal and Semiconductor Clusters. In: M. A. Duncan. Edit. New York: Elsevier Science B. V.p. 347-395.

Kückelmann U, Müller D. 1998. A new approach to the gas phase chemistry of ternary transition metal complexes: ion-beam induced reactions. Int. J. Mass Spectrom. Ion Processes. 172:71-78.

Kurinovich M A, Lee J K. 2002. The acidity of uracil and uracil analogs in the gas phase: Four surprisingly acidic sites and biological implications. J. Am. Soc. Mass Spectrom. 13:985-995.

Landry-Hum J, Bussière G D, C., C. R. 2001. Triplet electronic states in d^2 and d^8 complexes probed by absorption spectroscopy: A CASSCF/CASPT2 analysis of $[V(H_2O)_6]^{3+}$ and $[Ni(H_2O)_6]^{2+}$. Inorg. Chem. 40:2595-2601.

Larsen B S, Ridge D P. 1984. Structural Characterization Of Gas-Phase Complexes Of Alkanes, Alkenes, And Carbon-Monoxide With The Atomic Iron-Ion. J. Am. Chem. Soc. 106:1912-1922.

Lautens M, Klute W, Tam W. 1996. Transition metal-mediated cycloaddition reactions. Chemical Reviews. 96:49-92.

Lavanant H, Hecquet E, Hoppilliard Y. 1999. Complexes of L-histidine with Fe^{2+}, Co^{2+}, Ni^{2+}, Cu^{2+}, Zn^{2+} studied by electrospray ionization mass spectrometry. Int. J. Mass Spectrom. 185/186/187:11-23.

Leavell M D, Leary J A. 2001a. Stabilization and linkage analysis of metal-ligated sialic acid containing oligosaccharides. J. Am. Soc. Mass. Spectrom. 12:528-536.

Leavell M D, Leary J A. 2001b. Dissociation mechanisms for metal N-glycosides of N-acetyl neuraminic acid. Int. J. Mass Spectrom. 204:185-196.

Lee C, Yang W, Parr R G. 1988. Development of the Colle-Salvetti correlation-energy formula into a functional of the electron density. Phys. Rev. B. 37:785-789.

Lee J K. 2005. Insights into nucleic acid reactivity through gas-phase experimental and computational studies. Int. J. Mass Spectrom. 240:261-272.

Lei Q P, Amster I J. 1996. The reactions of ground state Cu^+ and Fe^+ with the 20 common amino acids. J. Am. Soc. Mass Spectrom. 7:722-730.

Liu F, Zhang X G, Armentrout P B. 2005. Activation of CH_4 by gas-phase Ni^+ and the thermochemistry of Ni-ligand complexes. Phys.Chem.Chem.Phys. 7:1054-1064.

Llamas-Saiz A L, Foces-Foces C, Mo O, Yanez M, Elguero E, Elguero J. 1995. The geometry of pyrazole: a test for ab initio calculations. J. Comput. Chem. 16:263-272.

Luna A, Alcamí M, Mó O, Yáñez M. 2000a. Cu^+ binding energies. Dramatic failure of the G2 method vs. good performance of the B3LYP approach. Chem. Phys. Lett. 320:129-138.

Luna A, Alcamí M, Mó O, Yáñez M. 2000b. Cu^+ reactivity trends in sp, sp^2, and sp^3 nitrogen, phosphorus and arsenic containing bases. Int. J. Mass Spectrom. 201:215-231.

Luna A, Alcamí M, Mó O, Yáñez M, Tortajada J. 2002. A theoretical study of the interaction between Ni^+ and small oxygen and nitrogen containing bases. Int. J. Mass Spectrom. 217:119-129.

Luna A, Amekraz B, Morizur J P, Tortajada J, Mo O, Yanez M. 1997. Reactions Between Guanidine and Cu^+ in the Gas Phase. An Experimental and Theoretical Study. J. Phys. Chem. A. 101:5931-5941.

Luna A, Morizur J P, Tortajada J, Alcamí M, Mó O, Yáñez M. 1998a. Role of Cu^+ Association on the Formamide -->Formamidic Acid -->(Aminohydroxy)carbene Isomerizations in the Gas Phase. J. Phys. Chem. A. 102:4652-4659.

Luna A, Amekraz B, Morizur J P, Tortajada J, Mó O, Yáñez M. 2000c. Reactions of urea with Cu^+ in the gas phase: An experimental and theoretical study. J. Phys. Chem. A. 104:3132-3141.

Luna A, Amekraz B, Tortajada J, Morizur J P, Alcamí M, Mó O, Yáñez M. 1998b. Modeling the interactions between peptide functions and Cu(I): Formamide-Cu^+ reactions in the gas phase. J. Am. Chem. Soc. 120:5411-5426.

Lynch B J, Truhlar D G. 2002. Obtaining the right orbitals is the first step to calculating accurate binding energies for Cu^+ ion. Chem. Phys. Lett. 361:251-258.

Ma J C, Doughterty D A. 1997. The Cation-π interaction. Chem. Rev. 97:1303-1324.

Ma S G, Wong P, Yang S S, Cooks R G. 1996. Gas-phase molecular, molecular pair, and molecular triplet Fe^+ affinities of pyridines. J. Am. Chem. Soc. 118:6010-6019.

Magnera T F, David D E, Michl J. 1989. Gas-phase water and hydroxyl binding-energies for monopositive 1st row transition-metal ions. J. Am. Chem. Soc. 111:4100-4101.

Marinelli P J, Squires R R. 1989. Sequential solvation of atomic transition-metal ions - the 2nd solvent molecule can bind more strongly than the 1st. J. Am. Chem. Soc. 111:4101-4103.

Mazurek U, Schwarz H. 2002. Reactions of group 8, 9,and 10 monocations (Fe^+, Co^+, Ni^+, Ru^+, Rh^+, Pd^+, Os^+, Ir^+, Pt^+) with phosphane in the gas phase. Chem. Eur. J. 8:2057-2066.

Mebel A M, Morokuma K, Lin M C. 1995. Modification of the Gaussian-2 theoretical-model - the use of coupled-cluster energies, density-functional geometries, and frequencies. J. Chem. Phys. 103:7414-7421.

Mercero J M, Matxain J M, Lopez X, York D M, Largo A, Eriksson L A, Ugalde J M. 2005. Theoretical methods that help understanding the structure and reactivity of gas phase ions. Int. J. Mass Spectrom. 240:37-99.

Meyer F, Khan F A, Armentrout P B. 1995. Thermochemistry of transition metal benzene complexes: Binding energies of $M(C_6H_6)_x^+$ (x = 1,2) for M = Ti to Cu. J. Am. Chem. Soc. 117:9740-9748.

Miller T M, Arnold S T, Viggiano A A, Miller A E S. 2004. Acidity of a nucleotide base: Uracil. J. Phys. Chem. A. 108:3439-3446.

Molina-Svendsen H, Bojesen G, McKenzie C J. 1998. Gas-phase reactivity of coordinatively unsaturated transition metal complex ions toward molecular oxygen. Inorg. Chem. 37:1981-1983.

Montgomery Jr. J A, Frisch M J, Ochterski J, Petersson G A. 1999. A complete basis set model chemistry. VI. Use of density functional geometries and frequencies. J. Chem. Phys. 110:2822-2827.

Noll R J, Yi S S, Weisshaar J C. 1998. Bimolecular $Ni^+(^2D_{5/2})$ + C_3H_8 reaction dynamics in real time. J. Phys. Chem. A. 102:386-394.

Ojima I, Tzamarioudaki M, Li Z Y, Donovan R J. 1996. Transition metal-catalyzed carbocyclizations in organic synthesis. Chemical Reviews. 96:635-662.

Oliveira M C, Marcalo J, Vieira M C, Ferreira M A A. 1999. Formation of some transition metal oxide cluster anions and reactivity towards methanol in the gas phase. Int. J. Mass Spectrom. 187:825-835.

Operti L, Rabezzana R. 2003. Gas-Phase Ion Thermochemistry in Organometallic Systems. Mass Spectrom. Rev. 22:407-428.

Palii S P, Zagorevskii D V, Gerbeleu N V, Dobrov A A, Nemchinova L A. 1999. Mass spectrometry of coordination compounds of transition metals with tetradentate ligands. 11. Isomeric quasi-macrocyclic Ni(II) complexes based on S-substituted isothiocarbohydrazides and the structure of "small" ions derived from them. Int. J. Mass Spectrom. 193:131-141.

Peake D A, Gross M L, Ridge D P. 1984. Mechanism Of The Reaction Of Gas-Phase Iron Ions With Neutral Olefins. J. Am. Chem. Soc. 106:4307-4316.

Perdew J P, Wang Y. 1992. Accurate and simple analytic representation of the electron-gas correlation-energy. Phys. Rev. B. 45:13244-13249.

Pis Diez R, Alonso J A. 2000. Theoretical evidence of bound metastable states in the doubly ionized nickel dimer Ni_2^{2+}. Chem. Phys. Lett. 332:481-486.

Pozniak B P, Dunbar R C. 1997. Monomer and dimer complexes of coronene with atomic ions. J. Am. Chem. Soc. 119:10439-10445.

Pulkkinen S, Noguera M, Rodríguez-Santiago L, Sodupe M, Bertran J. 2000. Gas phase intramolecular proton transfer in cationized glycine and chlorine substituted derivatives (M-Gly, M = Na^+, Mg^{2+}, Cu^+, Ni^+, and Cu^{2+}): Existence of zwitterionic structures? Chem. Eur. J. 6:4393-4399.

Raghavachari K, Trucks G W, J.A. P, Head-Gordon M. 1989. A 5th-order perturbation comparison of electron correlation theories. Chem. Phys. Lett. 157:479-483.

Rannulu N S, Amunugama R, Yang Z, Rodgers M T. 2004. Influence of the s and d orbital occupation on the binding of metal ions to imidazole. J. Phys. Chem. A. 108:6385-6396.

Ricca A, Bauschlicher J C W. 1997. Successive OH binding energies of $M(OH)_n^+$ for n = 1-3 and M =Sc, Ti, V, Co, Ni, and Cu. J. Phys. Chem. A. 101:8949-8955.

Ricca A, Bauschlicher J C W. 2002. Theoretical study of the interaction of water and imidazole with iron and nickel dications. J. Phys. Chem. A. 106:3219-3223.

Rodgers M T, Armentrout P B. 2000. Noncovalent metal-ligand bond energies as studied by threshold collision-induced dissociation. Mass Spectrom. Rev. 19:215-247.

Rodgers M T, Armentrout P B. 2002. Influence of d orbital occupation on the binding of metal ions to adenine. J. Am. Chem. Soc. 124:2678-2691.

Rodgers M T, Stanley J R, Amunugama R. 2000. Periodic trends in the binding of metal ions to pyridine studied by threshold collision-induced dissociation and density functional theory. J. Am. Chem. Soc. 122:10969-10978.

Rodríguez-Cruz S E, Jockusch R A, Williams E R. 1998. Hydration energies of divalent metal ions, $Ca^{2+}(H_2O)_n$ (n = 5-7) and $Ni^{2+}(H_2O)_n$ (n = 6-8), obtained by blackbody infrared radiative dissociation. J. Am. Chem. Soc. 120:5842-5843.

Rodríguez-Santiago L, Tortajada J. 2002. Experimental and theoretical studies on the gas phase reactivity of formamide-Ni^+ complexes generated by FAB and electrospray ionization. Int. J. Mass Spectrom. 219:429-443.

Rodríguez-Santiago L, Sodupe M, Tortajada J. 2001. Gas-phas reactivity of Ni^+ with glycine. J. Phys. Chem. A. 105:5340-5347.

Rodríguez-Santiago L, Noguera M, Sodupe M, Salpin J Y, Tortajada J. 2003. Gas phase reactivity of Ni^+ with urea. Mass Spectrometry and theoretical studies. J. Phys. Chem. A. 107:9865-9874.

Rue C, Armentrout P B, Kretzschmar I, Schröder D, Schwarz H. 2002. Guided ion beam studies of the reactions of Ni^+, Cu^+, and Zn^+ with CS_2 and COS. J. Phys. Chem. A. 106:9788-9797.

Rulísek L, Havlas Z. 2000. Theoretical studies of metal ion selectivity.1. DFT calculations of interaction energies of amino acid side chains with selected transition metal ions (Co^{2+}, Ni^{2+}, Cu^{2+}, Zn^{2+}, Cd^{2+}, and Hg^{2+}). J. Am. Chem. Soc. 122:10428-10439.

Sanekata M, Misaizu F, Fuke K. 1995. Reactions of singly charged alkaline-earth metal-ions with water clusters - characteristic size distribution of product ions. J. Am. Chem. Soc. 117:747-754.

Satterfield M, Brodbelt J S. 2000. Enhanced detection of flavonoids by metal complexation and electrospray ionization mass spectrometry. Anal. Chem. 72:5898-5906.

Schröder D, Zummack W, Schwarz H. 1994. Reaction-Products, Directionalities, And Mechanisms Of Iron(I)-Mediated Ch-Bond, Cc-Bond, And Co-Bond Activation Of Aliphatic Carboxylic-Acids In The Gas-Phase. J. Am. Chem. Soc. 116:5857-5864.

Schröder D, Weiske T, Schwarz H. 2002. Dissociation behavior of $Cu(urea)^+$ complexes generated by electrospray ionization. Int. J. Mass Spectrom. 219:729-738.

Schultz R H, Armentrout P B. 1991. Threshold Collisional Activation Of $Fe^+.C_3H_8$ - Probing The Potential-Energy Surface. J. Am. Chem. Soc. 113:729-730.

Schultz R H, Armentrout P B. 1993. Gas-phase metal-ion ligation - collision-induced dissociation of $Fe(H_2O)_x^+$ and $Fe(CH_4)_x^+$ (x=1-4). J. Phys. Chem. 97:596-603.

Schwarz H. 2004. On the spin-forbiddeness of gas-phase ion-molecule reactions: a fruitful intersection of experimental and computational studies. Int. J. Mass Spectrom. 237:75-105.

Schwarz H, Schröder D. 2000. Concepts of metal-mediated methane functionalization. An intersectionof experiment and theory. Pure Appl. Chem. 72:2319-2332.

Sicilia E, Russo N. 2004. Structures, harmonic frequencies and interconversion potential energy profile of $Ni^{+}(C_2H_2)_2$ complexes. J. Mol. Struct. (THEOCHEM). 709:167-170.

Sievers M R, Jarvis L M, Armentrout P B. 1998. Transition-metal ethene bonds: Thermochemistry of $M^{+}(C_2H_4)_n$ (M = Ti-Cu, n = 1 and 2) complexes. J. Am. Chem. Soc. 120:189-1899.

Sim F, St-Amant A, Papai I, Salahub D R. 1992. Gaussian density functional calculations on hydrogen-bonded systems. J. Am. Chem. Soc. 114:4391-4400.

Smith G, Leary J A. 1996. Differentiation of diastereomeric nickel(II) N-glycoside complexes using tandem mass spectrometry and kinetic energy release measurements. J. Am. Chem. Soc. 118:3293-3294.

Smith G, Leary J A. 1998. Mechanistic studies of diastereomeric nickel(II) N-glycoside complexes using tandem mass spectrometry. J. Am. Chem. Soc. 120:13046-13056.

Smith G, Leary J A. 1999. Synthesis and analysis of electrospray ionization-generated five-coordinate diastereomeric Ni-N-glycoside complexes using a quadrupole ion trap mass spectrometer. Int. J. Mass Spectrom. 193:153-160.

Smith G, Pedersen S F, Leary J A. 1997. Stereoselective beta-hydrogen elimination from nickel(II)-N-glycoside complexes. Journal of Organic Chemistry. 62:2152-2154.

Sodupe M, Bauschlicher J C W. 1991. Theoretical-study of the bonding of the 1st-row and 2nd-row transition-metal positive-ions to acetylene. J. Phys. Chem. 95:8640-8645.

Sodupe M, Bauschlicher J C W, Langhoff S R, Partridge H. 1992. Theoretical-study of the bonding of the 1st-row transition-metal positive-ions to ethylene. J. Phys. Chem. 96:2118-2122.

Stiefel E I, Matsumoto K. 1996. Transition Metal Sulfur Chemistry. Washington DC: American Chemical Society.

Surya P I, Ranatunga D R A, Freiser B S. 1997. Infrared multiphoton dissociation of $MC_4H_6^{+}$ [M=Fe, Co, or Ni; C_4H_6= 1,3-butadine or $(C_2H_2)(C_2H_4)$]. J. Am. Chem. Soc. 119:3351-3357.

Surya P I, Roth L M, Ranatunga D R A, Freiser B S. 1996. Infrared multiphoton dissociation of transition metal containing ions: $MC_nH_{2n}^{+}$ (M = Fe, Co, Ni; n = 2-5). J. Am. Chem. Soc. 118:1118-1125.

Thomas J L C, Bauschlicher J C W, Hall M B. 1997. Binding of nitric oxide to first-transition-row metal cations: An ab initio study. J. Phys. Chem. 101:8530-8539.

Thompson C J, Aguirre F, Husband J, Metz R B. 2000. Photofragment spectroscopy and dynamics of $NiOH^{+}$ and $NiOH^{+}(H_2O)$. J. Phys. Chem. A. 104:9901-9905.

Tonkyn R, Ronan M, Weisshaar J C. 1988. Multicollision Chemistry Of Gas-Phase Transition-Metal Ions With Small Alkanes - Rate Constants And Product Branching At 0.75 Torr Of He. J. Phys. Chem. 92:92-102.

Trofimenko S. 1967. Boron-pyrazole chemistry IV. carbon- and boron-substituted poly(1-pyrazolyl)borates. J. Am. Chem. Soc. 89:6288-6294.

Trofimenko S. 1968. Molybdenum complexes with non-inert-gas configuration. J. Am. Chem. Soc. 90:4754-4755.

Tsierkezos N G, Schröder D, Schwarz H. 2003. Gas-phase solvation behavior of Ni(II) in water/N,N-dimethylformamide mixtures. J. Phys. Chem. A. 107:9575-9581.

Tsierkezos N G, Schröder D, Schwarz H. 2004. Complexation of nickel(II) by ethylenediamine investigated by means of electrospray ionization mass spectrometry. Int. J. Mass Spectrom. 235:33-42.

Vachet R W, Callahan J H. 2000. Quadrupole ion trap studies of the structure and reactivity of transition metal ion pair complexes. J. Mass Spectrom. 35:311-320.

Vachet R W, Hartman J R, Callahan J H. 1998. Ion-molecule reactions in a quadrupole ion trap as a probe of the gas-phase structure of metal complexes J. Mass Spectrom. 13:1209-1225.

Vachet R W, Hartman J R, Gertner J W, Callahan J H. 2001. Investigation of metal complex coordination structure using collision-induced dissociation and ion-molecule reactions in a quadrupole ion trap mass spectrometer. Int. J. Mass Spectrom. 204:101-112.

van Koppen P A M, Bowers M T, Fisher E R, Armentrout P B. 1994. Relative energetics of C-H and C-C bond activation of alkanes: Reactions of Ni^+ and Fe^+ with propane on the lowest energy (adiabatic) potential energy surfaces. J. Am. Chem. Soc. 116:3780-3791.

van Koppen P A M, Brodbeltlustig J, Bowers M T, Dearden D V, Beauchamp J L, Fisher E R, Armentrout P B. 1990. C-H Bond Activation As The Initial Step In The Co+-Mediated Demethanation Of Propane - The Critical Role Of Angular-Momentum At The Rate-Limiting Transition-State. J. Am. Chem. Soc. 112:5663-5665.

van Koppen P A M, Brodbeltlustig J, Bowers M T, Dearden D V, Beauchamp J L, Fisher E R, Armentrout P B. 1991. Transition-Metal Ion Mediated C-H And C-C Bond Activation Of Alkanes - Dynamic Coupling Between Entrance And Exit Channel Transition-States. J. Am. Chem. Soc. 113:2359-2369.

Walker N R, Grieves G A, Walters R S, Duncan M A. 2003. The metal coordination in $Ni^+(CO_2)_n$ and $NiO_2^+(CO_2)_m$ complexes. Chem. Phys. Lett. 380:230-236.

Walker N R, Walters R S, Grieves G A, Duncan M A. 2004. Growth dynamics and intracluster reactions in $Ni^+(CO_2)_n$ complexes via infrared spectroscopy. J. Chem. Phys. 121:10498-10507.

Walter D, Armentrout P B. 1998. Sequential bond dissociation energies of $M^+(NH_3)_x$ (x = 1-4) for M= Ti-Cu. J. Am. Chem. Soc. 120:3176-3187.

Walters R S, Jaeger T D, Duncan M A. 2002. Infrared spectroscopy of Ni+(C2H2)n complexes: Evidence for intracluster cyclization reactions. J. Phys. Chem. A. 106:10482-10487.

Walters R S, Pillai E D, Duncan M A. 2005a. Solvation dynamics in $Ni^+(H_2O)_n$ clusters probed with infrared spectroscopy. J. Am. Chem. Soc. 127:16599-16610.

Walters R S, Pillai E D, Schleyer P v R, Corminboeuf C, Duncan M A. 2005b. Vibrational spectroscopy and structures of $Ni^+(C_2H_2)_n$ (*n* = 1-4) complexes. J. Am. Chem. Soc. 127:17030-17042.

Watanabe H, Iwata S, Hashimoto K, Misaizu F, Fuke K. 1995. Molecular-orbital studies of the structures and reactions of singly charged magnesium-ion with water clusters, $Mg+(H_2O)_n$. J. Am. Chem. Soc. 117:755-763.

Weisshaar J C. 1993. Bare transition metal atoms in the gas phase: Reactions of M, M^+, and M^{2+} with hydrocarbons. Acc. Chem. Res. 26:213-219.

Wen D, Yalcin T, Harrison A G. 1995. Fragmentation reactions of Cu^+-cationated alpha-amino acids. Rapid Commun. In Mass Spectrom. 9:1599-1599.

Williams S M, Brodbelt J S. 2004. MS^n characterization of protonated cyclic peptides and metal complexes. J. Am. Soc. Mass Spectrom. 15:1039-1054.

Williams S M, Brodbelt J S, Huang Z L, Lai H G, Marchand A P. 2003. Complexation of silver and co-recovered metals with novel aza-crown ether macrocycles by electrospray ionization mass spectrometry. Analyst. 128:1352-1359.

Wilson S R, Yasmin A, Wu Y H. 1992. Bipyridyl Amino-Acid Metal-Complexes And Their Characterization By Electrospray Mass-Spectrometry. Journal Of Organic Chemistry. 57:6941-6945.

Wong P S H, Ma S, Wang F, Cooks R G. 1997a. Stereoelectronic effects and gas phase Co^+, Ni^+, $CpFe^+$, $CpCo^+$ and $CpNi^+$ affinities of pyridines studied by the kinetic method. J. Organom. Chem. 539:131-139.

Wong P S H, Ma S, Yang S S, Cooks R G, Gozzo F C, Eberlin M N. 1997b. Sulfur trifluoride cation (SF_3^+) affinities of pyridines determined by the kinetic method: Stereoelectronic effects in the gas phase. J. Am. Soc. Mass. Spectrom. 8:68-75.

Yalcin T, Wang J Y, Wen D, Harrison A G. 1997. C-C and C-H bond activation in the fragmentation of the $[M+Ni]^+$ adducts of aliphatic amino acids. J. Am. Soc. Mass Spectrom. 8:749-755.

Yamashita M, Fenn J B. 1984. Electrospray ion-source - another variation on the free-jet theme. J. Phys. Chem. 88:4451-4459.

Yang S S, Bortolini O, Steinmetz A, Cooks R G. 1995. Relative cyanide cation ($^{+}$CN) affinities of pyridines determined by the kinetic method using multiple-stage (MS(3)) mass-spectrometry. J. Mass. Spectrom. 30:184-193.

Yi S S, Blomberg M R A, Siegbahn P E M, Weisshaar J C. 1998. Statistical modeling of gas-phase organometallic reactions base on density functional theory: Ni^{+} + C_3H_8. J. Phys. Chem. A. 102:395-411.

Zhang D, Tao W A, Cooks R G. 2001a. Chiral resolution of D- and L-amino acids by tandem mass spectrometry of Ni(II)-bound trimeric complexes. Int. J. Mass Spectrom. 204:159-169.

Zhang Q, Kemper P R, Bowers M T. 2001b. $Fe(CH_4)_n^{+}$ and $Ni(CH_4)_n^{+}$ clusters: Experimental and theoretical bond energies for n =1-6. Int. J. Mass Spectrom. 210/211:265-281.

Zhao X, Xin B, Xing X P, Zhang X, Wang G H, Gao Z. 2001. Reactions of first-row transition metal ions with propargyl alcohol in the gas phase. Rapid Commun. Mass Spectrom. 15:1317-1321.

Zhou M, Andrews L. 2000. Reactions of laser-ablated Fe, Co, and Ni with NO: Infrared spectra and density functional calculations of MNO^{+} and $M(NO)_x$ (M = Fe, Co, x = 1-3; M = Ni, x = 1, 2), and $M(NO)_x^{-}$ (M = Co, Ni; x = 1,2). J. Phys. Chem. A. 104:3915-3392.